Received: 4 November 2019 | Revised: 26 March 2020 | Accepted: 22 May 2020

DOI: 10.1002/rnc.5121

SPECIAL ISSUE ARTICLE

WILEY

Digital implementation of sliding-mode control via the implicit method: A tutorial

Bernard Brogliato[1] | **Andrey Polyakov**[2]

[1]Univ. Grenoble-Alpes, INRIA, CNRS, Grenoble INP, LJK, Grenoble, France

[2]Univ. Grenoble-Alpes, INRIA Lille Nord-Europe, Villeneuve-d'Ascq, France

Correspondence
Bernard Brogliato, Univ. Grenoble-Alpes, INRIA, CNRS, Grenoble INP, LJK, Grenoble 38000, France.
Email: bernard.brogliato@inria.fr

Summary

The objective of this article, is to provide a clear presentation of the discretization of continuous-time sliding-mode controllers, also known in the automatic control literature as the emulation method, when the implicit (backward) Euler scheme is used. First-order, second-order, and homogeneous controllers are considered. The main theoretical results are recalled in each case, and the focus is put on the discrete-time implementation structure and on the algorithms which allow the designer to solve, at each time-step, the one-step generalized equations which are needed to compute the controllers. The article ends with some open issues.

KEYWORDS

discrete-time, homogeneous systems, sliding-mode control

1 | INTRODUCTION

The digital implementation of sliding-mode controllers (SMC), has long been known as being a tough issue, where the mere possibility of realizing SMC through discretization, was questioned. It happens indeed that the so-called emulation method [design the controller in continuous-time, and next discretize the plant via zero-order hold (ZOH) or else], which often relies on the existence of a small enough sampling time so that the continuous-time properties are recovered, does not work well when sliding-mode (set-valued) controllers[1] are considered, because fundamental properties like global asymptotic stability and the mere existence of sliding modes, may not be preserved after the discretization. In addition, the control input and the sliding variable are affected by chattering, which is highly undesirable. As we shall see in this article, it is in fact quite possible to realize discrete-time SMC, provided the right discretization method is employed to calculate the continuous-time control input to be applied on the plant. Roughly speaking (details are given in the sequel), the widely used *explicit* discretization method, is replaced by an *implicit* discretization method.

The fundamental idea originates from numerical simulation and analysis of mechanical systems with unilateral contact and set-valued friction, in particular the Moreau-Jean algorithm.[1-4] This is close also to so-called proximal algorithms in optimization[5,6] as introduced in Reference 7, as well as discretization of differential inclusions with maximal monotone set-valued part.[8-10] All these algorithms are based on an implicit discretization of the set-valued part of the dynamics, and a strong use of Convex or nonsmooth analysis, complementarity theory, and variational inequalities theory. However, the control problem has its own specific features, so it is not always a straightforward task to transfer such ideas from contact mechanics or optimization, to sliding-mode control.

[1]The word "discontinuous" is most often used in the SMC literature, however, we prefer the word "set-valued" which corresponds to the mathematical framework of differential inclusions.

Work supported by the ANR project Digitslid no ANR-18-CE40-0008-01.

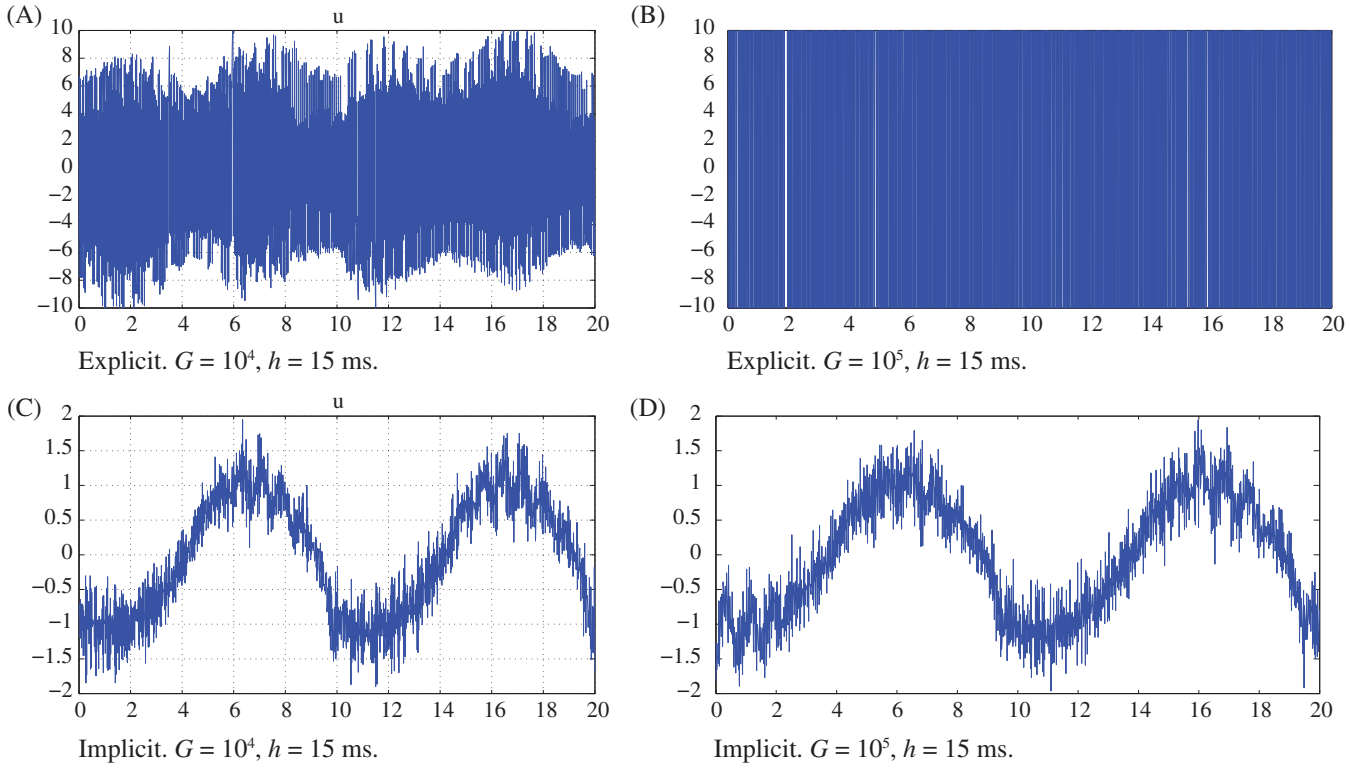

FIGURE 1 Typical experimental results for explicit (A, B) and implicit (C, D) SMC (control signals). SMC, sliding-mode controllers [Colour figure can be viewed at wileyonlinelibrary.com]

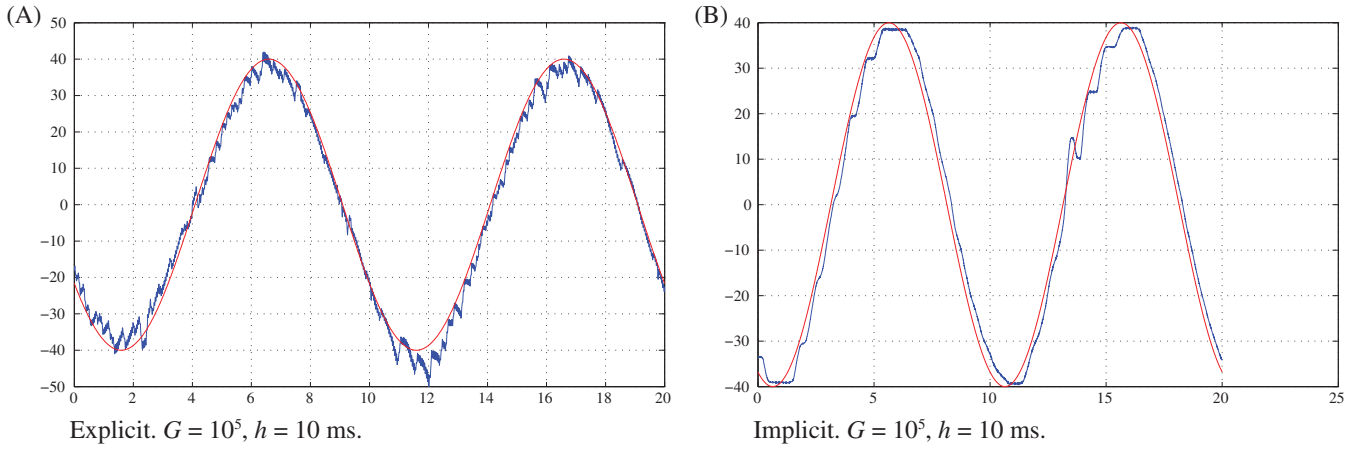

FIGURE 2 Typical experimental results for explicit (A) and implicit (B) SMC (output signals). SMC, sliding-mode controllers [Colour figure can be viewed at wileyonlinelibrary.com]

The basic motivation for the development of a novel scheme of the digital implementation of SMC is the suppression of the so-called *numerical* (or *digital*) *chattering effect*, that is, unavoidable when an explicit method is used, even in the ideal case without any perturbation.[11-14] Typical results obtained experimentally in References 15,16 on an electropneumatic system controlled with a first-order SMC are shown in Figures 1 and 2, where the discontinuous part of the controller (Figure 1A,B for the explicit method, Figure 1C,D for the implicit method) and the output (Figure 2A for the explicit method, Figure 2B for the implicit one) are depicted. The SMC gain is denoted as G, h is the sampling time. It appears clearly that the implicit method drastically decreases the amplitude and the chattering of the controller, without modifying the basic SMC structure.

In addition to the chattering drawback, it is known that explicit discretization yields only local stability for some homogeneous systems[17] [18, section V.C], see also Reference 19 for an interesting analysis of explicit Euler discretization of HOSMC. This remains true for first-order SMC when the continuous equivalent control is explicitly discretized [20, section VII.A], and even if the continuous-time system enjoys global asymptotic and exponential stability. In short, the main advantage and power of the implicit method is that it "copies" most of the nice properties of the continuous-time SMC:

- **P1:** Drastic decreasing of numerical chattering at both the output (the variable to be regulated) and the input (no longer any bang-bang signal which damages actuators) see Figures 1 and 2.
- **P2:** Keeps the continuous-time controller structure (no additional control gains or parameters).
- **P3:** Allows for large sampling periods without significant deterioration of closed-loop performances (the sampling times indicated in Figures 1 and 2 are typical of what may be chosen in practical implementations).
- **P4:** Performs a kind of regularization (with a saturation-like function), but *after* the discretization, in a systematic and automatic way, contrary to the explicit method which requires a regularization *before* the time-discretization (without any guarantee of numerical chattering suppression unless a long and tedious design work is performed, and decreasing the control system's accuracy).
- **P5:** Allows to get robustness with respect to matched bounded disturbances, as well as parameter uncertainties, but also unmatched disturbances (using a backstepping approach).
- **P6:** Convergence of not only the output toward its continuous-time counterpart when $h \to 0$, but also of the input (impossible to obtain with explicit method).
- **P7:** Preserves finite-time convergence toward the attractive surface (even in case of codimension ≥ 2 surface, that is, several attractive surfaces[2]).
- **P8:** Preserves Lyapunov stability properties of the continuous-time controller.
- **P9:** Allows one to define in a rigorous way the discrete-time sliding surfaces, and the sliding modes of the dynamics.
- **P10:** The set-valued controller selection remains insensitive to the control gain variations during the discrete-time sliding mode, as predicted by Filippov's and Utkin's equivalent control approaches (see Figure 1C,D for an experimental illustration).
- **P11:** Reproduces the equivalent control during sliding modes, with almost-exact compensation (up to a delay equal to the sampling period) of the disturbance.

Properties **P1**, **P3**, **P10**, and **P11** have been verified experimentally in References 15,16,20,21 on two different setups: an electropneumatic system, and an inverted pendulum on a cart. Property **P10** may be, in fact, the best illustration of the drastic difference between the explicit and the implicit methods. The price to pay, is that the controller is less simple to calculate than its explicit counterpart. However, as we shall see in the sequel, the degree of complexity of the computations of most implicit controllers, remains low, and is not at all an obstacle to their real-time implementation (especially in view of **P3**).

The differences between the explicit and the implicit Euler methods and the superiority of the latter in nonsmooth gradient methods in optimization, and in the simulation of mechanical systems with impacts and unilateral constraints, are well known.[1,3,4,6,22] *One may see the analysis of these two methods in SMC and homogeneous systems, as a new field of investigation, besides optimization and contact mechanics.*

We should also mention the analysis of the implicit Euler method for linear complementarity systems and relay systems, with main applications in circuits with nonsmooth components.[2,23,24] In sliding-mode control and observation, the implicit approach has been initiated and deeply analyzed by two main research groups, in France,[15,16,18,20,21,25-36] and in Japan.[37-51] We may also mention[52-54] (who apply a kind of semi-implicit discretization method based on pseudo linear representations), as well as the pioneering work in Reference 55 where the implicit Euler discretization was advocated for the first time in automatic control for a scalar system with known perturbation (see Remark 1 below), and with a short analysis of its finite-time convergence properties. It is noteworthy that both [55, pp274-275] and [3, section 5] therefore presented similar contributions, the first one in the automatic control scientific community, the second one in the

[2]The attractive sets will most of the time be hyperplanes of the form $Cx = 0$, $C \in \mathbb{R}^{m \times n}$. When $m \geq 2$ we will indifferently use the words surface, or surface of codimension m.

contact mechanics scientific community. Several experimental validations led on various kinds of setups, confirm the above theoretical and numerical findings.[15,16,20,21,37,38,40-43,46,47,56]

In this article, we start in Section 2 with the simplest scalar example, to illustrate the main features of the implicit approach applied to the first-order SMC. The closed-loop structure is analyzed in Section 2.5. Then we proceed with more complex cases (still dealing with first-order SMC) in Section 3: n-dimensional LTI systems with matched perturbation in Section 3.1, n-dimensional LTI systems with matched perturbation and parameter uncertainty in Section 3.2, Lagrangian systems with matched perturbation and parameter uncertainty in Section 3.3. Other schemes which illustrate the features of the implicit method are briefly summarized in Section 3.4: a backstepping algorithm for planar systems with unmatched perturbations in Section 3.4.1, an improved algorithm with perturbation estimation to improve the precision in Section 3.4.2, a fixed-time convergence nonlinear system in Section 3.4.3, parabolic, proxy-based, and amplitude-and-rate saturated SMC in Sections 3.4.4,3.4.5, and 3.4.6, respectively. It is shown that the implicit method possesses a common feedback structure, where the input is calculated by a so-called *generalized equation* (GE) which keeps the same structure in all cases. Section 4 is devoted to second-order SMC: the twisting controller in Section 4.1, and the supertwisting in Section 4.2. Homogeneous systems are treated in Section 5. Conclusions are in Section 6 and some algorithmic details are given in the Appendix.

Notation and definitions. Positive definiteness of a matrix: $\mathbb{R}^{n\times n} \ni M \succ 0$ means that $x^\top Mx > 0$ for all vector $x \neq 0$ (the matrix M needs not be symmetric), I_n is the $n\times n$ identity matrix. The minimum and maximum eigenvalues of $M \in \mathbb{R}^{n\times n}$ are denoted as $\lambda_{\min}(M)$ and $\lambda_{\max}(M)$. The induced matrix norm $\|M\|_m = \sup_{\|x\|=1}\|Mx\|$. The set $\mathbb{B}_n \stackrel{\Delta}{=} \{x \in \mathbb{R}^n \mid \|x\| \leq 1\}$ represents the unit closed ball with center at the origin in $\mathbb{R}^n$ with the Euclidean norm. The set-valued signum function is $\mathrm{sgn}(x) = +1$ if $x > 0$, -1 if $x < 0$, and $[-1, +1]$ if $x = 0$. When $x \in \mathbb{R}^n$, we set $\mathrm{sgn}(x) = (\mathrm{sgn}(x_1), \mathrm{sgn}(x_2), \dots, \mathrm{sgn}(x_n))^\top$. The domain of a set-valued function $F : \mathbb{R}^n \rightrightarrows \mathbb{R}^m$ is $\mathrm{dom}(F) = \{x \in \mathbb{R}^n \mid F(x) \neq \emptyset\}$. The interior of a set S is denoted as $\mathrm{int}(S)$.

Let $K \subseteq \mathbb{R}^n$ be a closed nonempty convex set. Its indicator function is $\psi_K(x) = 0$ if $x \in K$, $\psi_K(x) = +\infty$ if $x \notin K$. The subdifferential of Convex analysis of the indicator function is the normal cone to K, that is, $\partial\psi_K(x) = \mathcal{N}_K(x)$, where $\mathcal{N}_K(x) = \emptyset$ if $x \notin K$, and $\mathcal{N}_K(x) = \{z \in \mathbb{R}^N \mid \langle z, v - x\rangle \leq 0 \text{ for all } v \in K\}$. Let K be convex polyhedral, represented as $K = \{x \in \mathbb{R}^n \mid C_i x + d_i \geq 0,\ 1 \leq i \leq p\} = \{x \in \mathbb{R}^n \mid Cx + d \geq 0\}$. Then $\mathcal{N}_K(x) = \{w \in \mathbb{R}^n \mid w = -\sum_{i=1}^p C_i^\top \lambda_i,\ 0 \leq \lambda_i \perp C_i x + d_i \geq 0\} = \{w \in \mathbb{R}^n \mid w = -C^\top\lambda,\ 0 \leq \lambda \perp Cx + d \geq 0\}$ [57, examples 5.2.6].

The support function of the closed convex nonempty set K, is $\sigma_K(x) = \sup_{v\in K}\langle x, v\rangle$. It is the conjugate function $\psi_K^\star(\cdot)$ of the indicator $\psi_K(\cdot)$, and vice versa. Both the indicator and the support functions are convex proper lower semicontinuous. One has:

$$x \in \partial\sigma_K(y) \Leftrightarrow y \in \mathcal{N}_K(x), \tag{1}$$

for any x and $y \in \mathbb{R}^n$: the set-valued mappings $\partial\sigma_K(\cdot)$ and $\mathcal{N}_K(\cdot)$ are inverse mappings. Let $K = [-1, 1] \subset \mathbb{R}$, then $\sigma_{[-1,1]}(x) = |x|$, and $\partial\sigma_{[-1,1]}(x) = \mathrm{sgn}(x) = \partial|x|$ (the set-valued signum function), and $x \in \mathrm{sgn}(y) \Leftrightarrow y \in \mathcal{N}_{[-1,1]}(x)$. If $x \in \mathbb{R}^n$, then $\partial\,\|x\|_1 = \mathrm{sgn}(x)$, where $\|x\|_1 = \sum_{i=1}^n |x_i|$.

Let now $x \in \mathbb{R}^n$ and $y \in \mathbb{R}^n$ be given, and $M = M^\top \succ 0$, then

$$M(x - y) \in -\mathcal{N}_K(x) \Leftrightarrow x = \mathrm{proj}_M[K; y], \tag{2}$$

where the orthogonal projection is $\mathrm{proj}_M[K, y] = \mathrm{argmin}_{z\in K}\frac{1}{2}(z - y)^\top M(z - y)$ (this is the orthogonal projection in the metric defined by M). Using the normal cone definition, this is equivalent to the problem: find $x \in K$ such that

$$\langle y - x, x - v\rangle \geq 0, \quad \text{for all } v \in K, \tag{3}$$

which is a variational inequality. Given $\lambda \in \mathbb{R}^m$, $M \in \mathbb{R}^{m\times m}$, and $q \in \mathbb{R}^m$, a linear complementarity problem (LCP) is a nonsmooth problem of the form: $\lambda \geq 0$, $w = M\lambda + q \geq 0$, $w^\top\lambda = 0$, rewritten compactly as $0 \leq \lambda \perp w = M\lambda + q \geq 0$.

Let $f : \mathbb{R} \to \mathbb{R}^m$ be a right-continuous step function, discontinuous at finitely many time instants t_k and t_0, $t \in \mathbb{R}$ with $t_0 < t$. The variation of $f(\cdot)$ on $[t_0, t]$ is defined as:

$$\mathrm{Var}_{t_0}^t(f) \stackrel{\Delta}{=} \sum_k \|f(t_k) - f(t_{k-1})\|,$$

with $k \in \mathbb{N}^*$ such that $t_k \in (t_0,t]$. If $f(\cdot)$ is continuously differentiable with bounded derivatives then the variation of $f(\cdot)$ on $[t_0,t]$ is defined as:

$$\mathrm{Var}_{t_0}^{t}(f) \stackrel{\Delta}{=} \int_{t_0}^{t} \|\dot{f}(\tau)\| \mathrm{d}\tau. \tag{4}$$

Let $\mathcal{M} : \mathbb{R}^n \rightrightarrows \mathbb{R}^n$ be a set-valued mapping. It is *monotone* if for any x and $y \in \mathrm{dom}(\mathcal{M}) \subseteq \mathbb{R}^n$, and any $x' \in \mathcal{M}(x)$, $y' \in \mathcal{M}(y)$, one has $\langle x-y,x'-y' \rangle \geq 0$. It is *strongly* monotone if $\langle x-y,x'-y' \rangle \geq \|x-y\|^2$ for some $\alpha > 0$. It is *maximal* if it cannot be enlarged without destroying its monotonicity. The subdifferential of a convex proper lower semicontinuous function, defines a maximal monotone operator (for instance, the normal cone to a convex nonempty closed set, is maximal monotone, and the subdifferential of its support function is also maximal monotone).

A function $f : \mathbb{R}_+ \to \mathbb{R}_+$ belongs to the set $\mathcal{K}$ if it is continuous, monotone increasing and $f(0) = 0$.

2 | A SIMPLE EXAMPLE

2.1 | Continuous-time system

Let us start with the simplest scalar system:

$$\dot{x}(t) = u(t) + d(x(t), t),$$

with unknown disturbance $|d(x,t)| \leq M < +\infty$, $x(0) = x_0 \in \mathbb{R}$ and known upperbound M. The classical SMC for the considered system is $u(x(t)) = -(M+\delta)\mathrm{sgn}(x(t))$, $\delta > 0$. More rigorously, we should write:

$$u(t) = -\lambda(t), \text{ with } \lambda(t) \in (M+\delta)\ \mathrm{sgn}(x(t)),$$

which means that $u(t)$ is an element (a selection) of the set $\mathrm{sgn}(x(t))$: the controller is *set-valued* (another name is *multivalued*). We assume that $d(\cdot,\cdot)$ satisfies basic requirements for this set-valued closed-loop system to be well posed with absolutely continuous solutions, for instance, in the sense of Filippov's differential inclusions (other choices are possible[8,9]). This is more than a mathematical fuss, because it means that once the origin $x^* = 0$ is attained (after a finite-time t^*), then there exists a $\lambda(x(t),t)$ such that $u(x(t),t) = -d(x(t),t)$ for all $t \geq t^*$: the equivalent control which acts on the system when the sliding mode is activated, *exactly* compensates for the perturbation. Obviously, this is doable only because of the set-valuedness of the control input. It is noteworthy that during sliding modes, the value of $u(t)$ does not depend on the controller gain $G \stackrel{\Delta}{=} M + \delta$: it takes values inside the interval $[-M-\delta, M+\delta]$, and these values depend only on $d(x(t),t)$: increasing δ has no influence on $u(t)$ (property **P10**).

2.2 | Digital implementation

Let us now turn our attention to the discrete-time realization of this set-valued controller. The first step is the choice of a plant discretization. In such a simple case, the ZOH exact discretization, and the Euler discretizations are very close one to each other, and differ only by the approximation of the disturbance on a sampling interval $[t_k,t_{k+1})$. We shall denote the disturbance approximation as d_k, so that the plant's discretization reads as:

$$x_{k+1} = x_k + hu_k + hd_k, \quad k \geq 0, \tag{5}$$

$h = t_{k+1} - t_k > 0$ is the sampling period, $d_k = d(x_k,t_k)$ for the Euler method, $d_k = \int_{t_k}^{t_{k+1}} d(x(t),t)dt$ for the exact method. Since our goal is to explain the difference between the explicit and the implicit methods, we shall not focus on this issue

from now on. For simplicity let us assume that $M+\delta=1$. The explicit method reads as:

$$\begin{aligned}&(a)\ x_{k+1}=x_k+hu_k+hd_k\\&(b)\ u_k=-\mathrm{sgn}(x_k),\end{aligned}\tag{6}$$

which means that one applies the staircase input $\bar{u}_k(t)=u_k$ for all $t\in[t_k,t_{k+1})$. We shall see later the reason why we did not write $u_k\in-\mathrm{sgn}(x_k)$, but an equality. The implicit method is designed as follows:

$$\begin{aligned}&(a)\ x_{k+1}=x_k+hu_k+hd_k\\&(b)\ \tilde{x}_{k+1}=x_k+hu_k\\&(c)\ u_k=-\lambda_{k+1}\\&(d)\ \lambda_{k+1}\in\mathrm{sgn}(\tilde{x}_{k+1}),\end{aligned}\tag{7}$$

and one applies the staircase input $\bar{u}_k(t)=-\lambda_{k+1}$ for all $t\in[t_k,t_{k+1})$. The method is said implicit, because if $d(x(t),t)\equiv 0$, then $\tilde{x}_{k+1}=x_{k+1}$ and (7) (d) holds, so that we obtain in the unperturbed case the *difference inclusion*:

$$x_{k+1}-x_k\in-h\ \mathrm{sgn}(x_{k+1}).\tag{8}$$

Let us make a stop here. In (6) (b), the input is available directly, since $x_k=x(t_k)$ is measured at time t_k (see, however, Section 2.4). Such is not the case neither in (7), nor in (8) where the input $u_k\in-\mathrm{sgn}(x_{k+1})$. At this stage, it could be thought that the implicit method yields an anticipative input. However, such is not the case as we shall see next. See also Remark 1 for further comments on the design of (7) (b) (c) (d).

In fact, (7) (b) (c) (d) have to be solved as follows (solving (8) follows the same lines). First notice that (7) (b) (c) (d) can be rewritten as

$$\tilde{x}_{k+1}-x_k\in-h\ \mathrm{sgn}(\tilde{x}_{k+1}),\tag{9}$$

which is a *GE* mimicking (8) but with unknown $\tilde{x}_{k+1}$, which is a dummy variable needed to make calculations (or could be seen as the state of an unperturbed system mimicking the plant).

- A GE is a nonlinear problem involving a set-valued mapping, of the form

$$0\in F(x),\ F:\mathrm{dom}(F)\subseteq\mathbb{R}^n\rightrightarrows\mathbb{R}^p.$$

  One example is $0\in f(x)+\mathcal{N}_K(x)$ with $f:\mathbb{R}^n\to\mathbb{R}^p$ a single-valued function, $K\subseteq\mathbb{R}^n$ a closed convex set, that is, widely studied.[58,59] In general a GE can be written with complementarity problems, variational inequalities, inclusions into normal cones, and so on. Key properties for existence and uniqueness of solutions are monotonicity, convexity.
- In numerical analysis, an ODE $\dot{x}(t)=f(x(t))$, $x(0)=x_0$, $f(\cdot)$ Lipschitz continuous, can be discretized with an implicit Euler method, yielding a nonlinear problem $g(x_{k+1})\overset{\Delta}{=}x_{k+1}-hf(x_{k+1})-x_k=0$ to be solved at each step with an iterative method. In our set-valued setting, the implicit method yields a GE of the form $G(\tilde{x}_{k+1})\ni 0$, (9) being one example with $G(\tilde{x}_{k+1})=\tilde{x}_{k+1}-x_k+h\ \mathrm{sgn}(\tilde{x}_{k+1})$.

It is not difficult to see that the GE in (9) has a unique solution for any x_k and $h>0$, either relying on general results as in References 59 or 60 (which rely on the fundamental property of monotonicity of operators), or by simple inspection: the intersection between the line $\tilde{x}_{k+1}\mapsto\tilde{x}_{k+1}-x_k$ and the graph of the set-valued mapping $\tilde{x}_{k+1}\mapsto-h\ \mathrm{sgn}(\tilde{x}_{k+1})$, is unique, see Figure 3 (left) . Four cases are depicted: case (1) $x_k<-h\Rightarrow\tilde{x}_{k+1}=x_k+h$, cases (2) and (3) $x_k\in[-h,h]\Rightarrow\tilde{x}_{k+1}=0$, case (4) $x_k>h\Rightarrow\tilde{x}_{k+1}=x_k-h$. As expected from (9), $\tilde{x}_{k+1}$ depends only on known quantities. The role played by the monotonicity of both operators in Figure 3 (left) is clear, for if one considers instead $\tilde{x}_{k+1}\mapsto h\ \mathrm{sgn}(\tilde{x}_{k+1})$, uniqueness of intersections in all cases is lost.

Remark 1. Notice that since $d(x,t)$ is unknown, solving the GE(x_{k+1}): $x_{k+1}-x_k-hd_k\in-h\mathrm{sgn}(x_{k+1})$ to calculate the so-called equivalent controller is impossible (and this is certainly the reason why the work presented in Reference 55 has

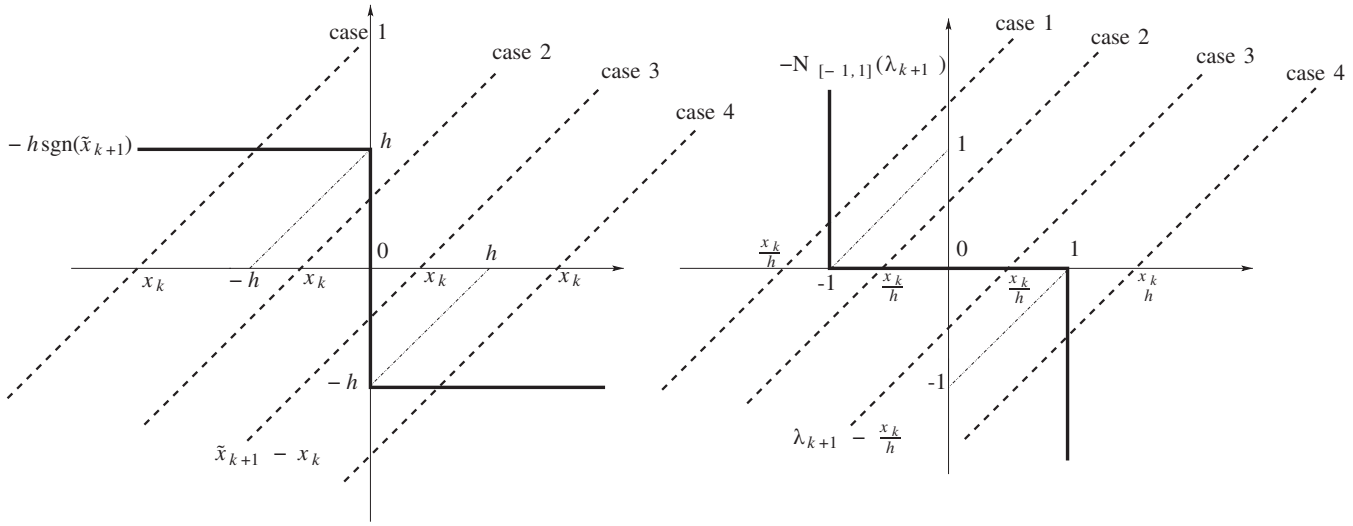

FIGURE 3 The generalized equations in (7) (b) (c) (d) (left) and in (12) (right)

not been applied further, as witnessed even in recent articles[61]). This is why $\tilde{x}_{k+1}$ has been defined through (7) (b)(c)(d), to allow for the GE($\tilde{x}_{k+1}$) (9). In a sense, (7) (b) represents a virtual unperturbed system.[26] The interpretation of this fact, is that it is not possible to find automatically a selection of the set-valued term, which solves GE(x_{k+1}). This is the big difference with respect to the continuous-time setting. In discrete-time, the controller will be able to compensate for the perturbation, but with a delay equal to h.

A graphical interpretation of the GE (9) is interesting in this simple case, but it is not sufficient to deal with more complex cases to come later. To that aim, it is convenient to use to tools from Convex analysis. Without going too deeply into the details, let us state that the GE in (9) is *equivalent* to the GE:

$$\tilde{x}_{k+1} \in \mathcal{N}_{[-1,+1]}\left(\frac{\tilde{x}_{k+1} - x_k}{-h}\right) = -\mathcal{N}_{[-1,+1]}\left(\frac{\tilde{x}_{k+1} - x_k}{h}\right), \tag{10}$$

which is obtained by *inverting* the set-valued signum function as in (1). From (10), and using (2), one obtains equivalently to (10):

$$\tilde{x}_{k+1} = x_k + h\ \mathrm{proj}\left[[-1,1]; -\frac{x_k}{h}\right]. \tag{11}$$

Let us now turn our attention to the control. Using (1) and (7) (d), one infers that $\tilde{x}_{k+1} \in \mathcal{N}_{[-1,1]}(\lambda_{k+1})$, hence from (7) (b) (c) it follows that

$$\lambda_{k+1} - \frac{x_k}{h} \in -\mathcal{N}_{[-1,1]}(\lambda_{k+1}). \tag{12}$$

The graphical interpretation of the GE (12) is obtained by reversing the graphs in Figure 3 (from the left subfigure to the right subfigure). Then using (7) (c) and (2) (or, merely using (7) (b) and (11)), it follows that the implicit controller is given as:

$$u_k = \mathrm{proj}\left[[-1,1]; -\frac{x_k}{h}\right].$$

Remark 2. The variables $\tilde{x}_{k+1}$ and λ_{k+1} are *conjugate* variables, in the sense that they satisfy an equivalence as (1). In a more general setting, the first one represents the "virtual" sliding variable, and the second one is a selection of the set-valued control signal. In this sense, the implicit discretization does represent the time-discretization of the set-valued continuous-time closed-loop system.

Let us explain the projection in (13). At $t=t_k$, one measures $x(t_k)$, and calculates u_k as the point of $[-1,1]$ that is the closest to $-\frac{x_k}{h}$ in $[-1,1]$, as follows:

Algorithm 1

1. If $-\frac{x_k}{h} \geq 1 \Leftrightarrow x_k \leq -h$, then $u_k = 1$,
2. If $-\frac{x_k}{h} \leq -1 \Leftrightarrow x_k \geq h$, then $u_k = -1$,
3. If $-\frac{x_k}{h} \in [-1,1] \Leftrightarrow x_k \in [-h,h]$, then $u_k = -\frac{x_k}{h}$.

Then the staircase input (a right-continuous step function) $\bar{u}(\cdot)$ is defined as: $\bar{u}(t) = u_k$ for all $t \in [t_k, t_{k+1})$, $k \geq 0$. It is noteworthy that when the trajectory is far from the origin, then both the implicit and the explicit controllers are the same. The big difference between both, exists close to Σ_d. *In this scalar case, the implicit controller is very easy to implement by performing three simple on-line tests.*

It requires, however, actuators which are capable of attaining continuous values (ie, step-motors or the like, cannot realize implicit controllers: they behave like an explicit Euler discretization). The above developments prove that the discrete-time system is *well posed*, in the sense that one is able to compute a *unique* value of the control input at each step $k \geq 0$. The notion of a discrete-time sliding surface has been mentioned. Let us define it now for our simple system (see also [62, definition 5.1]).

Definition 1. Consider the closed-loop system (7). The discrete-time sliding surface is defined as:

$$\Sigma_d = \{(x_k, u_k) \mid \tilde{x}_{k+1} = 0\}.$$

Thus, on Σ_d one has $u_k = -\frac{x_k}{h} \in [-1,1]$ (in fact this is the definition of a discrete-time sliding phase that is taken in [20, remark 1]), so that from (5) $x_{k+1} = hd_k$. Hence if the system remains on Σ_d, at the next step one has $\tilde{x}_{k+2} = x_{k+1} + hu_{k+1} = 0$, and the input is $u_{k+1} = -d_k$, applied on $t \in [t_{k+1}, t_{k+2})$[3]: *the implicit controller compensates for the perturbation, with a delay h* (see **P10** and **P11**). It is noteworthy that the notion of a sliding surface is defined from $\tilde{x}_{k+1}$, the virtual or dummy unperturbed state variable, and not from x_{k+1} itself (in the absence of perturbation, both are equal one to each other).

2.3 | Closed-loop analysis

The properties of the closed-loop system (5) (13) can be studied, along the lines of References 20,25-27, and are summarized now.

Theorem 1. [20, 25-27] *Consider the difference inclusion closed-loop system (5) (13), that is, the implicit time-discretization of the set-valued system* $\dot{x}(t) = u(t) + d(x(t), t)$, $u(t) \in -\text{sgn}(x(t))$, $x(0) = x_0$, *with* $|d(x,t)| < 1$ *for all t and x. Let* $h = t_{k+1} - t_k > 0$ *be given.*

1. *In the unperturbed case, the origin of the unperturbed system in (8) is globally Lyapunov stable, with same Lyapunov function in continuous-time and in discrete-time.*
2. *With a suitable choice of the feedback gain, the solutions to the perturbed system (7) attain* Σ_d *in a finite number of steps and stay in it, that is, there exists* $k^* < +\infty$ *such that* $\tilde{x}_{k+1} = 0$ *for all* $k > k^*$.
3. *Let the solution to the continuous-time system attain the sliding surface at* t^*. *The control input* $\bar{u}(\cdot)$ *converges to its continuous-time counterpart* $u(\cdot)$ *in the following sense:*
   (a) *Let* $d(t)$ *be uniformly continuous. For all strictly decreasing sequences* $\{h_n\}_{n\in\mathbb{N}}$, *one has* $\lim_{h_n \to 0} \text{esssup}_{t\in I} |\bar{u}(t) - u(t)| = 0$ *for all time intervals* $I \subseteq [t^*, +\infty)$.
   (b) *Let* $d(t)$ *be continuously differentiable and with bounded derivative. For all strictly decreasing sequences* $\{h_n\}_{n\in\mathbb{N}}$ *and all* $t > t^*$, *one has* $\lim_{h_n \to 0} \text{Var}_{t^*}^{t}(\bar{u}) = \text{Var}_{t^*}^{t}(u)$.
4. *On the sliding surface* Σ_d, *one has* $u_k = -d_{k-1} \in [-1,1]$ *on* $t \in [t_k, t_{k+1})$, *and* $x_k = hd_{k-1}$ *(the disturbance is attenuated by a factor h),* $k \geq 1$.

We recall that $\bar{u}(\cdot)$ is the staircase input: $\bar{u}(t) = u_k$ for all $t \in [t_k, t_{k+1})$, $k \geq 0$. The time t^* and the integer k^* depend on the initial data. The variation is defined in (4). Item 1 follows from [18, theorem 5] and [20, section V.C]. Item 2

[3]This input is the discrete-time equivalent input in Utkin's sense, which or course is unknown but is the consequence of applying the controller in (13).

is proved in References 26 and 20. Item 3 is proved in [20, section V.C]. Item 4 is proved in Reference 26. It is noteworthy that the explicit method (6) possesses also some convergence properties, see, for instance, [1, theorem 9.5] [63, theorem 2.2], from which the convergence of solutions to (6) toward some solution to the continuous-time DI, can be proved under a linear growth condition on $d(x,t)$. It is also possible to show that the sequence $\{x_k\}_{k\in\mathbb{N}}$ generated by (6), is bounded for any initial data and any $h>0$. This can be proved with the Lyapunov-like function $V_k = x_k^2$, which satisfies along (6): $V_{k+1} - V_k < 0$ for all $|x_k| > \frac{h(1+2M+M^2)}{1-M}$, where $|d_k| \leq M < 1$. The analysis of the trajectories while they wander in a ball of radius proportional to h and centered at the origin, shows that the controller switches between -1 and $+1$. This is, however, quite insufficient for SMC analysis, where one is interested by the closed-loop behavior for $h>0$, not as $h \to 0$.

2.4 | Explicit vs implicit: Further comments

The explicit method in (6) yields digital chattering.[11-13,64-66] This results in a bang-bang input as in Figure 1A,B, because the explicitly discretized controller behaves like a step motor, that is incapable of reaching any value other than $+1$ and -1.

- In order to cope with this issue, one may, as is commonly done in the SMC literature, replace the signum multifunction by a saturation or sigmoid, which approximates it. First, accuracy is necessarily decreased, second the parameter-tuning process so that chattering is effectively decreased, may not be easy at all[16,67] (see also Remark 7), third adding a saturation destroys the sliding mode (this issue being directly related to the controller set-valuedness on the attractive surface), fourth it is not clear how this regularization performs when the attractive surface has codimension ≥ 2 (and tuning the gains in that case is even less easy, see Reference 68 for details on *sigmoid blending*) and this is even more true after discretization,[69,70] fifth this adds parameters in the control, which may not be desirable, sixth and finally this may in some cases destroy stability [71, remark 5]. In short, and contrarily to a widely spread idea in the SMC scientific community, adding saturations is far from being a miracle cure to chattering. In fact, the process of parameters tuning[4] so that the performance remains good, is rarely given in the articles, letting one think that this is an automatic, easy process. An enlightening example in $\mathbb{R}^2$ has been worked out numerically in Reference 16. Its conclusions is that tuning the saturation width and the sampling time, in order to minimize input and output chattering, is at best a difficult process.
- A second option is to filter out chattering oscillations by incorporating low-pass filters in the control loop, however, this also introduces nonwanted effects like phase lags and additional parameters to tune, and it necessarily implies less accuracy. The analysis of the digital implementation of SMC using low-pass filters is far from being complete.
- Another solution, could be to add a *selection procedure* in order to allow for the system to choose an element of the set $\mathrm{sgn}(x_k)$. In numerical analysis, the minimum norm selection is sometimes chosen [1, section 9.2.4.1], which is sufficient to get convergence toward solutions to the continuous-time differential inclusion. In our control setting, this is clearly not very appropriate, since the minimum norm element of $\mathrm{sgn}(x_k)$ is either 1 or -1 outside zero, or 0 at zero: it is not possible to counteract the perturbation with such a selection. Actually, the right selection is unknown, since this is the perturbation itself (see in this respect Remark 1). Moreover, numerical approximations do not allow for an exact calculation of zero, so that the decision of whether or not the system has reached the origin, necessarily implies to define a boundary layer containing zero, within which it is decided that $\mathrm{sgn}(x_k) = [-1,1]$ for all x_k in this boundary layer. This is an additional parameter to be tuned. Such a zero detection issue is not present in the implicit method, where u_k is obtained by solving (13) at each step k.
- It happens from (13) and Algorithm 1, that u_k is nothing but the saturation function of x_k, with saturation width equal to $[-h,h]$. Consequently, one interpretation of the implicit method, is that it applies a saturation (a regularization of the set-valued input), in an automatic way, *after* the discretization process. This is quite different from adding a saturation in the continuous-time closed-loop, and discretizing afterward, especially in cases more complex that the simplest scalar example.
- As alluded to in the introduction, the idea of using an implicit Euler discretization was fist advocated in Reference 55, in a simple scalar case (and with the idea of inverting the set-valued sign function). However, the idea

[4]Here parameters mean the discretization parameter h and the regularization parameters, like the saturation width.

FIGURE 4 The implicit controller structure

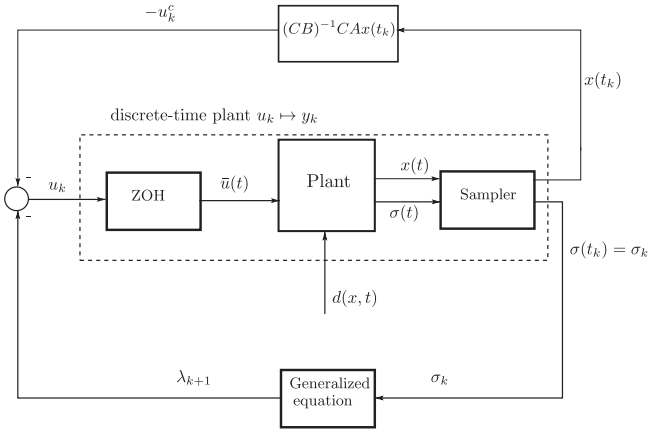

was not pushed forward much because the so-called equivalent controller could not be calculated, since it depends on the disturbance which is unknown.[62,72] As pointed out earlier, the main contribution of Reference 26 and subsequent articles, is to avoid computing directly the equivalent control, and use instead a disturbance-free auxiliary system that yields a solvable GE. The equivalent control idea is also used in Reference 72, forcing $\sigma_{k+1} = 0$, with an explicit Euler approximation of the anticipative terms depending on future states, and adding an integrator to increase the accuracy in the vicinity of the sliding surface by estimating the disturbance from previous states and inputs.

- The issue of measurement noise which may pollute the sliding variable, is a major issue in SMC. Actually the implicit discretization approach is not a miracle cure for that sort of uncertainties. As indicated in Reference 21, one needs to perform an optimal tuning of the filters' parameters in order to guarantee that the closed-loop system keeps good performance. The implicit approach performance slightly decreases when sampling times become too small (see, for instance, [16, figures 3.2.4, 3.2.5] [21, figures 11, 12]): measurement noise may be the cause of this behavior. However, it continues to drastically supersede the explicit approach even for small sampling times. In this setting the use of exact[73] or of algebraic differentiators,[74,75] which behave better than linear filters when they are correctly implemented, may be a promising path.

2.5 | Closed-loop structure and GEs

The discretized closed-loop system (7), or (5) (13), has the general structure in Figure 4, where $x(t)$ is the plant's state, while $\sigma(t)$ is the sliding variable. The variable u_k^c denotes the "equivalent" part of the controller, which is zero in the above scalar case (because $A = 0$). In the above scalar case, one has $x(\cdot) = \sigma(\cdot)$, however, in general these two signals are not the same. The block "Generalized equation" corresponds to (7) (b) (c) (d), equivalently to (13): it computes the variable λ_{k+1} as the "output" of the GE in (12). The discrete-time plant $u_k \mapsto y_k$ usually uses a ZOH method for simulation and real implementation, however, it may be another discretization for the control design (for instance, if the plant is nonlinear, the calculations yielding the exact ZOH method are impossible to make, and in such a case another discrete-time model like Euler may be chosen, see Sections 3.2 and 3.3).

Other ways to formulate equivalently the GE feedback block for the above scalar system are as follows.

- **Variational inequalities:** Starting from (10) and (12) and using the normal cone definition, one finds:

$$\begin{gathered}\text{Find } \tilde{x}_{k+1} \in \mathbb{R} \text{ such that: } \langle \tilde{x}_{k+1}, \tilde{x}_{k+1} - x_k - hv \rangle \geq 0 \quad \text{for all } v \in [-1,1] \\ \text{and} \\ \text{Find } \lambda_{k+1} \in [-1,1] \text{ such that: } \langle h\lambda_{k+1} - x_k, v - \lambda_{k+1} \rangle \geq 0 \quad \text{for all } v \in [-1,1].\end{gathered} \tag{14}$$

These are variational inequalities of the first kind. Let us focus on the second VI in (14). It can be rewritten equivalently as

$$\langle h\lambda_{k+1} - x_k, v - \lambda_{k+1}\rangle + \psi_{[-1,1]}(v) - \psi_{[-1,1]}(\lambda_{k+1}) \geq 0, \text{ for all } v \text{ and } \lambda_{k+1} \in \mathbb{R}.$$

As such this is a VI of the second kind, and the existence of a unique solution is easily deduced from [60, corollary 3]. One can also rely on [59, corollary 2.2.5, theorem 2.3.3] to infer the same conclusion from (12).

- **Complementarity problems:** Another formulation of the GE in (12), is obtained by using complementarity theory tools. To this end, and without going into details on the relationships between normal cones to polyhedral convex sets and complementarity problems (see the introduction for some details), one remarks by inspection that $\mathcal{N}_{[-1,1]}(\lambda_{k+1}) = \{z \in \mathbb{R} \mid z = -\gamma_k^1 + \gamma_k^2,\ 0 \leq \gamma_k^1 \perp \lambda_{k+1} + 1 \geq 0,\ 0 \leq \gamma_k^2 \perp 1 - \lambda_{k+1} \geq 0\}$. Thus, we obtain an equivalent formulation of (12):

$$\begin{cases} \lambda_{k+1} - \frac{x_k}{h} = -z = \gamma_k^1 - \gamma_k^2 \\ 0 \leq \gamma_k^1 \perp \lambda_{k+1} + 1 \geq 0 \\ 0 \leq \gamma_k^2 \perp 1 - \lambda_{k+1} \geq 0, \end{cases} \tag{15}$$

where γ_k^1 and γ_k^2 are two slack variables. From (15), we can obtain the following LCP:

$$0 \leq \Gamma_k \perp \begin{pmatrix} 1 & -1 \\ -1 & 1 \end{pmatrix} \Gamma_k + \begin{pmatrix} \frac{x_k}{h} + 1 \\ -\frac{x_k}{h} + 1 \end{pmatrix} \geq 0, \tag{16}$$

with unknown $\Gamma_k = (\gamma_k^1, \gamma_k^2)^\top$. Notice that same calculations can be led with u_k instead, and we get then the LCP:

$$\begin{gathered} 0 \leq \bar{\Gamma}_k \perp \begin{pmatrix} 1 & -1 \\ -1 & 1 \end{pmatrix} \bar{\Gamma}_k + \begin{pmatrix} -\frac{x_k}{h} + 1 \\ \frac{x_k}{h} + 1 \end{pmatrix} \geq 0 \\ u_k = -\frac{x_k}{h} - \bar{\gamma}_k^1 + \bar{\gamma}_k^2 \end{gathered} \tag{17}$$

The matrix of these LCPs is not full rank, hence it is not a P-matrix. However, one notices that these LCPs have a special structure, because both terms in their right-hand sides cannot vanish simultaneously. They can be solved by inspection with an enumerative algorithm:

Algorithm 2

1. If $-\frac{x_k}{h} < -1$, then $\gamma_1^k = 0$ and $\gamma_2^k = \frac{x_k}{h} - 1 > 0$, and $\lambda_{k+1} = 1$.
2. If $-\frac{x_k}{h} > 1$, then $\gamma_2^k = 0$ and $\gamma_1^k = -\frac{x_k}{h} - 1 > 0$, and $\lambda_{k+1} = -1$.
3. If $-1 \leq -\frac{x_k}{h} \leq 1$, then $\gamma_1^k = \gamma_2^k$ and $\lambda_{k+1} = \frac{x_k}{h}$.

It is noteworthy that Algorithm 2 is via (7) (c) the same as Algorithm 1 which solves the projection (13). *The first conclusion to be drawn from this simple example, is that the implicit controller is the solution to a GE, which can be expressed with various mathematical formalisms: inclusion in a normal cone, variational inequality, projection on a convex set, complementarity problem. This is crucial not only for the well-posedness analysis of the discretized closed-loop system, but also for the controller on-line calculation.*

3 | FIRST-ORDER SLIDING-MODE CONTROL

Let us now turn our attention to first-order SMC, applied to n-dimensional systems.

3.1 | Linear time-invariant *n*-dimensional systems with matched disturbances

This problem was tackled in References 20,25,26. Let us consider the following closed-loop system:

$$\begin{cases} \dot{x}(t) = Ax(t) + Bu(t) + Bd(x(t), t), \quad x(0) = x_0, \\ u(t) = u^c(t) + u^s(t) \\ \sigma(t) = Cx(t) \\ u^s(t) \in -G\ \mathrm{sgn}(\sigma(t)), \end{cases} \tag{18}$$

where notations are the same as in Figure 4, $u^c(\cdot)$ denotes the continuous part of the input, $u^s(\cdot)$ its set-valued part (which we denoted as $u(\cdot)$ in Section 2), and $y(\cdot) = \sigma(\cdot)$, $G \in \mathbb{R}^{p\times p}$ is a control gain, $C \in \mathbb{R}^{p\times n}$ is a control parameter which is part of the control design, $B \in \mathbb{R}^{n\times p}$, $p \geq 1$.

Assumption 1. The $p \times p$ matrix CB is positive definite, the plant matrices A and B are known, the disturbance $d(x,t)$ is unknown with known upperbound M such that $\|d(x,t)\| \leq M$ for all x and t.

The classical first-order SMC is designed, with

$$u^c(t) = -(CB)^{-1}CAx(t)$$

(which guarantees the invariance of the surface $\sigma(t) = 0$ in the unperturbed case —for this reason $u^c(\cdot)$ is sometimes named the *nominal* control law—, and is obtained by setting $\dot{\sigma}(t) = 0$ —for this reason $u^c(\cdot)$ is sometimes named the *equivalent* control law—), and $u^s(t) \in -G\ \mathrm{sgn}(\sigma(t))$, resulting in the set-valued dynamics:

$$\begin{cases} \dot{\sigma}(t) = CBu^s(t) + CBd(x(t), t) \\ \quad u^s(t) \in -G\ \mathrm{sgn}(\sigma(t)), \end{cases} \tag{19}$$

which belongs to the class of set-valued Lur'e systems[5], see Figure 6A. Provided that G is large enough to counteract the disturbance, the system in (19) possesses a globally attractive sliding surface $\{x \in \mathbb{R}^n \mid \sigma(x) = 0\}$.

3.1.1 | Discrete-time SMC design: Calculation of the input

Let us discretize the plant with a ZOH method, with sampling time $h = t_{k+1} - t_k > 0$:

$$x_{k+1} = e^{Ah}x_k + B_h\bar{u}^c(t) + B_h\bar{u}^s(t) + d_k, \quad t \in [t_k, t_{k+1}), \tag{20}$$

with $B_h \overset{\Delta}{=} \int_{t_k}^{t_{k+1}} e^{A(t_{k+1}-\tau)}Bd\tau$, $d_k = \int_{t_k}^{t_{k+1}} e^{A(t_{k+1}-\tau)}Bd(x(\tau),\tau)d\tau$, $\bar{u}^c(t) = u_k^c$ and $\bar{u}^s(t) = u_k^s$ for all $t \in [t_k, t_{k+1})$, define the staircase input. The discrete-time counterpart of the unperturbed version of (19) is proposed as follows:

$$\begin{aligned} \tilde{\sigma}_{k+1} &= \sigma_k + CB_h\ u_k^s \\ u_k^s &\in -G\ \mathrm{sgn}(\tilde{\sigma}_{k+1}) \end{aligned} \tag{21}$$

This is the counterpart of (7) (b) (c) (d), and (20) together with (21) is exactly the generalization of (7). Assume that $G = \mathrm{diag}(g)$, $g > 0$ large enough to counteract the disturbance, which guarantees that (19) is globally finite-time Lyapunov stable [77, chapter 4, section 3]. The extension of Definition 1 is as follows.

Definition 2. The discrete-time sliding mode corresponds to

$$\{(x_k, u_k^s) \mid \tilde{\sigma}_{k+1} = 0 \ \Leftrightarrow\ u_k^s \in (-g, g)^p \ \Leftrightarrow\ \mathcal{N}_{[-g,g]^p}(u_k^s) = \{0\}\}.$$

[5]That is, systems with a static feedback nonlinearity which is set-valued.[2,76]

The counterparts of (12) and of (14) are the inclusion and the VI:

$$\begin{gathered} CB_h u_k^s + \sigma_k \in -\mathcal{N}_{[-g,g]^p}(u_k^s) \\ \Updownarrow \\ \text{Find } u_k^s \in [-g,g]^p \text{ such that } \langle \sigma_k + CB_h u_k^s, v - u_k^s \rangle \geq 0, \quad \text{for all } v \in [-g,g]^p. \end{gathered} \tag{22}$$

In the scalar case of Section 2, $CB_h = h$ and $\frac{1}{h}\mathcal{N}_{[-1,1]}(u_k^s) = \mathcal{N}_{[-1,1]}(u_k^s)$ due to a basic property of cones. Let $CB_h = (CB_h)^\top \succ 0$, then from (22), and using (2), one can express u_k^s as an orthogonal projection, as follows:

$$u_k^s = \text{proj}_{CB_h}\left[[-g,g]^p; -(CB_h)^{-1}\sigma_k\right] \tag{23}$$

which is the counterpart of (13). Once again, general results in References 59,60 could be used to assert existence and uniqueness of u_k^s in view of the monotonicity property of the ingredients in (22) and (21) (the monotonicity of $CB_h \succ 0$, and of the normal cone and of the signum multifunctions). In practice, the solution to (22) can be found solving a quadratic problem, or an LCP solver like Lemke's algorithm,[1] see Section A1 for details on the complementarity problem associated with (22). Let us now pass to the discretized continuous part u_k^c, which was absent in the scalar case of the foregoing sections. It may be computed in different ways at $t = t_k$:[20]

1. *Exact input:* this is calculated as the above "equivalent" continuous-time controller $u^c(\cdot)$, solving $\sigma_{k+1} = Ce^{Ah}x_k + CB_h u_k^c$ with $\sigma_{k+1} = \sigma_k$ [6]: $u_k^c = (CB_h)^{-1}C(I_n - e^{Ah})x_k$, so that using (20):

$$x_{k+1} = (e^{Ah} + B_h(CB_h)^{-1}C(I_n - e^{Ah}))x_k + B_h u_k^s + d_k. \tag{24}$$

2. *Explicit input:* this is a straightforward copy of $u^c(t)$, replacing $x(t)$ by $x(t_k)$, that is: $u_{k,exp}^c = -(CB)^{-1}CAx_k$, so that using (20):

$$x_{k+1} = (e^{Ah} - B_h(CB)^{-1}CA)x_k + B_h u_k^s + d_k. \tag{25}$$

3. *Implicit input:* $u_{k,imp}^c = -(CB)^{-1}CA\bar{x}_{k+1}$, with $\bar{x}_{k+1} = (I_n + B_h(CB)^{-1}CA)^{-1}e^{Ah}x_k$ obtained from (20) with $d_k = 0$ and $u_k^s = 0$, replacing $x(t)$ by $\bar{x}_{k+1}$ in $u^c(t)$, so that using (20):

$$x_{k+1} = (I_n - B_h(CB)^{-1}CA(I_n + B_h(CB)^{-1}CA)^{-1})e^{Ah}x_k + B_h u_k^s + d_k.$$

4. *Midpoint input:* $u_{k,mid}^c = \frac{1}{2}(u_{k,exp}^c + u_{k,imp}^c)$, combining the above two inputs.

The role of $u^c(\cdot)$ is to maintain the invariance of the sliding surface, clearly each one of the above four discretizations preserves approximately this property in a different way. An important point has to be made here: in general, and even in the absence of perturbation, the discretization of $u^c(\cdot)$ implies that $\tilde{\sigma}_{k+1} \neq \sigma_{k+1}$. However, the exact input in item 1 guarantees that $\tilde{\sigma}_{k+1} = \sigma_{k+1}$ when $d(x,t) \equiv 0$, indeed using (24) gives $Cx_{k+1} = Cx_k + CB_h u_k^s$, that is, exactly $\tilde{\sigma}_{k+1}$ in (21). But, the explicit input of item 2 gives from (25): $\sigma_{k+1} = Cx_{k+1} = C(e^{Ah} - B_h(CB)^{-1}CA)x_k + CB_h u_k^s$, that is, not $\tilde{\sigma}_{k+1}$ in (21). Similarly for the other two discretizations in items 3 and 4.

Assumption 2. Let β be the smallest eigenvalue of $\frac{1}{2}(CB_h + (CB_h)^\top)$. The controller gain g satisfies for all $k \in \mathbb{N}$: $\|Cd_k\| \leq g\beta$.

One sees that the condition on the gain G differs from the continuous-time case, where it would be stated as $g > \sup_{t\in\mathbb{R}^+, x\in\mathbb{R}^n} \|d(x,t)\|$.

Remark 3. It is worth noting (item 1) that $\sigma_{k+1} = \sigma_k$ is a fixed point condition which is *the* discrete-time counterpart of $\dot{\sigma}(t) = 0$, quite different from imposing $\sigma_{k+1} = 0$ which is a dead-beat input condition, yielding $u_k^{db} = -(CB_h)^{-1}Ce^{Ah}x_k$ instead of u_k^c. The exact input in item 1 satisfies $u_k^c = -h(CB_h)^{-1}CAx_k + (CB_h)^{-1}\mathcal{O}(h^2)$, while $u_k^{db} = -(CB_h)^{-1}C(I_n + Ah) +$

[6] From [20, lemma 6], one has $CB_h \succ 0$ provided h is small enough.

$(CB_h)^{-1}\mathcal{O}(h^2)$. Both inputs clearly possess quite different behaviors when $h \ll 1$, as u_k^{db} grows unbounded when h vanishes, while u_k^c does not.

3.1.2 | Discrete-time SMC design: Closed-loop analysis

We therefore have at our disposal four discretizations of $u^c(\cdot)$ and two discretizations of $u^s(t)$. They can be combined as wanted, though clearly the closed-loop system will be influenced significantly. Let us now state a recapitulating theorem, similar to Theorem 1.

Theorem 2. [20, lemma 7, propositions 1, 2, 3, 4, lemmae 9, 10, 11, corollary 1] *Let Assumption 1 hold, and let $h > 0$ be small enough so that $CB_h > 0$.*

1. *The GEs (21) and (22) always have a unique solution, hence u_k^s is uniquely defined at each step $k \geq 0$.*
2. *Let u_k^c be the exact input of item 1. Then in the absence of disturbance, $\tilde{\sigma}_{k+1} = \sigma_{k+1} = Cx_{k+1}$ and (21) has a unique equilibrium $\sigma^* = 0$ that is globally finite-time Lyapunov stable, with Lyapunov function $V(\sigma_k) = g\ \|\sigma_k\|_1$. Let us consider a nonzero matched perturbation, and let Assumption 2 hold. Then:*
   (a) *The sliding surface Σ_d is attained after a finite number of steps.*
   (b) *During the sliding-mode phase on Σ_d, we have $u_{k+1}^s = -(CB_h)^{-1}Cd_k$, that is, the control compensates for the ZOH perturbation with one step delay.*
   (c) *The staircase input $\bar{u}^s(\cdot)$ converges toward its continuous-time counterpart $u^s(\cdot)$ during sliding-mode phases, with same assumptions on the perturbation as in Theorem 1 item 3.*
   (d) *The controller $\bar{u}^s(\cdot)$ is insensitive to the gain G increase when the system is in the sliding mode.*
3. *Consider (20) and let $u^s(\cdot) \equiv 0$ and $d(x,t) \equiv 0$. The accuracy measured by the error $\Delta\sigma_k \stackrel{\Delta}{=} \sigma_{k+1} - \sigma_k$ depends on the discretization of the continuous input $u^c(\cdot)$ discretization:*
   (a) *with $u_{k,exp}^c$ or $u_{k,imp}^c$, $\Delta\sigma_k = \mathcal{O}(h^2)$,*
   (b) *with $u_{k,m}^c$, $\Delta\sigma_k = \mathcal{O}(h^3)$.*
4. *Let $\epsilon_k \stackrel{\Delta}{=} \|\sigma_{k+1}\|$ be the discretization error when $\|\sigma_k\|$ is small enough.*
   (a) *Consider (20) with $d_k = 0$ for all $k \geq 0$. Suppose that the closed-loop state is in an $\mathcal{O}(h^2)$-neighborhood of the sliding surface Σ_d at t_k, that is, $\sigma_k = \mathcal{O}(h^2)$. If $u_k^s = u_{k,epl}^s = -G\ \mathrm{sgn}(\sigma_k)$, then $\epsilon_k = \mathcal{O}(h)$ and the system exits the $\mathcal{O}(h^2)$-neighborhood.*
   (b) *Let the system (20) be in Σ_d. If $d_k = 0$ for all $k \geq 0$, and if $u_k^s = u_{k,imp}^s$ in (23), then ϵ_k has the same order as $\Delta\sigma_k$ in the foregoing item 3 (a) and (b). If $d_k \neq 0$, then the order is 1 due to the perturbation.*

The convergence result in item 2 (c) proves that the implicit input, does represent a good approximation of the set-valued continuous-time input. Convergence results will also be shown in Sections 3.2 and 3.3 in more complex cases. But, item 2 (d) proves that the implicit scheme has very good properties not only as h approaches 0, but when it takes positive values (and experimental results show that such positive values could be large in practice). The result of item 3 is a measure of the error introduced by the discretization of $u^c(\cdot)$, on the invariance property guaranteed by $u^c(\cdot)$ on the sliding surface in the unperturbed case. The result of item 4 (b), shows that the implicit method on the set-valued part of the input, yields in the absence of perturbation and when combined with a midpoint continuous input discretization, a precision in h^3. The proof of these assertions is in Reference 20. It is also shown in Reference 20 (mainly through simulations) that the explicit discretization $u_{k,\exp}^c$ can destabilize the closed-loop system, even if the implicit input u_k^s in (23) is applied. Such instability phenomenon due to an explicit discretization is also shown in Reference 54 on a differentiator example.

- The conclusions drawn for the scalar case of Sections 2 and 2.5, extend to n-dimensional systems with matched disturbances, under the positive definiteness of the $p \times p$ matrices CB and CB_h. However, the discretization of the continuous part of the input (the equivalent, or nominal, part of the controller), plays an important role in the stability and the accuracy of the closed-loop system.
- The monotonicity property plays a major role in the existence and uniqueness of the controller at each step k (item 1 in Theorem 2), that is, in the solvability with uniqueness of the feedback block in Figure 4. This is used for more general set-valued controllers in References 31 (Section 3.3) and 32 (Section 3.2).

It is noteworthy that the Lyapunov stability results of item 2 in Theorem 2, concern only the reduced order p system (21). The stability of the complete closed-loop system with dimension n constructed from (20), is not shown yet. One may expect that if C is chosen such that the continuous-time closed-loop system is stable in some sense, then provided solutions to the discretized system converge toward those of the continuous-time one, the stability properties are preserved after discretization, at least for small enough $h>0$. We may, however, be interested to get results for positive h not "small enough," a concept that has mainly a mathematical interest, but may lack of practical interest. Results in this direction are given in Section 3.2.

3.2 | Linear time-invariant n-dimensional systems with matched disturbances and parameter uncertainty

In this section, the robust control problem is made further complex,[32] by considering parameter uncertainties in (18), that is:

$$\dot{x}(t) = (A + \Delta_A(x(t),t))x(t) + Bu(t) + Bd(x(t),t), \quad x(0) = x_0, \tag{26}$$

where A is known, and $\Delta_A(x,t)$ contains all uncertainties related to the transition matrix, and is nonlinear, time-varying. We are therefore placing ourselves in a quite general robust control framework.

3.2.1 | Continuous-time SMC design

Throughout this section, the following assumption holds true.

Assumption 3. **(i)** The pair (A,B) is stabilizable. **(ii)** The matrix $B \in \mathbb{R}^{n\times p}$, where $p<n$, has full column rank. **(iii)** For all $t\in[0,+\infty)$ the uncertainty matrix-function $\Delta_A(t,\cdot)$ is locally Lipschitz continuous and satisfies $\Delta_A(t,x)\Lambda\Delta_A^\top(t,x) \prec I_n$ for all $x\in\mathbb{R}^n$ and for some known $n\times n$ matrix $\Lambda=\Lambda^\top \succ 0$. **(iv)** For all $t\in[0,+\infty)$ the external disturbance $d(t,\cdot)$ is locally Lipschitz continuous. Moreover, there exists $M>0$ such that $\sup_{t\geq 0, x\in\mathbb{R}^n}\|d(t,x)\| \leq M < +\infty$.

Just as we did in Section 3.1, we split the controller in a continuous (nominal, equivalent) part $u^c(\cdot)$ and a set-valued part $u^s(\cdot)$. The sliding variable is designed from an optimization process as $\sigma = Cx$, $C\in\mathbb{R}^{p\times n}$, CB nonsingular, and $C=(B^\top P^{-1}B)^{-1}B^\top P^{-1}$ for some $P=P^\top\succ 0$. The overall controller structure is depicted in Figure 5, where the lower feedback system is the design and analysis model, while the upper diagram represents the implementation via a ZOH method. The "generalized equation" blocks share the same structure. The overall control synthesis makes sense, since as we shall see later, the "error" between the "output" of the real closed-loop system, and that of the design system, becomes arbitrarily small when the sampling period decreases.

It is noteworthy that the only difference between the classical explicit controller, and the implicit one, lies in the block "Generalized equation" in Figures 4 and 5.

The continuous part $u^c(\cdot)$ of the controller (the nominal, or the equivalent control), is chosen as in Section 3.1: $u^c(t) = -(CB)^{-1}CAx(t) = -CAx(t)$. The control synthesis is made in Reference 32, starting from a state variable change $z=Mx$, $z=(z_1^\top,\sigma^\top)^\top$, $M\in\mathbb{R}^{n\times n}$ full rank, which allows one to rewrite the system (26) as:

$$\begin{aligned} &(i)\ \ \dot{z}_1(t) = B_\perp^\top(A+\hat{\Delta}_A(t,z(t)))PB_\perp(B_\perp^\top PB_\perp)^{-1}z_1(t) + B_\perp^\top(A+\hat{\Delta}_A(t,z(t)))B\sigma(t)\\ &(ii)\ \ \dot{\sigma}(t) = u^s(t) + \hat{d}(t,z(t)) + \hat{d}_m(t,z(t)), \end{aligned} \tag{27}$$

where, $\hat{\Delta}_A(t,z) \overset{\Delta}{=} \Delta_A(t,T^{-1}z)$, $\hat{d}(t,z) \overset{\Delta}{=} d(t,T^{-1}z)$, $\hat{d}_m(t,z) \overset{\Delta}{=} (B^\top P^{-1}B)^{-1}B^\top P^{-1}\Delta_A(t,M^{-1}z)M^{-1}z$, $B_\perp\in\mathbb{R}^{n\times(n-p)}$ is an orthogonal complement of B. The advantage of the state variable change, is that the dynamics is split into two parts: one that is unperturbed, and the other one is the sliding variable dynamics that is disturbed. This is quite nice for the SMC design, because in general, parametric uncertainties could create unmatched perturbations. Both subdynamics are coupled, however. The set-valued controller is designed as follows:

$$-u^s(t) \in K\sigma(t) + g(z(t))\mathcal{M}(\sigma(t)), \tag{28}$$

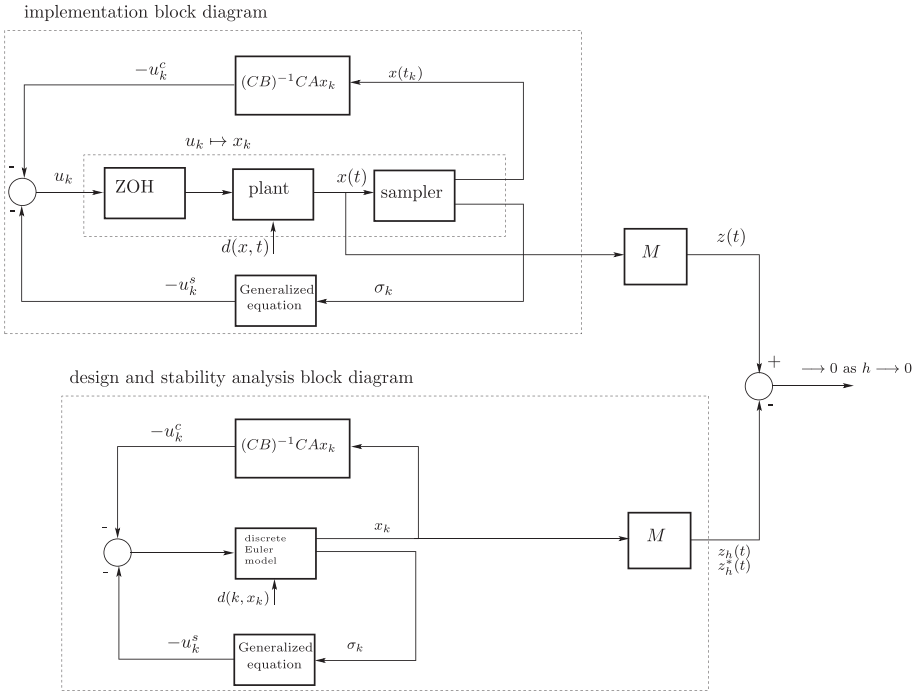

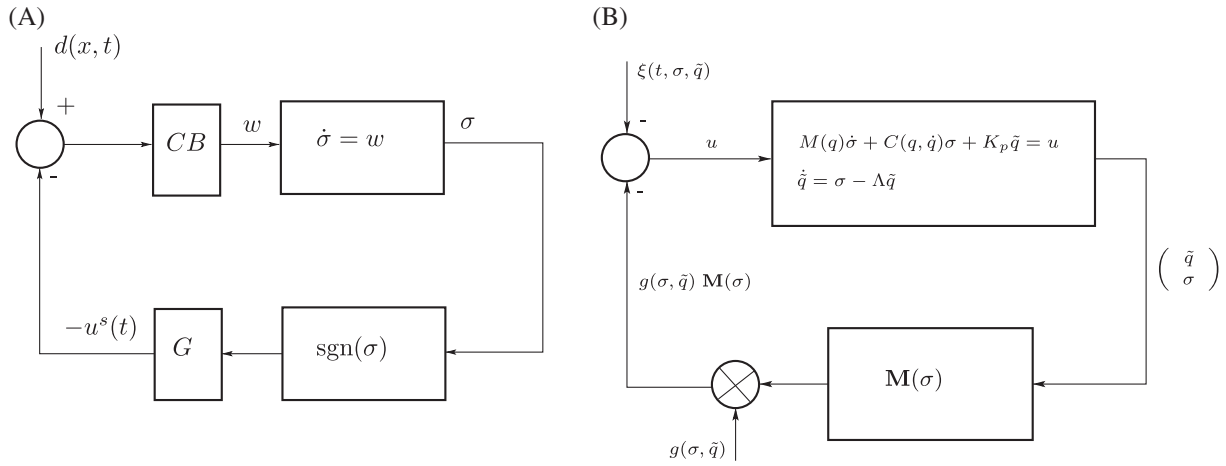

FIGURE 5 The implicit digital controller structure

FIGURE 6 The closed-loop set-valued Lur'e system structure

where $\mathbb{R}^{p\times p} \ni K \succ 0$, $g : \mathbb{R}^n \to \mathbb{R}_+$ is a positive function depending on the system state z, and $\mathcal{M} : \mathbb{R}^m \rightrightarrows \mathbb{R}^m$ is a set-valued maximal monotone operator (thus, $(K + g\mathcal{M})(\cdot)$ is maximal monotone for all constant $g > 0$). The gain K and the matrix P are the solution to a specific LMI involving Λ (see Assumption 3 **(iii)**). The closed-loop system is made of (27) with (28). The sliding variable dynamics in (27) *(ii)* (28) possesses the same feedback structure as in Figure 6A.

Remark 4. Considering maximal monotone operators in (28), allows one to enlarge the set of multivalued controllers $u^s(t)$. It encompasses the signum multifunction as in (18).

It is proved in [32, theorems 22, 24, 25, corollary 26], that the closed-loop system (27) (28) possesses, under some conditions on K, P, $\gamma(\cdot)$, $\mathrm{dom}(\mathcal{M}) = \mathbb{R}^p$, and under Assumption 3, a unique solution in the Caratheodory sense[7], for any initial conditions, with a unique equilibrium that is globally Lyapunov stable, while finite-time stability occurs for

[7]The proof does not follow from Filippov's theory (due to maximal monotone set-valued terms), nor from maximal monotone differential inclusions (due to the presence of $\gamma(z)$ in (28)), and thus requires some careful developments [32, appendix A].

the σ-dynamics in (27). On the sliding surface $\Sigma = \{x \in \mathbb{R}^n \mid Cx = 0\}$, the controller $u^s(\cdot)$ compensates exactly for the equivalent disturbance, as seen from (27).

3.2.2 | Discrete-time SMC design: Calculation of the input

In the context of this article, the first step is to choose a discretization for the plant model (26). Computing a ZOH discretization is impossible, because the plant is nonlinear. Let us choose an explicit Euler discretization:

$$x_{k+1} = (I_n + hA)x_k + hBu_k + Bd(k, x_k) + h\Delta_A(k, x_k)x_k. \tag{29}$$

The nominal input u_k^c is calculated as the exact input, from $\sigma_{k+1} = \sigma_k$ and (29) without perturbation and uncertainty: $u_k^c = \frac{1}{h}(CB)^{-1}(\sigma_k - C(I_n + hA)x_k)$. The set-valued input is chosen as $-u_k^s \in g\ \mathcal{M}(\sigma_{k+1})$, with a constant gain $g > 0$. After some calculations, one obtains the discrete-time system:

$$\begin{cases} z_{k+1}^1 = B_\perp^\top (I_n + hA + h\hat{\Delta}_A(k, z_k))XB_\perp (B_\perp^\top XB_\perp)^{-1} z_k^1 + B_\perp^\top (I_n + hA + h\hat{\Delta}_A(k, z_k))B\ \sigma_k \\ \sigma_{k+1} = \tilde{\sigma}_{k+1} + h(\hat{d}(k, z_k) + C\hat{\Delta}_A(k, z_k)M^{-1}z_k), \end{cases} \tag{30}$$

where $C = (B^\top X^{-1}B)^{-1}B^\top X^{-1}$, $X = X^\top > 0$ satisfies some suitable LMI recalled in Theorem 3 below (using Assumption 3 **(i)**), and one sets:

$$\begin{aligned} \tilde{\sigma}_{k+1} &= \sigma_k + hu_k^s \\ u_k^s + K\tilde{\sigma}_{k+1} &\in -g\ \mathcal{M}(\tilde{\sigma}_{k+1}) \end{aligned} \tag{31}$$

The framed system in (31) is quite similar to (21), taking into account that $CB = I_p$. It represents the GE to be solved at each step t_k to calculate u_k^s. The dummy variable $\tilde{\sigma}_{k+1}$ is as in Section 3.1 and is used to define the discrete-time sliding surface Σ_d.

Remark 5. It is clear that the state variable $x_k \neq x(t_k)$ where $x(t)$ is the solution to the plant's dynamics (26), and similarly $z_k^1 \neq z_1(t_k)$, $\sigma_k \neq \sigma(t_k)$. In all rigor we should denote the variables of the lower feedback system in Figure 5, as $\tilde{x}_k$, $\tilde{z}_k^1$ and $\tilde{\sigma}_k$ to highlight this fact. We, however, prefer to keep the used notation and to keep the notation $\tilde{\cdot}$ for the dummy "unperturbed" sliding variable $\tilde{\sigma}_{k+1}$, to be consistent with the foregoing sections.

The input u_k^s is nonanticipative, and an extension of (23) is as follows:

$$u_k^s = -\frac{1}{h}(I_p - (I_p + h\ (K + g\mathcal{M}))^{-1})(\sigma_k) \tag{32}$$

In Convex analysis, the mapping $J_{\mathcal{M}}^h(\cdot) \stackrel{\Delta}{=} (I_p + h\ \mathcal{M})^{-1}(\cdot)$ is called the *resolvent* with index h associated with the maximal monotone map $\mathcal{M}(\cdot)$, and $\mathcal{M}_{\mathcal{M}}^h(\cdot) \stackrel{\Delta}{=} \frac{1}{h}(I_p - (I_p + h\ \mathcal{M})^{-1})(\cdot)$ is its Yosida approximation, hence $u_k^s = -\mathcal{M}_{K+g\mathcal{M}}^h(\sigma_k)$. It is single-valued, Lipschitz continuous and nonexpansive. The point is here: how to calculate such a resolvent in practice, that is, how to solve the GE block in Figure 5 ? Let us explain this now. First, it is convenient to compute $\tilde{\sigma}_{k+1}$ from (31). From (32) it follows that $(I_n + hK)\tilde{\sigma}_{k+1} - \sigma_k \in -hg\mathcal{M}(\tilde{\sigma}_{k+1})$ or, equivalently, for $\theta > 0$,

$$\begin{gathered} \theta\sigma_k - \theta(I_p + hK)\tilde{\sigma}_{k+1} \in \theta hg\ \mathcal{M}(\tilde{\sigma}_{k+1}) \Leftrightarrow \theta\sigma_k + (I_p - \theta I_p - \theta hK)\tilde{\sigma}_{k+1} \in (I_p + \theta hg\ \mathcal{M})(\tilde{\sigma}_{k+1}) \\ \Updownarrow \\ \tilde{\sigma}_{k+1} = J_{\mathcal{M}}^{\theta hg}(\theta\sigma_k + (I_p - \theta(I_p + hK))\tilde{\sigma}_{k+1}). \end{gathered} \tag{33}$$

The key is that for $\theta > 0$ small enough, the right-hand side of the last equation in (33) is a contraction, and the method of successive approximations can be used to solve this fixed point problem. We shall see an example of such solver in

Section 3.3. More details are also provided in Section D1. Once $\tilde{\sigma}_{k+1}$ has been computed from (33), then u_k^s can be obtained using (31).

Example 1. Let $\mathcal{M}(\cdot) = \text{sgn}(\cdot)$ as in Section 2, then $J^h_{\mathcal{M}}(x) = (1 + h\ \text{sgn})^{-1}(x) = \begin{cases} x - h\ \text{sgn}(x) & \text{if } |x| > h \\ 0 & \text{if } |x| \leq h \end{cases}$, and $\mathcal{M}^h(x) = \frac{1}{h}(1 - J^h_{\mathcal{M}})(x) = \begin{cases} \text{sgn}(x) & \text{if } |x| > h \\ \frac{x}{h} & \text{if } |x| \leq h \end{cases}$. We recover the saturation function as the Yosida approximant of the signum multifunction, coherently with the discussion in Section 2.4. Other examples of mappings are given in References 31,32,78, like $\mathcal{M}(\cdot) = \partial f(\cdot)$ with $f(x) = \max_i |x_i| = \|x\|_\infty, f(x) = \sum_{i=1}^p |x_i| = \|x\|_1||, f(x) = \|x\|_2, f(x) = \psi_K(x)$ with K a closed convex nonempty set.

Example 2. Let us choose $f(\sigma) = \|\sigma\|_\infty$ and $\mathcal{M}(\sigma) = \partial f(\sigma)$. Then $\mathcal{M}^h(\sigma) = \text{proj}[\mathbb{B}^1_p; \frac{\sigma}{h}]$, where $\mathbb{B}^1_p = \{x \in \mathbb{R}^p \mid \|x\|_1 \leq 1\}$. Using (32), we find that in this case the set-valued controller is an extension of both (13) and (23).

3.2.3 | Discrete-time SMC design: Closed-loop stability analysis

Let us now state a recapitulating theorem:

Theorem 3. [32, lemma 34, corollary 35, theorem 37, corollary 40, section 4.5] *Let the matrices X and K satisfy the LMIs in Section B1, and $\{0\} \in \text{int}(\mathcal{M}(0))$. Let also Assumption 3 hold, and CB be full rank. Then, the following holds true:*

1. *The subsystem $z^1_{k+1} = B_\perp^\top(I_n + hA + h\hat{\Delta}_A(k, z_k))XB_\perp(B_\perp^\top XB_\perp)^{-1}z^1_k$, obtained by setting $\sigma_k = 0$ in (30), is globally asymptotically stable with Lyapunov function $V(z^1_k) = \frac{1}{2}z^{1T}_k(B_\perp^\top XB_\perp)^{-1}z^1_k$.*
2. *$\sigma_k \in hg\mathcal{M}(0)$ for some $k \in \mathbb{N} \Leftrightarrow \tilde{\sigma}_{k+1} = 0$. In addition, if for some $k_0 \in \mathbb{N}$, $\tilde{\sigma}_{k_0+1} = 0$, then $\tilde{\sigma}_{k_0+n} = 0$ for all $n \geq 1$, whenever $\hat{d}(k, z_k) + C\hat{\Delta}_A(k, z_k)M^{-1}z_k \in g\ \mathcal{M}(0)$ for all $k \geq k_0$.*
3. *Let the matched disturbance $\hat{d}(k, z_k) + C\hat{\Delta}_A(k, z_k)M^{-1}z_k \in g\ \mathcal{M}(0)$ for all $k \geq k^*$ for some $0 < k^* < +\infty$. Then, in the discrete-time sliding phase the control input u_k^s satisfies $u_k^s = \hat{d}_{k-1} + C\hat{\Delta}_A(k, z_k)M^{-1}z_k$.*
4. *During the discrete-time sliding phase, the controller u_k^s is independent of the gain g.*
5. *Let $L_c \subset \mathbb{R}^n$ be the compact set $L_c \stackrel{\Delta}{=} \left\{ \begin{pmatrix} z^1 \\ \sigma \end{pmatrix} \in \mathbb{R}^n \mid \frac{1}{2}z^{1\top}(B_\perp^\top XB_\perp)^{-1}z^1 + \frac{1}{2}\sigma^\top\sigma \leq c^2 \right\}$. Then, for any initial condition $z_0 = \begin{pmatrix} z^{1\top}_0 & \sigma^\top_0 \end{pmatrix}^\top$ which lies in L_c for some $c > 0$, there exists $h > 0$ small enough and fixed such that for $g > 0$ satisfying $g\varepsilon = \rho + W + (\sqrt{\overline{\kappa}} + 2h\|K\|^2)\overline{z}$, where $\overline{z} \stackrel{\Delta}{=} \max\{\|z\|, z \in L_c\}$ and $\rho > 0$ is an arbitrary constant, $\overline{\kappa}$ is such that $\|C\hat{\Delta}_A(k, z_k)M^{-1}z_k\| \leq \sqrt{\overline{\kappa}}\|z_k\|$, the origin of the discrete-time closed-loop system (30) (31) is semiglobally practically stable. In fact, for any initial condition $z_0 \in L_c$ the trajectories converge to a ball $c^*_h\mathbb{B}_n$ where $c^*_h < c$ and $\lim_{h\to 0} c^*_h = 0$.*
6. *Let the gain $g > 0$ satisfy $g\varepsilon = \rho + (1 + \alpha)(r + W + \sqrt{\overline{\kappa}}\overline{z}) + \max\left\{ 2h\|K\|^2\overline{z}, \frac{(W+\sqrt{\overline{\kappa}}\overline{z})^2}{r} \right\}$ for some constants $\rho, r > 0$ and $\varepsilon > 0$ such that $\varepsilon\mathbb{B}_p \subset \mathcal{M}(0)$. Then, there exists $k_0 > 0$, $k_0 = k_0(\alpha, r)$, which is finite and such that the variable $\tilde{\sigma}_{k_0} = 0$. Moreover, $\tilde{\sigma}_k = 0$ for all $k \geq k_0$, that is, the discrete-time sliding phase is reached in a finite number of steps.*
7. *Consider the following piecewise continuous functions: $z^1_h(t) \stackrel{\Delta}{=} z^1_k + \frac{t-t_k}{h}(z^1_{k+1} - z^1_k)$, $\sigma_h(t) \stackrel{\Delta}{=} \sigma_k + \frac{t-t_k}{h}(\sigma_{k+1} - \sigma_k)$ for all $t \in [t_k, t_{k+1}]$, and the step functions $\tilde{\sigma}^*_h(t) \stackrel{\Delta}{=} \tilde{\sigma}_{k+1}$, $\sigma^*_h(t) \stackrel{\Delta}{=} \sigma_k$, $z^{1*}_h(t) \stackrel{\Delta}{=} z_k$, for all $t \in (t_k, t_{k+1}]$. Then $z^1_h \to z^1$, $\sigma_h \to \sigma$, $z^{1*}_h \to z^1$, $\sigma^*_h \to \sigma$, strongly in $\mathcal{L}_2([0, t]; \mathbb{R}^{n-p})$ or $\mathcal{L}_2([0, t]; \mathbb{R}^p)$ for any $t > 0$. Moreover, (z^1, σ) is a solution to the differential inclusion (27) (28).*

It is noteworthy that the stability of the complete system (30) (31) (and not just that of the reduced order sliding variable (31) as in Theorem 2) is proved in Theorem 3 item 5, with a Lyapunov function that is the same as the one used in the continuous-time case. Item 3 in Theorem 3 means, as in Section 3.1, that the set-valued controller compensates for the disturbance with a delay of one step h. The value of c^*_h in item 5, is given explicitly in [32, equation (98)]. The value of $\overline{\kappa}$ in items 5 and 6, is explicitly given in [32, equation (42)]. Items 1 to 6 concern the analysis and design model of the plant, using the Euler discretization (29). However, item 7 proves that the lower feedback system in Figure 5, is a good approximation of the upper one. This is confirmed by numerical simulations where the upper block in Figure 5 is simulated.

- The system analyzed in this section is more complex than that of Section 3.1, because it is nonlinear, and with parametric uncertainties. Nevertheless, the results in Theorem 3 prove that the implicit digital implementation of the SMC, guarantees strong closed-loop properties.
- Simulation results in Reference 32 with $n=5$ and $p=2$, indicate that input and output chattering are drastically decreased with the implicit method, which also tolerates large sampling times $h>0$ without deteriorating too much the closed-loop performance.
- The GE to be solved to compute u_k^s at each step, can in general be solved with a successive approximations method, or explicitly in certain cases (in a way similar to the simpler systems in Sections 2 and 3.1).
- Once again, maximal monotonicity appears as a key property for the existence and the uniqueness of the set-valued input u_k^s (discrete-time system's well posedness), and for the continuous-time system's well posedness.
- As alluded to in Section 2.4, the implicit method performs a kind of regularization *after* the discretization. This is visible again in (32) through the use of Yosida approximations.

3.2.4 | Experimental results

Extensive experimental results have been reported for the above SMC in References 15,16,20 on two laboratory experimental setups: an electropneumatic system,[15,16] and an inverted pendulum on a cart.[20] They confirm most of the properties in the list in Section 1: almost suppression of input and output chattering **P1**, insensitivity of the controller to the gain magnitude during the sliding mode **P10** (which is henceby experimentally proved to exist, **P9**), allows for large sampling times while keeping good performances **P3**, all of this without changing the controller's structure **P2**. Other experimental results can be found in Kikuuwe et al articles (see the introduction for a list), which all confirm chattering suppression.

3.3 | Lagrangian systems with matched disturbances and parameter uncertainty

The systems in the foregoing section are nonlinear due to uncertainties. Let us turn our attention now to systems which are intrinsically nonlinear, Lagrange systems:

$$M(q(t))\ddot{q}(t)+C(q(t),\dot{q}(t))\dot{q}(t)+G(q(t))+F(t,q(t),\dot{q}(t))=\tau(t), \tag{34}$$

where $q,\dot{q},\ddot{q}\in\mathbb{R}^n$ are the vectors of generalized positions, velocities and accelerations, respectively. The matrix $\mathbb{R}^{n\times n}\ni M(q)=M(q)^\top>0$, denotes the inertia matrix of the system. The term $C(q,\dot{q})\dot{q}\in\mathbb{R}^n$ represents the centripetal and Coriolis forces acting on the system. The term $G(q)\in\mathbb{R}^n$ is the vector of gravitational forces. The vector $F(t,q,\dot{q})\in\mathbb{R}^n$ accounts for unmodeled dynamics and external disturbances. Finally, the vector $\tau\in\mathbb{R}^n$ represents the control input forces. We assume that $C(q,\dot{q})$ is defined using the so-called *Christoffel's symbols*, so that the skew-symmetry property of the matrix $\dot{M}(q)-2C(q,\dot{q})$ holds [76, lemma 6.17].

3.3.1 | Continuous-time SMC design

Just as we did in the foregoing section, let us make a brief summary of the continuous-time SMC design and analysis, before passing to the digital framework. We suppose that the inertial parameters are not known exactly, so that estimates $\hat{M}(q)$, $\hat{C}(q,\dot{q})$ and $\hat{G}(q)$ of the matrices $M(q)$, $C(q,\dot{q})$ and $G(q)$ have to be used in the controller. As we shall see, the proposed controller shares many similarities with that in Section 3.2. Let us set:

$$\begin{cases} u^c(q,\dot{q},t)=\hat{M}(q)\ddot{q}_{\mathrm{r}}+\hat{C}(q,\dot{q})\dot{q}_{\mathrm{r}}+\hat{G}(q)-K_p\tilde{q} \\ -u^s(\sigma,\tilde{q})\in g(\sigma,\tilde{q})\ \mathcal{M}(\sigma) \\ \tau(q,\dot{q},t)=u^c(q,\dot{q},t)+u^s(\sigma,q,t), \end{cases} \tag{35}$$

where: $\tilde{q} = q - q_d$, $q_d(\cdot)$ is a desired trajectory, $\sigma = \dot{\tilde{q}} + \Lambda\tilde{q}$, $-\Lambda$ is Hurwitz, $K_p = K_p^\top \succ 0$, $K_p\Lambda = \Lambda^\top K_p \succ 0$, $\dot{q}_r = \dot{q}_d - \Lambda\tilde{q}$, the gain $g(\cdot,\cdot)$ is locally Lipschitz continuous, $\mathcal{M}(\cdot)$ is a maximal monotone operator. The control objective is the tracking of the desired trajectory $q_d(\cdot)$ for any initial conditions. The next assumption gathers some classical assumptions on boundedness of the inertial terms, on regularity of the dynamics, and a property of the set-valued term.

Assumption 4. **(i)** $0 < k_1 \leq \| M(q)\|_m \leq k_2$, $\|C(q,\dot{q})\|_m \leq k_C\|\dot{q}\|$, $\|G(q)\| \leq k_G \| q\|$, $\|F(t,q,\dot{q})\| \leq k_F$, for some known positive constants k_1, k_2, k_C, k_G and k_F, **(ii)** there exists a constant k_3 such that, for all $x, y \in \mathbb{R}^n$, $\|M(x) - M(y)\|_m \leq k_3 \| x - y\|$, **(iii)** the function $h : \mathbb{R}^n \times \mathbb{R}^n \to \mathbb{R}^n$ defined by $h(x_1,x_2,x_3) \stackrel{\Delta}{=} C(x_1,x_2)x_3$ is locally Lipschitz continuous, **(iv)** the function $F(t,x_1,x_2)$ is continuous in t and uniformly locally Lipschitz continuous in (x_1,x_2) (ie, the Lipschitz constant is independent of t), **(v)** the function $G(\cdot)$ is Lipschitz continuous and satisfies $0 = G(0) \leq G(x)$ for all $x \in \mathbb{R}^n$, **(v)** let $\mathcal{M}(\cdot) = \partial\Phi(\cdot)$, then $\Phi : \mathrm{dom}(\Phi) = \mathbb{R}^n \to \mathbb{R} \cup \{+\infty\}$ is a convex proper lower semicontinuous function, $0 = \Phi(0) \leq \Phi(w)$ for all $w \in \mathbb{R}^n$, and $0 \in \mathrm{int}(\partial\Phi(0)) \Leftrightarrow$ there exists $\alpha > 0$ such that $\Phi(\cdot) \geq \alpha\| \cdot \|$, **(vi)** $0 < \hat{k}_1 \leq \|\hat{M}(q)\|_m \leq \hat{k}_2$, $\|\hat{C}(q,\dot{q})\|_m \leq \hat{k}_C\|\dot{q}\|$, $\|\hat{G}(q)\| \leq \hat{k}_G\|q\|$, for all $(t,q,\dot{q}) \in \mathbb{R}_+ \times \mathbb{R}^n \times \mathbb{R}^n$ and some known positive constants $\hat{k}_1$, $\hat{k}_2$, $\hat{k}_C$ and $\hat{k}_G$, **(vii)** the estimated matrices satisfy the skew-symmetry property $\frac{d}{dt}\hat{M}(q(t)) = \hat{C}(q(t),\dot{q}(t)) + \hat{C}^\top(q(t),\dot{q}(t))$.

The estimated matrices and vectors are therefore supposed to respect the structure of the real ones and to keep their fundamental properties, but with approximate inertia parameters. The closed-loop system (34) (35) can be rewritten equivalently as follows:

$$\begin{cases} M(q)\dot{\sigma} + C(q,\dot{q})\sigma + K_p\tilde{q} + \xi(t,\sigma,\tilde{q}) \in -g(\sigma,\tilde{q})\ \mathcal{M}(\sigma) \\ \dot{\tilde{q}} = \sigma - \Lambda\tilde{q}, \quad \sigma(0) = \sigma_0,\ \tilde{q}(0) = \tilde{q}_0, \\ \xi(t,\sigma,\tilde{q}) = F(t,q,\dot{q}) + \Delta M(q)\ddot{q}_r + \Delta C(q,\dot{q})\dot{q}_r + \Delta G(q), \end{cases} \tag{36}$$

where $\Delta M(q) = M(q) - \hat{M}(q)$, $\Delta C(q,\dot{q}) = C(q,\dot{q}) - \hat{C}(q,\dot{q})$ and $\Delta G(q) = G(q) - \hat{G}(q)$. The system in (36) is reminiscent of the Slotine and Li algorithm, and it possesses the set-valued Lur'e system feedback structure[2] depicted in Figure 6B.

Most importantly for the control design, the equivalent disturbance satisfies $\|\xi(t,\sigma,\tilde{q})\| \leq \beta(\sigma,\tilde{q})$, where $\beta(\sigma,\tilde{q}) = c_1 + c_2\|\sigma\| + c_3\|\tilde{q}\| + c_4\|\tilde{q}\|\|\sigma\| + c_5\|\tilde{q}\|^2$, for known positive constants c_i, $i = 1, \dots, 5$. Despite $\mathcal{M}(\cdot)$ is maximal monotone, the well posedness of (36) cannot be inferred directly from general results on maximal monotone differential inclusions, due to the presence of both $M(q)$ and $g(\sigma,\tilde{q})$ that destroy the monotonicity in general.[79] Under suitable condition on $g(\cdot,\cdot)$ and α in Assumption 4 **(v)**, the existence of solutions to (36) is proved in [31, theorem 1] (see also Reference 80) with continuous $\sigma(\cdot)$ and $\tilde{q}(\cdot)$, $\dot{\sigma}(\cdot)$ essentially bounded on bounded sets, and with uniqueness in case of constant gain $g > 0$. The robust stability is also shown, with global stability of the origin and global convergence of $\sigma(\cdot)$ to zero in finite-time for state-dependent $g(\sigma,\tilde{q})$, and semiglobal asymptotic stability with constant $g > 0$. One uses the Lyapunov-like function $V(\sigma,t) = \frac{1}{2}\sigma^\top M(q(t))\sigma$, or $H(\sigma,\tilde{q}) = \frac{1}{2}\sigma^\top M(q(t))\sigma + \frac{1}{2}\tilde{q}^\top K_p\tilde{q}$.

Remark 6. In the context of tracking control of Lagrangian systems, the sliding variable $\sigma(\cdot)$ is naturally of dimension n and the sliding surface of codimension n.

3.3.2 | Discrete-time SMC design: Calculation of the input

Once the continuous-time design has been done, the next step is to design the digital controller. As we shall see, this shares some common features with the material of Section 3.2, but Lagrangian systems possess their own features as well. Mimicking (29), let us start with the following Euler discretization of the plant (34):

$$\begin{cases} M(q_k)\frac{\dot{q}_{k+1} - \dot{q}_k}{h} + C(q_k,\dot{q}_k)\dot{q}_{k+1} + G(q_k) + F(t_k,q_k,\dot{q}_k) = \tau_k \\ q_{k+1} = q_k + h\dot{q}_k. \end{cases} \tag{37}$$

We do not repeat here the discussion after (29), let us just mention that the overall structure in Figure 5 will also apply. The proposed controller is:

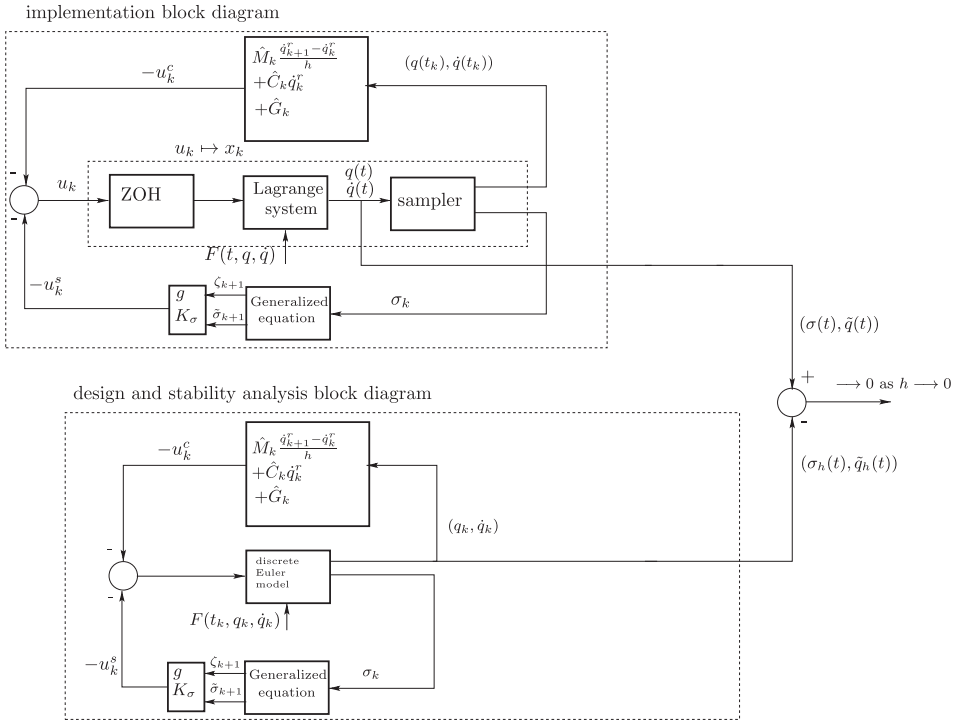

FIGURE 7 The implicit digital controller structure

$$\begin{cases} u^c_k = \hat{M}_k\frac{\dot{q}^r_{k+1}-\dot{q}^r_k}{h} + \hat{C}_k\dot{q}^r_{k+1} + \hat{G}_k \\ -u^s_k \in K_\sigma\tilde{\sigma}_{k+1} + g\,\partial\Phi(\tilde{\sigma}_{k+1}) \\ q^r_{k+1} = q^r_k + h\dot{q}^r_k, \quad \tau_k = u^c_k + u^s_k, \end{cases} \tag{38}$$

where $\dot{q}^r_k = \dot{q}^{\mathrm{d}}_k - \Lambda\tilde{q}_k$, $K_\sigma = K_\sigma^\top \succ 0$, $g>0$ is constant. One difference between the continuous-time and the discrete-time inputs, is that the term $K_p\tilde{q}$ in $u^c(t)$ in (35), is transferred into $K_\sigma\tilde{\sigma}_{k+1}$ in u^s_k. One notices that $\dot{q}^r_{k+1}$ is available at $t=t_k$, using (37). After some manipulations, one obtains the discrete-time closed-loop system:

$$\begin{cases} (M_k\sigma_{k+1} - M_k\sigma_k + hC_k\sigma_{k+1} + hK_\sigma\tilde{\sigma}_{k+1} - h\xi_k = -hg\,\zeta_{k+1} \\ \tilde{q}_{k+1} = (I_n - h\Lambda)\tilde{q}_k + h\sigma_k, \end{cases} \tag{39}$$

and

$$\begin{aligned} &\hat{M}_k\tilde{\sigma}_{k+1} - \hat{M}_k\sigma_k + h\hat{C}_k\tilde{\sigma}_{k+1} + hK_\sigma\tilde{\sigma}_{k+1} = -hg\,\zeta_{k+1} \\ &\zeta_{k+1} \in \partial\Phi(\tilde{\sigma}_{k+1}) \end{aligned} \tag{40}$$

where $\tilde{\sigma}_{k+1}$ is a dummy variable as in (21) and (31). Notice that the equivalent counterpart of the sliding-variable dynamics in (19) and (27) (28), is given here by the first equation in (36), and its discrete-time counterpart is in (40), and is the GE similar to (21) and (31). The overall controller structure is depicted in Figure 7. Let us concentrate on the "Generalized equation" block in Figure 7. Let us define $\hat{\mathcal{A}}_k \stackrel{\Delta}{=} (\hat{M}_k + h\hat{C}_k + hK_\sigma)$. It defines a strongly monotone operator when $\frac{\hat{k}_1}{2} + h\lambda_{\min}(K_\sigma) - \frac{\|\hat{\epsilon}\|_m}{2} \geq 0$, where $\hat{\epsilon} = o(h)$ satisfies $\hat{M}_{k+1} - \hat{M}_k = h\hat{C}_k + h\hat{C}_k^\top + \hat{\epsilon}_k$ and $M_{k+1} - M_k = hC_k + hC_k^\top + \epsilon_k$ (this is an approximate version of the above skew-symmetry property). It follows from tools from variational inequality theory that in such a case, the "Generalized equation" feedback block is given by:

$$\begin{aligned} &\zeta_{k+1} = -\tfrac{1}{hg}\left(\hat{\mathcal{A}}_k\tilde{\sigma}_{k+1} - \hat{M}_k\sigma_k\right) \\ &\tilde{\sigma}_{k+1} = \mathrm{Prox}_{\mu hg\,\Phi}((I_n - \mu\hat{\mathcal{A}}_k)\tilde{\sigma}_{k+1} + \mu\hat{M}_k\sigma_k) \end{aligned} \tag{41}$$

where $\mu > 0$ is such that $0 < \hat{\mathcal{A}}_k + \hat{\mathcal{A}}_k^\top - \mu \hat{\mathcal{A}}_k^\top \hat{\mathcal{A}}_k$. The Prox(·) map is a rather classical tool of Convex analysis[8], and we shall give an example next that clarifies its meaning. The important point at this stage, is to see that the "Generalized equation" feedback block represented in (41), defines an unique nonanticipative controller u_k^s in (38). The next step is how to solve it in real-time implementations. We suggested in Section 3.2, that the fixed-point problem (33) can be solved with successive approximations methods [81, section 14]. This is indeed a fast method, certainly more suitable for real-time implementation than other solvers like semismooth Newton methods. Let us choose $\Phi(\sigma) = \alpha\|\sigma\|_1$, $\alpha > 0$, so that $\partial\Phi(\sigma) = \alpha\ (\text{sgn}(\sigma_1), \text{sgn}(\sigma_2), \ \dots\ , \text{sgn}(\sigma_n))^\top$, then the algorithm (41) to be implemented at each t_k, $k \geq 0$, to calculate $\tilde{\sigma}_{k+1}$, and using a method of successive approximations, is as follows Reference 31:

Algorithm 3

1. Set $\mu > 0$ small enough such that $0 < \hat{\mathcal{A}}_k + \hat{\mathcal{A}}_k^\top - \mu \hat{\mathcal{A}}_k^\top \hat{\mathcal{A}}_k$ holds.
2. Set $j = 0$ and set $x^0 \in \mathbb{R}^n$.
3. Compute x^{j+1} as

$$v^j = (I - \mu\hat{\mathcal{A}}_k)x^j + \mu\hat{M}k\sigma_k,$$
$$x^{j+1} = v^j - \mu\ \text{proj}\left[[-c, c]^n; \frac{v^j}{\mu}\right],$$

   where $c = hg\alpha$ and the set $[-c,c]^n$ represents the n-cube in $\mathbb{R}^n$ centered at the origin with edge length equal to $2c$.
4. If $\|x^{j+1} - x^j\| > \varepsilon$, then increase j and go to step 3. Else, set $\tilde{\sigma}_{k+1} = x^{j+1}$ and stop.

The constant ε represents the precision of the algorithm. We provide in Section C1 more details on the GE($\tilde{\sigma}_{k+1}$), in particular how it may be solved with an LCP, hence recovering what happens for the other cases in (17), (A2) and (D5).

A big difference between SMC and optimization or contact mechanics, is that the dimension of the problem represented by the "Generalized equation" feedback block in Figures 4,5, *and* 7, *is proportional to the codimension of the sliding surface (ie, p in Sections* 3.1 *and* 3.2, *n in Section* 3.3), *and thus remains small (while in contact mechanics the contact LCP dimension may reach several hundred thousands).*

3.3.3 | Discrete-time SMC design: Closed-loop stability analysis

Let us state now a recapitulating theorem which summarizes the results in Reference 31.

Theorem 4 [31, lemma 6, corollary 2, theorems 4, 5, 6] *Let Assumption 4 hold.*

1. *Suppose that $h > 0$ is such that $\|\hat{\epsilon}_k\|_m \leq \min(\hat{k}_1, 2h\lambda_{\min}(K_\sigma))$, and that $\left\|\frac{\hat{M}_k\sigma_k}{h}\right\| \leq g\alpha$. Then $\tilde{\sigma}_{k+1} = 0$. Moreover, suppose that $M_k = \hat{M}_k$, $C_k = \hat{C}_k$ (no parametric uncertainty), that ξ_k is uniformly bounded by some constant $0 < \overline{F} < +\infty$ and that the gain satisfies $2\frac{\hat{k}_2}{\hat{k}_1}\overline{F} \leq g\alpha$. Then, $\tilde{\sigma}_{k_0+1} = 0$ for some $k = k_0$ implies that $\tilde{\sigma}_{k_0+n} = 0$ for all $n \geq 1$.*
2. *The equivalent control which maintains the constraint $\tilde{\sigma}_{k+n} = 0$ for all $n \geq 1$ is given by $\zeta_{k+2}^{eq} = \frac{1}{hg}\hat{M}_{k+1}\mathcal{B}_k^{-1}\left((M_k - \hat{M}_k)\sigma_k - h\xi_k\right)$, with $\mathcal{B}_k = M_k + hC_k$.*
3. *Consider the discrete-time dynamical system (39) (40), without parametric uncertainty ($M_k = \hat{M}_k$, $C_k = \hat{C}_k$) and ξ_k uniformly bounded by $\overline{F}$. Then, the origin $(\sigma^\star, \tilde{\sigma}^\star) = 0$ is globally practically stable whenever $g\alpha \geq \max\left\{\frac{2\hat{k}_2}{\hat{k}_1}\overline{F}\left(1 + \frac{\overline{F}}{\hat{k}_1\hat{r}}\right), 2\hat{k}_2\sqrt{\frac{\hat{k}_2}{\hat{k}_1}\left(\hat{r} + \frac{2\overline{F}}{\hat{k}_1}\right)}\right\}$, for some $0 < \hat{r}$ small enough and fixed. Moreover, $\tilde{\sigma}_k$ reaches the origin in a finite number of steps k^*, and $\tilde{\sigma}_k = 0$ for all $k \geq k^* + 1$.*
4. *Consider the discrete-time dynamical system (39) (40). Then, there exist constants $\hat{r}_\sigma > 0$, $\delta^* > 0$, $\overline{\beta}$, $\mathcal{F}(h)$ and $h^* > 0$ such that, for all $h \in (0, \min\{\delta^*, h^*\}]$, the origin of (39) is semiglobally practically stable whenever g and α satisfy $g\alpha > \max\left\{\frac{2\hat{k}_2}{\hat{k}_1}\overline{\beta}\left(1 + \frac{\overline{\beta}}{\hat{k}_1\hat{r}_\sigma}\right), 2\hat{k}_2\sqrt{\frac{\hat{k}_2}{\hat{k}_1}\left(\hat{r}_\sigma + \frac{2\mathcal{F}(h)}{\hat{k}_1}\right)}\right\}$. Moreover, $\tilde{\sigma}_k$ reaches the origin in a finite number of steps k^*, and $\tilde{\sigma}_k = 0$ for all $k \geq k^* + 1$.*

[8]Its use is widely spread in optimization, and this may be the first time it is applied in SMC.

5. *Assume that the spectrum of $I_n - h\Lambda$ is in the interior of the unitary circle. Then, if there is no disturbance (ie, $\xi \equiv 0 \Rightarrow \sigma_k = \tilde{\sigma}_k$), the origin of (39) (40) is globally finite-time Lyapunov stable, while $\tilde{q}_k \to 0$ asymptotically.*
6. *Let $(\sigma_k, \tilde{q}_k)$ be a solution to the closed-loop discrete-time system (39) (40), and let the functions $\sigma_h(t) \overset{\Delta}{=} \sigma_{k+1} + \frac{t_{k+1}-t}{h}(\sigma_k - \sigma_{k+1})$, $\tilde{q}_h(t) \overset{\Delta}{=} \tilde{q}_{k+1} + \frac{t_{k+1}-t}{h}(\tilde{q}_k - \tilde{q}_{k+1})$, for all $t \in [t_k, t_{k+1})$, be the piecewise-linear approximations of σ_k and $\tilde{q}_k$, respectively. Then, we can find a subsequence of sampling times h converging to zero, such that $(\sigma_h, \tilde{q}_h)$ converges to $(\sigma, \tilde{q})$, where $(\sigma, \tilde{q})$ is a solution to (36) with constant g and $\mathcal{M}(\cdot) = \partial\Phi(\cdot)$.*

Item 1 means that if the control gain is large enough, then the system remains in the discrete-time sliding surface once it has been reached. The stability analysis is led with the positive definite functions $V_1(\tilde{\sigma}_k) = \tilde{\sigma}_k^\top \hat{M}_k \tilde{\sigma}_k$ and $V_2(\sigma_k)) = \sigma_k^\top \hat{M}_k \sigma_k$, while $V(\sigma) = \sigma^\top(q)\sigma$ is used in the continuous-time setting. The equivalent controller in item 2 is obviously not implementable, since the perturbation is unknown. However, it shows (similarly to the foregoing sections) that the implicit controller compensates for the disturbance, with a one-step delay. Also the magnitude of the equivalent controller, does not diverge as $h \to 0$, because one can prove that $\sigma_{k+1} = -h\hat{\mathcal{B}}_k^{-1}\xi_k$, $\hat{\mathcal{B}}_k = \hat{M}_k + h\hat{C}_k$, in the discrete sliding surface. Items 3 and 4, are interesting because they connect the discrete-time sliding surface, with the discrete plant's state stability. The constants $\overline{\beta}$ and $\mathcal{F}(h)$ in item 4 can be calculated from known quantities, see the proof of [31, theorem 5]. Item 5 proves that in the ideal unperturbed case, the implicit method guarantees a very strong stability of the closed-loop system. Item 6 guarantees, in a similar way as item 7 in Theorem 3, that the lower feedback system in Figure 7 is a good approximation of the upper system which represents the controlled plant.

The stability analyses presented in the foregoing sections for the implicit controllers (Theorems 1-3 *and* 4), *are all led with Lyapunov functions which are very close, or equal to their continuous-time counterparts. Consequently, the implicit approach mimics the continuous-time framework.*

3.3.4 | Numerical simulations

Simulations are presented in Reference 31, on a two-degree-of-freedom planar manipulator, following the "Implementation block diagram" in Figure 7. They confirm that the implicit approach supersedes the explicit one. However, they reveal also that the discrete-time sliding phase is never reached exactly (in the configuration of Figure 7) because of the nonexact plant discretization (37). Thus, small chattering is present (however, much smaller than with the explicit approach), which is absent in the pure discrete/discrete setting (the "design and stability analysis block diagram" in Figure 7). An important additional conclusion of these numerical tests, is that the closed-loop system is unstable with the explicit controller $-u_k^s = K_\sigma \sigma_k + g\ \partial\Phi(\sigma_k)$ (instead of (38)), for $h > h^* > 0$ and some h^*, while it remains stable with the implicit method.

The fact that the explicit method requires much smaller sampling periods than the implicit one to attain less good performances, may constitute one of the most important, if not the most important advantage of the implicit approach.

3.4 | Further case studies of the implicit method

Let us provide a brief overview of further studies on the implicit discretization of SMCs.

3.4.1 | Backstepping nested SMC algorithm for unmatched perturbations

It is worth recalling that the popular backstepping method, has been originally proposed in References 82-85 in an SMC contact for the control of triangular systems (named therein block control, see [76, p544] for a short history of backstepping). More recently a nested SMC controller has been proposed to cope with unmatched perturbations,[33] for planar systems as:

$$\begin{cases} \dot{x}_1(t) = x_2(t) + d_1(x_1(t), t) \\ \dot{x}_2(t) = u(t) + d_2(x_2(t), t). \end{cases} \tag{42}$$

The goal is to regulate $x_1(\cdot)$ to a neighborhood of zero, with a backstepping nested controller of the form $u(x_1, x_2) \in -g_2\Xi(x) - g_3\text{sgn}(\Xi(x))$, $\Xi(x) \in x_2 + g_1\text{sgn}(x_1)$, $g_1,g_2,g_3 > 0$ constant gains. The implicit discrete-time input is calculated solving a two-step GE. Comparisons are made with a first-order SMC and an H_∞ controller on stirred-tank reactors in series, through numerical simulations, and seem to be in favor of the nested SMC input. It is noteworthy that if $d_1(\cdot)$ is time differentiable with bounded first derivative, the system in (42) can be reduced to a double integrator with matched disturbance $\ddot{x}_1(t) = u(t) + \frac{d}{dt}(d_1(x_1(t), t)) + d_2(x_1(t), t)$, and the twisting algorithm (see Section 4.1) can be applied, yielding $(x_1(t), \dot{x}_1(t)) \to (0, 0)$ so that $x_2(t) \to -d_1(x(t),t)$ as $t \to +\infty$. However, on one hand this is a restrictive assumption on the disturbance, on the other hand the twisting algorithm applies to dimension 2 systems, while the backstepping nested approach should be extendable to dimension $n \geq 3$ systems.

3.4.2 | Perturbation estimation to increase the precision

One way to improve the accuracy of discrete-time SMC, is to use the fact that since the controller compensates for the perturbation with a one-step delay, the perturbation is known (or estimated) with a one-step delay and this estimation could be used to approximately compensate at the next step (if the perturbation does not vary too abruptly). In this respect the implicit method certainly represents a great advantage compared with the implicit one, because the discrete sliding surface is given a rigorous definition and it is attained in finite-time, see Theorems 1 and 2. Such ideas were proposed for instance, in Reference 72 in which, however, only the continuous (equivalent) part of the controller is considered in the analysis. The work in Reference 30 uses similar ideas with an implicit discretization of the equivalent-based SMC, and proves that accuracy is improved proportionally to the disturbance estimation accuracy.

3.4.3 | Fixed-time convergence

It is proved in Reference 29 that the implicit Euler method allows one to preserve the fixed-time convergence property of a nonlinear system with SMC. Though the type of controller considered in Reference 29 has little practical interest (because it has a cubic term in the input, yielding high overshoot), it shows a further property of the implicit discretization, namely, the hyperexponential convergence rate (while the explicit discretization may yield instability of the closed-loop system[17]).

3.4.4 | Parabolic SMC filtering

Basically, the problem studied in References 37,41,43,47,56,86,87 concerns noise reduction filtering, and is written as

$$\begin{cases} \dot{x}_1(t) = x_2(t) \\ \dot{x}_2(t) \in -\frac{k_1+1}{2}\text{sgn}(\sigma(t)) - \frac{k_1-1}{2}\text{sgn}(x_2(t)) \\ \sigma \stackrel{\Delta}{=} x_2 + \text{sgn}(x_1 - u)\sqrt{2k_2|x_1 - u|}, \end{cases} \tag{43}$$

where $k_1 > 1$, $k_2 > 0$, $u(\cdot)$ is the filter input while $y = x_1$ is its output. Such filters can remove impulsive and high-frequency noise, with smaller phase lag than linear filters. Improved versions of the basic parabolic scheme are proposed in References 86,87, with extensive numerical simulations and comparative numerical analysis in open and closed-loop. They are implemented digitally with an implicit Euler method and various experimental validations are reported: force projecting master-slave systems with one- and six-degree-of-freedom manipulators,[43,47] racing wheel,[41] ultrasonic sensor and optical encoder.[37,56]

3.4.5 | Proxy-based SMC

Proxy-based SMC has been developed in the setting of haptic systems control[38,46,49,88][9], parallel robots control,[89] control of an active ankle foot orthosis for paretic patients,[90] control of a piezoelectric-actuated nanopositioning stage[91]. It

[9]Apparently the article [88] is the first article where the implicit method has been advocated in the context of digital proxy-based SMC.

applies to Lagrangian systems (34), and combines a PID controller with a first-order SMC. The continuous-time design and controller discretization, are presented in References 38,46,88, with experimental validations. The continuous-time closed-loop stability is analyzed in Reference 49.

3.4.6 | Amplitude-and rate-saturated controller

These are introduced in References 39,48, to control linear invariant systems with matched perturbations, as in (18). The input is defined through a differential inclusion as:

$$\begin{cases} \dot{u}(t) \in -g\ \mathrm{sgn}\left(u(t) + \mathrm{sat}\left(\frac{Cx}{\gamma(x(t),u(t))}\right)\right) \\ \gamma(x,u) = \min\left(\gamma_c, \frac{|CAx|+CB|u|+CBM}{g}\right), \end{cases} \tag{44}$$

with $C \in \mathbb{R}^{1\times n}$, $CB > 0$, $|d(t)| \le M$, $\gamma(x,u) \le \gamma_c$, sat$(\cdot)$ is the usual saturation function, with saturation width $\alpha > M$. The objective is to get an input that satisfies $|u| \le \alpha$ and $|\dot{u}| \le g$. It is shown that sliding mode exists, and an implementable implicit Euler discretization of $u(\cdot)$ is calculated.

4 | SECOND-ORDER SLIDING-MODE CONTROL

Let us now turn our attention to second-order SMC, and focus on the twisting and the supertwisting controllers. Though it is sometimes admitted that higher order SMC (HOSMC) suppresses chattering, such is not the case, as witnessed by simulation and experimental results, for the supertwisting[40,92,93] and the twisting[14,21,50] schemes. It is thus worth investigating their implicit discretization.

4.1 | Twisting algorithm

The twisting algorithm has been one of the first HOSMC to be presented in the literature. It was proposed in Reference 94 with a full stability analysis, see also a stability analysis with a weak Lyapunov function in Reference 95. Given a sliding-variable that is of relative degree 2 with respect to the control input, that is, $\ddot{\sigma}(t) = a(x(t),t) + b(x(t),t)u(t)$, $0 < b_{\min} \le |b(x,t)| \le b_{\max}$, $|a(x,t)| \le a_{\max}$, the twisting scheme takes the form:

$$u^s(t) \in -g_1\ \mathrm{sgn}(\sigma(t)) - g_2\ \mathrm{sgn}(\dot{\sigma}(t)), \quad g_1 > 0, \quad g_2 > 0, \tag{45}$$

yielding a differential inclusion $\ddot{\sigma}(t) \in a(x(t),t) - b(x(t),t)g_1\ \mathrm{sgn}(\sigma(t)) - b(x(t),t)g_2\ \mathrm{sgn}(\dot{\sigma}(t))$. Conditions guaranteeing the global finite-time stability of the origin $(\sigma^\star, \dot{\sigma}^\star) = (0,0)$ have been derived in References 94,95, they are simply $g_1 > g_2 > 0$ when $a(x,t) \equiv 0$ and $b(x,t) = 1$. To illustrate the big difference between the twisting algorithm and the schemes studied in the foregoing sections, let us start with the simplest case, where $a(x,t) \equiv 0$ and $b(x,t) = 1$. It is known that the explicit Euler discretization of the input, that is, $u^s_k = -g_1\ \mathrm{sgn}(\sigma_k) - g_2\ \mathrm{sgn}(\dot{\sigma}_k)$, yields chattering, as shown experimentally in Reference 21 and analytically in Reference 14 (though it may possess interesting accuracy properties when combined with disturbance estimation[96]). The ZOH discretization yields, with an implicit control

$$u^s_k \in -g_1\ \mathrm{sgn}(\sigma_{k+1}) - g_2\ \mathrm{sgn}(\dot{\sigma}_{k+1}) \tag{46}$$

to be computed at $t = t_k$ and applied on $[t_k, t_{k+1})$:

$$\begin{aligned} &\Sigma_{k+1} = A_h\Sigma_k + B_h\lambda^s_{k+1} \\ &\lambda^s_{k+1} \in -\mathrm{sgn}(\Sigma_{k+1}) \end{aligned} \iff B_h\lambda^s_{k+1} + A_h\Sigma_k \in -\mathcal{N}_{[-1,1]}(\lambda^s_{k+1}), \tag{47}$$

FIGURE 8 The closed-loop set-valued Lur'e system structure

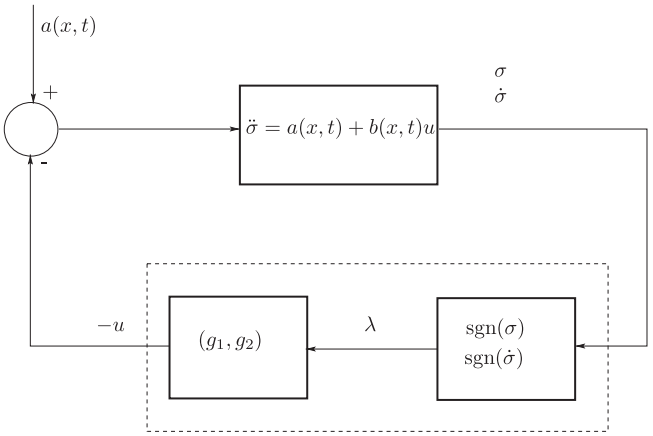

with $\Sigma_k = (\sigma_k, \dot{\sigma}_k)^\top$, $A_h = e^{Ah} = \begin{pmatrix} 1 & h \\ 0 & 1 \end{pmatrix}$, $A = \begin{pmatrix} 0 & 1 \\ 0 & 0 \end{pmatrix}$, $B_h = hg_1 b_k \begin{pmatrix} \frac{h}{2} & \beta\frac{h}{2} \\ 1 & \beta \end{pmatrix}$, $g_2 = \beta g_1$, with the approximation $b_k = b(x_k,k)$. One sees that $\lambda^s_{k+1} = (\lambda^s_{1,k+1}, \lambda^s_{2,k+1})^\top$ in (47) plays the same role as λ_{k+1} in (7) (c) (d), with $u^s_k = g_1\lambda^s_{1,k+1} + g_2\lambda^s_{2,k+1}$. The equivalence is obtained by using (1), which gives $\Sigma_{k+1} \in -\mathcal{N}_{[-1,1]}(u^s_k)$. This GE is under the canonical form as in the left-hand side of (2), but unfortunately B_h is an indefinite matrix, thus $\lambda^s_{k+1} \mapsto B_h\lambda^s_{k+1} + A_h\Sigma_k$ is not a monotone operator, general results[59,60] about the uniqueness of such GE do not apply, and finally (2) cannot be used so that (47) does not define a projection as (13) or (23). Henceby the GE in (47) is less nice than its first-order SMC counterparts in (21), (or (22)), (31) and even (40).

The twisting algorithm yields a GE for the calculation of the implicit input, that is, less tractable than its first-order SMC counterparts. This is mainly due to the loss of monotonicity of a crucial feedback operator.

Actually, the block diagrams in Figure 6A and in Figure 8, where $u^s = -(g_1, g_2)\lambda^s$, $\lambda^s_1 \in \mathrm{sgn}(\sigma)$, $\lambda^s_2 \in \mathrm{sgn}(\dot{\sigma})$, are similar Lur'e set-valued systems. However, the feedback static nonlinearity within the dashed block $(\sigma, \dot{\sigma}) \mapsto -u$ loses the maximal monotonicity property due to the sum of the two signum multifunctions.

4.1.1 | Discrete-time twisting design: Calculation of the input

Let us rewrite the GE (47) in a more general setting with nonzero term $a(x,t) = a_{\mathrm{nom}}(x,t) + d(x,t)$, where $a_{\mathrm{nom}}(x,t)$ is its nominal known part and $d(x,t)$ is its unknown uniformly bounded part (a disturbance or uncertainty). Let us set the GE($\tilde{\Sigma}_{k+1}$):

$$\begin{cases} \tilde{\Sigma}_{k+1} = A_h\Sigma_k + F_{h,a} + B_h\lambda^s_{k+1} \\ \lambda^s_{k+1} \in -\mathrm{sgn}(\tilde{\Sigma}_{k+1}) \end{cases} \tag{48}$$

with $\tilde{\Sigma}_k = \begin{pmatrix} \tilde{\sigma}_k \\ \dot{\tilde{\sigma}}_k \end{pmatrix}$, which is the counterpart of (7) (b) (c) (d), (21), (31) and (40). The vector $F_{h,a} = \begin{pmatrix} \frac{h^2 a_k}{2} \\ ha_k \end{pmatrix}$ stems for possible nonzero $a_{\mathrm{nom}}(x,t)$, with the explicit Euler approximation $a_k = a_{\mathrm{nom}}(x_k,k)$. As we saw in Sections 3.2 and 3.3, see Remark 5, there are two possible reasons for $\tilde{\Sigma}_{k+1} \neq \Sigma(t_{k+1})$: a nonexact discretization of the differential inclusion $\ddot{\sigma}(t) \in a(x(t),t) - b(x(t),t)g_1\ \mathrm{sgn}(\sigma(t)) - b(x(t),t)g_2\ \mathrm{sgn}(\dot{\sigma}(t))$ due to nonlinear terms, and/or the presence of uncertainties. Here both are present due to the approximation a_k and due to $d(x,t)$. The (approximate) plant discretization is now given by $\Sigma_{k+1} = A_h\Sigma_k + B_h\lambda^s_{k+1} + F_{h,a} + F_{h,d}$, with $F_{h,d} = \int_{t_k}^{t_{k+1}} e^{A(t_{k+1}-\tau)}Bd(x(\tau),\tau)d\tau$. The difference between $\tilde{\Sigma}_{k+1}$ and Σ_{k+1} on one time step, is therefore equal to $F_{h,d}$.

Let us use once again the inversion $\tilde{\Sigma}_{k+1} \in -\mathcal{N}_{[-1,1]^2}(\lambda^s_{k+1})$ of the second equation in (48). Henceby the GE($\tilde{\Sigma}_{k+1}$) in (48) can be rewritten equivalently as the GE(λ^s_{k+1}) (its dual, or conjugate GE):

$$A_h\Sigma_k + F_{h,a} + B_h\lambda^s_{k+1} \in -\mathcal{N}_{[-1,1]^2}(\lambda^s_{k+1}). \tag{49}$$

The following holds true.

Proposition 1 [21, lemma 1, proposition 1] *[35, lemma 2]*

1. *The GE($\tilde{\Sigma}_{k+1}$) in (48) has always a unique solution for any Σ_k, $F_{h,a}$ and any $h>0$.*
2. *The control input value $u_k^s = g_1\lambda_{k+1}^s + g_1\beta\lambda_{k+1}^s$ is always unique also, and nonanticipative.*
3. *The multipliers $\lambda_{k+1}^s \in \mathbb{R}^2$, solutions to the GE in (49), are unique whenever $\tilde{\Sigma}_{k+1} \neq 0$.*

The existence of solutions in item 1 is a straightforward application of [59, corollary 2.2.5]. However, the proof of uniqueness of solutions in items 1 and 2 requires specific developments that do not follow from general results on uniqueness of solutions to such GE, see Reference 21. Nonanticipativeness in item 2 comes directly from the GE(λ_{k+1}^s). As noted in [21, remark 2], item 3 also holds in the continuous-time setting.

Solving the controller GE: The overall structure of the discrete-time implementation of the twisting scheme, follows that of the block diagrams shown in Figures 5 and 7. Clearly the GE(λ_{k+1}^s) in (49) can be rewritten as an LCP, in a way quite similar to Sections A1,C1, and D1, or as a variational inequality. As alluded to above, the problems encountered in SMC are of low dimension (here, two variables). The GE(λ_{k+1}^s) can be solved on-line using the algorithm in Reference 97, which is available in the software package SICONOS[1][10]. Due to its low dimension with nine possible cases, the GE(λ_{k+1}^s) can also be solved enumeratively. The algorithm which has been used to obtain the experimental results described in Section 4.1.3 is explicitly written in [98, appendix C.2]. It is a MATLAB code of about 120 lines long. On the contrary, the MATLAB code used for the scalar SMC is about 10 lines long, see [98, appendix C.1].

4.1.2 | Discrete-time twisting design: Closed-loop analysis

Let us start with the following definition.

Definition 3. The discrete-time sliding surface is

$$\Sigma_d \overset{\Delta}{=} \{(\tilde{\sigma}_k, \dot{\tilde{\sigma}}_k) \in \mathbb{R}^2 \mid (\tilde{\sigma}_k, \dot{\tilde{\sigma}}_k) = (0,0) \ \Leftrightarrow \ \lambda_k^s \in (-1,1)^2\},$$

where $(\tilde{\sigma}_k, \dot{\tilde{\sigma}}_k)$ is the solution to the GE in (48).

Proposition 2. *Let us consider the above discretization of the system $\ddot{\sigma}(t) = a(x(t),t) + b(x(t),t)u(t)$, with the implicit discrete-time twisting controller $u_k^s \in -g_1\lambda_{1,k+1}^s - g_1\beta\lambda_{2,k+1}^s$, and λ_{k+1}^s solution to the GE in (49), to be applied at $t=t_k$.*

1. *On Σ_d one has $\sigma_k = \frac{h^2}{2}a_k$, $\dot{\sigma}_k = -ha_k$, $\lambda_{1,k+1}^s + \beta\lambda_{2,k+1}^s = 0$, $u_k^s = 0$.*
2. *Let $a(x,t) \equiv 0$ and $b(x,t) = 1$ (double-integrator system), $g_1 > g_2 > 0$, and the implicit twisting controller. Then [98, lemmae 2.3.10, 2.3.11, 2.3.12] [35, lemma 1]:*
   (a) *The segment $\{(0,\dot{\sigma}_k) \in \mathbb{R}^2 \mid |\dot{\sigma}_k| \leq \frac{h}{2}(g_1 - g_2)\}$ is invariant for the system (48).*
   (b) *The origin of the system (48) is reachable only from the line segment $S_0 \overset{\Delta}{=} \{(\sigma_k,\dot{\sigma}_k) \in \mathbb{R}^2 \mid \sigma_k + \frac{h}{2}\dot{\sigma}_k = 0, \ |\dot{\sigma}_k| \leq h(g_1+g_2)\}$.*
   (c) *S_0 is not an attracting set of the closed-loop discrete-time system, and the set of initial positions that can reach the origin is a union of countably many segments. Therefore, it has Lebesgue measure zero.*
3. *Let $d(x,t) \neq 0$, $|d(x,t)| \leq M < +\infty$, then on Σ_d one has $\Sigma_{k+1} = F_{h,d} = \mathcal{O}(h)$.*

The discretization used in the preliminary results in [26, equation (50)], differs from the above because an implicit Euler method was used to calculate the GE (48), not a ZOH method. It can be shown that both methods differ by an $\mathcal{O}(h^2)$ term premultiplying λ_{k+1}^s in the $\tilde{\sigma}_{k+1}$ dynamics. Nevertheless the conclusions drawn in [26, propositions 7, 8] agree with those in Proposition 2 item 1, in the sense that the term $a(x,t)$ is attenuated by a factor h^2 on the position and by a factor h on the velocity. The accuracy of the implicit twisting algorithm is therefore equivalent to that of the explicit scheme,[14,96] and could be improved with an disturbance estimation along the lines of Section 3.4.2, see Reference 96. Recall that in item 2, $\tilde{\Sigma}_k = \Sigma_k$ so that (47) and (48) are the same systems. The consequence of item 2, is that the system may cycle between two values $(0,\alpha)$ and $(0,-\alpha)$ with $|\alpha| \leq \frac{h}{2}(g_1+g_2)$, for some initial conditions. These cycles vanish as $h \to 0$. But

[10] https://nonsmooth.gricad-pages.univ-grenoble-alpes.fr/siconos/index.html

FIGURE 9 Normal cones to the set K

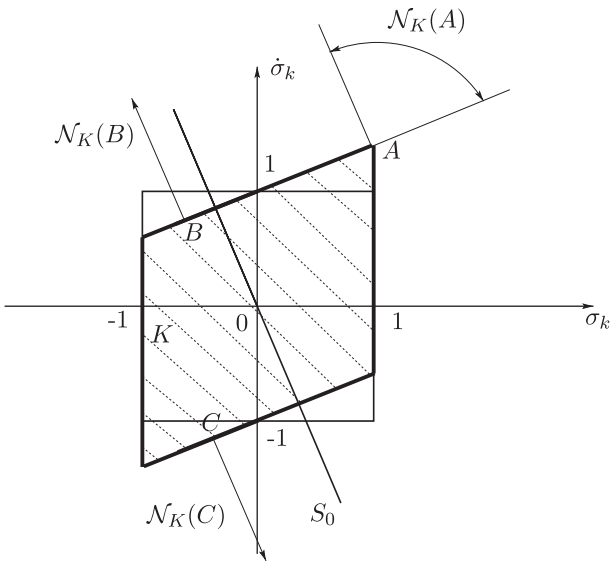

they hamper one to state asymptotic stability results for $h>0$. This means that the above implicit discretization of the input, is too simple to guarantee stronger stability property. This has motivated the study of a modified version of the *regular* discrete-time implicit twisting algorithm in (46), which guarantees global finite-time Lyapunov stability.[35] The modification does not lie in the arguments (the controller is still implicit), but in the controller structure. Specifically, let us assume that $a(x,t)\equiv 0$ and $b(x,t)=1$ as in item 2 of Proposition 2. We have seen that the implicit controller is calculated from $\Sigma_{k+1}\in -\mathcal{N}_{[-1,1]^2}(\lambda^s_{k+1})$, which allows the designer to construct and solve the GE in (49). This inclusion shows that the state at step $k+1$ must belong to minus the normal cone to the hypercube $[-1,1]^2$. If the segment S_0 does not belong to the normal cone, there is no chance to get the asymptotic stability. The idea is to set instead: $\Sigma_{k+1}\in -\mathcal{N}_K(\lambda^s_{k+1})$, with $K\subset\mathbb{R}^2$ a bounded polytopic convex set $K=\{x\in\mathbb{R}^2 \mid Ex\le b\}$, $E\in\mathbb{R}^{4\times 2}$ and $b\in\mathbb{R}^4$, designed such that the normal cone to K contains S_0, see Figure 9 where K defined with $E(h)=\begin{pmatrix}1 & 0\\ -\frac{h}{2} & 1\\ -1 & 0\\ \frac{h}{2} & -1\end{pmatrix}$ and $b=(1,1,1,1)^\top$ is depicted. Then we obtain the following.

Proposition 3 [35] *Let $a(x,t)\equiv 0$, $b(x,t)=1$, and the discretization $\Sigma_{k+1}=A_h\Sigma_k+B_h\lambda^s_{k+1}$, $u^s_k=g_1\lambda^s_{1,k+1}+g_2\lambda^s_{2,k+2}$. Let also $0<h<2$ and $g_1>\left(1+\frac{h}{2}\right)g_2>0$. Then the controller defined by $\Sigma_{k+1}\in-\mathcal{N}_K(\lambda^s_{k+1})$ renders the origin $(\sigma_k,\dot\sigma_k)=(0,0)$ the unique equilibrium of the closed-loop system, which is globally finite-time Lyapunov stable.*

The proof is led with the Lyapunov function $V(\sigma_k,\dot\sigma_k)=g_1|\sigma_k+\frac{h}{2}\dot\sigma_k|+\frac{1}{2}\dot\sigma_k^2-\frac{h}{2}g_2\lambda_{2,k}\dot\sigma_k$, which is close to its continuous-time counterpart in Reference 95.

4.1.3 | Experimental results

Thorough experimental results are presented in Reference 21, obtained on an electropneumatic system with dimension 4, see Figure 10, where the explicit input is $u^s_k=-g_1\mathrm{sgn}(\sigma_k)-g_2\mathrm{sgn}(\dot\sigma_k)$. It produces a high-frequency bang-bang signal (Figure 10 top). The conclusions drawn for first-order SMC are still valid: drastic decrease of input and output chattering, and insensitivity of the input with respect to the gain β increase.

It is noteworthy that in general, the second-order dynamics for $\sigma(\cdot)$ stems from a higher dimensional system that has relative degree two with respect to $\sigma(\cdot)$ seen as an output, so that $\sigma(\cdot)$ and $\dot\sigma(\cdot)$ are designed as functions of some measured output $y(\cdot)$ and of its derivatives, usually obtained as the output of linear filters that approximate differentiation (so-called "dirty filters" $\frac{\tau s}{s+\tau}$, $\tau>0$, which introduce phase lags[11]). This is a feature shared by the first-order SMC. A crucial fact

[11] This drawback may be alleviated by using sliding-mode differentiators instead.

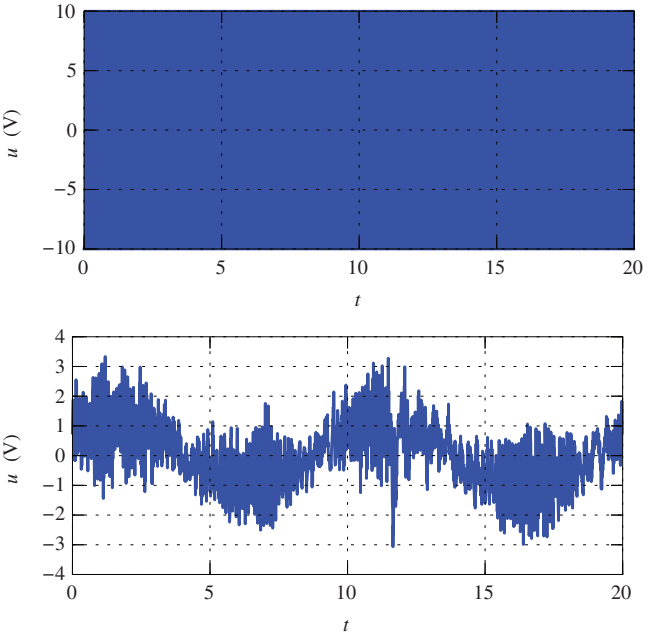

FIGURE 10 Explicit (top) and implicit (bottom) discrete-time twisting inputs, $h = 10$ ms [Colour figure can be viewed at wileyonlinelibrary.com]

noticed in Reference 21, is that the experimental results drastically depend on the correct tuning of "extra" parameters: time constants τ of the linear filters to construct $\sigma = Cx$ and possibly $\dot{\sigma}(\cdot)$, and entries of the "output" matrix C. A detailed presentation of the selection of these parameters is made in [21, section 5] and [98, section 4.1.3]. We reach once again the same conclusion as in the foregoing sections: the implicit method does not aim at improving the accuracy (at least, not theoretically), it aims at alleviating chattering and it allows one to get results close to the continuous-time behavior (in particular, **P2** and **P10** in the introduction). However, it is clear that the suppression of output chattering, may result in better accuracy of the implicit method compared with the explicit one, for same gains and sampling periods $h > 0$.

Remark 7. Saturations or sigmoid regularizations of both signum multifunctions can be applied to the twisting scheme. It is expected that tuning the saturations widthes and the sampling time $h > 0$ to alleviate chattering, will require an off-line process, likely to be more complex than the first-order SMC case studied in Reference 16. The complete analysis of the system's behavior in the boundary layer, is related directly to the time-discretization of a singularly perturbed system (where the singular parameter is the saturation width). The time discretization of singularly perturbed systems is known to be a tough issue, where the boundary layer dynamics strongly depends on the sampling time vs saturation width ratio.[69,70] Letting $x \stackrel{\Delta}{=} \sigma$ and $z \stackrel{\Delta}{=} \dot{\sigma}$, while a saturation with width $1 \gg \epsilon > 0$ is used to regularize both signum functions, the regularized twisting algorithm writes down inside the boundary layer with width 2ϵ:

$$\begin{cases} \dot{x}(t) = z(t) \\ \epsilon\, \dot{z}(t) = -g_1 x(t) - g_2 z(t). \end{cases} \tag{50}$$

Following References 69,70, the time-discretization with an explicit Euler method and fast sampling $h \approx \epsilon$ is equal to:

$$\begin{pmatrix} x_{k+1} \\ z_{k+1} \end{pmatrix} \approx \begin{pmatrix} 1 + \frac{hg_1}{g_2}\left(-1 + \frac{e^{-g_2}-1}{g_2}\right) & -\frac{h}{g_2}(e^{-g_2} - 1) \\ \frac{g_1}{g_2}(e^{-g_2} - 1) & e^{-g_2} \end{pmatrix} \begin{pmatrix} x_k \\ z_k \end{pmatrix}, \tag{51}$$

while for slow sampling it becomes

$$\begin{pmatrix} x_{k+1} \\ z_{k+1} \end{pmatrix} \approx \begin{pmatrix} 1 + \frac{hg_1}{g_2}(e^{-\beta g_2} - 1) & he^{-\beta g_2} \\ \frac{g_1}{g_2}(e^{-\beta g_2} - 1) & e^{-\beta g_2} \end{pmatrix} \begin{pmatrix} x_k \\ z_k \end{pmatrix}, \tag{52}$$

with $\beta \gg 1$, $h = \beta\epsilon$.

Remark 8. A continuous twisting algorithm has been proposed in Reference 99, and its implicit time-discretization is studied in Reference 50. Numerical simulations show that it supersedes the explicit one. Further theoretical work is needed to analyse the properties of this algorithm (finite-time stability, robustness). It would also be quite interesting to lead comparison studies between this implicit algorithm and the one in Reference 35.

4.2 | Supertwisting algorithm

The supertwisting algorithm can be used in the contexts of control,[94] observation and exact differentiation. In fact, despite it can attenuate chattering effects, its explicit Euler discretization is still prone to input and output chattering, as witnessed by analysis,[100] numerical simulations,[40,44] and experiments.[93] Its implementation with the implicit method is thus worth investigating. The supertwisting controller applies to a disturbed plant of the form:

$$\begin{cases} \dot{x}_1(t) = u(t) + \varphi(t) \\ \dot{\varphi}(t) = \Delta(t), \end{cases} \tag{53}$$

with the controller:

$$\begin{cases} u(t) = -g_1 \sqrt{|x_1(t)|}\, \mathrm{sgn}(x_1(t)) + \nu(t) \\ \dot{\nu}(t) \in -g_2\, \mathrm{sgn}(x_1(t)), \end{cases} \tag{54}$$

control gains $g_1 > 0$, $g_2 > 0$, giving the closed-loop system, where $x_2(\cdot) \overset{\Delta}{=} \nu(\cdot) + \varphi(\cdot)$:

$$\begin{cases} \dot{x}_1(t) = -g_1 \sqrt{|x_1(t)|}\, \mathrm{sgn}(x_1(t)) + x_2(t) \\ \dot{x}_2(t) \in -g_2\, \mathrm{sgn}(x_1(t)) + \Delta(t). \end{cases} \tag{55}$$

A basic assumption is $\sup_{t\geq 0}|\Delta(t)| \leq M$ for some known constant M. As is known, the dynamics in (55) also corresponds to that of a supertwisting observer for a dimension two system,[26,93,101] where the two states are the observation errors.

4.2.1 | Discrete-time supertwisting design: Calculation of the input

As in the foregoing sections, the first step is to choose a discrete-time model for the plant (53). Without going into details, let us propose:

$$\begin{cases} x_{1,k+1} = x_{1,k} + h u_k^s + h\overline{\varphi}_k \\ \varphi_{k+1} = \varphi_k + h\overline{\Delta}_k, \end{cases} \tag{56}$$

where $\overline{\varphi}_k$ and $\overline{\Delta}_k$ are an approximation of $\int_{t_k}^{t_{k+1}} \varphi(t)dt$ and of $\int_{t_k}^{t_{k+1}} \Delta(t)dt$, respectively. Then the implicit controller to be calculated at $t = t_k$ and applied on $t \in [t_k, t_{k+1})$ (ie, $\bar{u}^s(t) = u_k^s$ for all $t \in [t_k, t_{k+1})$), is obtained as Reference 36:

$$\begin{cases} u_k^s = -g_1 \sqrt{|\tilde{x}_{1,k+1}|}\, \mathrm{sgn}(\tilde{x}_{1,k+1}) + \nu_{k+1} \\ \nu_{k+1} \in \nu_k - g_2 h\, \mathrm{sgn}(\tilde{x}_{1,k+1}), \end{cases} \tag{57}$$

from which one can design the following GEs:

$$\begin{array}{l} \tilde{x}_{1,k+1} = x_{1,k} + h u_k^s \\ u_k^s = -g_1 \sqrt{|\tilde{x}_{1,k+1}|}\, \mathrm{sgn}(\tilde{x}_{1,k+1}) + \nu_{k+1} \\ \nu_{k+1} \in \nu_k - g_2 h\, \mathrm{sgn}(\tilde{x}_{1,k+1}) \end{array} \quad \leftrightarrow \quad \begin{array}{l} u_k^s = -g_1 \sqrt{|\tilde{x}_{1,k+1}|}\xi_{k+1} + \nu_{k+1} \\ \nu_{k+1} = \nu_k - g_2 h \xi_{k+1} \\ f(-g_2 h^2 \xi_{k+1}) \in \mathcal{N}_{[-1,1]}(\xi_{k+1}) \\ g(\tilde{x}_{1,k+1}) \in -g_2 h^2 \mathrm{sgn}(\tilde{x}_{1,k+1}) \end{array} \tag{58}$$

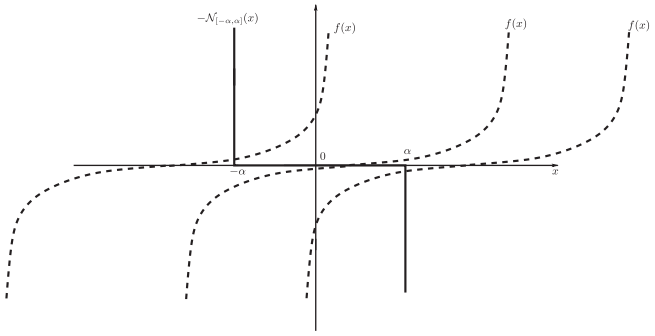

FIGURE 11 The generalized equation $f(x) \in -\mathcal{N}_{[-\alpha,\alpha]}(x)$, $\alpha > 0$

where $g(x) = x + hg_1\sqrt{|x|} - x_{1,k} - hv_k$, $f(y) = g^{-1}(x)$ (ie, the second GE in the right-hand side of (58) is just the inverse of the first one). The discrete-time system in (58) may be considered as a virtual unperturbed system. It happens that the GEs in (58) are solvable and their solution can be calculated analytically, so that the controller is given uniquely by the following algorithm:[36]

Algorithm 4

- **data**: $x_{1,k}$ and v_k, $a = h\lambda_1$, $h > 0$, $\lambda_1 > 0$, $\lambda_2 > 0$, $b_k = -x_{1,k} - hv_k$.
- **if** $b_k < -h^2\lambda_2$, **then** $\sqrt{|\tilde{x}_{1,k+1}|} = \frac{-a+\sqrt{a^2-4(b_k+\lambda_2 h^2)}}{2}$; $v_{k+1} = v_k - h\lambda_2$; $u_k = -\lambda_1\sqrt{|\tilde{x}_{1,k+1}|} + v_{k+1}$,
- **else if** $b_k \in [-h^2\lambda_2, h^2\lambda_2]$, **then** $u_k = v_{k+1} = -\frac{x_{1,k}}{h}$,
- **else if** $b_k > -h^2\lambda_2$, **then** $\sqrt{|\tilde{x}_{1,k+1}|} = \frac{-a+\sqrt{a^2+4(b_k-\lambda_2 h^2)}}{2}$; $v_{k+1} = v_k + h\lambda_2$; $u_k = \lambda_1\sqrt{|\tilde{x}_{1,k+1}|} + v_{k+1}$,
- **terminate**

The function $f(\cdot)$ is a strictly monotone continuous single-valued mapping, so the first GE in the right-hand side of (58) is a variational inequality of the class studied in Reference 59, and is an extension of (12) (or of (22)), while the second GE involving $g(\cdot)$ may be compared with (9) (or with (21)). This implies that these two GEs can be graphically interpreted as in Figure 3, changing the affine functions (dashed lines) by nonlinear strictly increasing curves, see Figure 11 [36, figure 2] [44, figure 2]. Thus, the supertwisting algorithm shares unexpected features with first-order SMC. The second GE in the right-hand side of (58), namely, $-g(\tilde{x}_{1,k+1}) \in g_2h^2\text{sgn}(\tilde{x}_{1,k+1})$, is graphically represented just by rotating the curves in Figure 11, in a similar way as done in Figure 3.

The implicit discretization of the supertwisting algorithm yields a uniquely solvable GE, and contrarily to the twisting scheme, it possesses some internal maximal monotonicity property.

As noticed at the end of Section 2.4, the implicit discretization in that case has the interpretation of regularizing the signum set-valued function. Does it have the same effect for the supertwisting algorithm ? This is shown in Reference 53, however, with a different kind of implicit discretization.

Remark 9. Semi-implicit schemes have been proposed in [26, section III.B.2] for the supertwisting algorithm. However, their analysis is very partial. Nevertheless semi-implicit schemes may be an interesting option to reduce on-line computations and improve the chattering behavior compared with the explicit method.

4.2.2 | Discrete-time supertwisting design: Closed-loop analysis

Preliminary results have been obtained for mixed twisting and supertwisting observer,[40] supertwisting observer and implicit discretization,[26,44] where numerical simulations and the calculation of the controller are shown.

Definition 4. The discrete-time sliding surface is defined as $\Sigma_d = \{(\tilde{x}_{1,k}, v_k) \in \mathbb{R}^2 \mid \tilde{x}_{1,k} = 0,\ v_k = 0\}$.

Let us summarize now the stability results in Reference 36.

Theorem 5. *The following is true:*

1. *The unique fixed point of the unperturbed (or virtual) closed-loop system (58) is* $(\tilde{x}_1^\star, v^\star) = (0, 0)$.

2. *Assume that the discrete-time state belongs to Σ_d for all t_i, $i \leq k+1$. Then $x_{1,k} = h^2\lambda_2\xi^1_{k+1}$ for some $\xi^1_{k+1} \in [-1,1]$, while $x_{1,k+1} = h^2\lambda_2\xi^2_{k+1} + h\overline{\varphi}_k$ for some $\xi^2_{k+1} \in [-2,2]$. If $\tilde{x}_{1,k+2} = 0$ and $v_{k+1} = 0$, then $x_{1,k+1}$ will also satisfy $x_{1,k+1} = h^2\lambda_2\xi^1_{k+2}$ for some $\xi^1_{k+2} \in [-1,1]$.*

Suppose that the perturbation $\Delta(t) \equiv 0$.

1. *Let $g_1 > 0$ and $0 < g_2 < \frac{g_1^2}{2\sqrt{2}}$. Then the origin of the discrete-time closed-loop system (58), is globally asymptotically stable in the sense of Lyapunov.*
2. *The sliding surface Σ_d is attained in a finite number of steps and is invariant.*

The proof of the global asymptotic stability (second item 1) is not trivial. Indeed it relies on the fact that the continuous-time system (55) admits a continuous Lyapunov function with convex level sets, continuously differentiable outside the origin. Previously discovered Lyapunov functions[102-104] do not meet such requirements. The Lyapunov function is not explicitly designed in Reference 36, but its existence is proved using the implicit Lyapunov function approach.[105]

5 | HOMOGENEOUS SYSTEMS

The foregoing sections were dedicated to show that the implicit discretization of first-order SMC carries the nice properties of continuous-time SMC, to the digital implementation setting. It is of interest to look for generalizations and further applications of this powerful feature. A property of first-order SMC in Section 3, is the maximal monotonicity of the set-valued controller, which plays a crucial role in the well posedness of both the continuous and the discrete-time algorithms. In particular it appears to be very useful for the solvability and uniqueness of solutions to the GE blocks in Figures 4,5, and 7. This property is lost for second-order SMC in Section 4. Indeed the twisting algorithm set-valued part is not monotone, however, it is **d**-homogeneous with degree $\nu = -r$ for any weighted dilation $\mathbf{d}(s) = \mathrm{diag}(e^{rs}) \in \mathbb{R}^{2\times 2}$, $r > 0$, $s \in \mathbb{R}$. The supertwisting set-valued right-hand side is not monotone (though, as we saw, it has some internal monotonicity properties), but it is **d**-homogeneous with degree $\nu = -r$ for any weighted dilation $\mathbf{d}(s) = \mathrm{diag}(e^{rs}, e^{\frac{r}{2}s}) \in \mathbb{R}^{2\times 2}$, $r > 0$, $s \in \mathbb{R}$. These two examples suggest that the homogeneity property could be used for the study of HOSMC that could enable one to design discrete-time methods which keep the nice properties of continuous-time HOSMC after their digitalization. This is the objective of References 18,34.

5.1 | Motivating example

To explain the key idea of the later constructions, let us consider two scalar nonlinear control systems:[34]

$$\begin{cases} \dot{x}(t) = u(x(t)) \\ u(x) = -2\sqrt{|x|}\mathrm{sgn}(x) \end{cases} \quad y\sqrt{x}\mathrm{sgn}x) \Leftrightarrow \quad \begin{cases} \dot{y}(t) = \tilde{u}(y(t)) \\ \tilde{u}(y) \in -\mathrm{sgn}(y). \end{cases}$$

The first system (x-system) has a continuous right-hand side. The control u appears, for example, as a part of the supertwisting controller (see Section 4.1.3). The second system (y-system) is the conventional first-order sliding mode system (see Section 2). Both systems are finite-time stable, that is, the state of each system vanishes in a finite time. These two systems are topologically equivalent (homeomorphic on $\mathbb{R}$ and diffeomorphic on $\mathbb{R} \setminus \{0\}$). More precisely, if $x(\cdot, x_0)$ is the solution to the first system with $x(0) = x_0 \in \mathbb{R}$, then $y(\cdot, y_0) = \sqrt{|x(\cdot, x_0)|}\mathrm{sgn}(x(\cdot, x_0))$ is the solution to the second system with $y(0) = y_0 = \sqrt{|x_0|}\mathrm{sgn}(x_0)$, and vice versa. Both control systems admit an implicit Euler discretization as follows:

$$\begin{cases} x_{k+1} = x_k + hu_k \\ u_k = -2\sqrt{|x_{k+1}|}\mathrm{sgn}(x_{k+1}) \end{cases} \quad \Leftrightarrow \quad \begin{cases} y_{k+1} = y_k + h\tilde{u}_k \\ \tilde{u}_k \in -\mathrm{sgn}(y_{k+1}). \end{cases}$$

The topological equivalence between these two systems is destroyed after discretization. Indeed, for the first system one has

$$\begin{cases} x_{k+1} = (\sqrt{h^2 + |x_k|} - h)^2 \mathrm{sgn}(x_k) \neq 0 \\ u_k = 2(h - \sqrt{h^2 + |x_k|})\ \mathrm{sgn}(x_k) \end{cases} \quad \text{for all } k \geq 0,$$

provided that $x_0 \neq 0$, but the implicit scheme for the second equation gives (see Section 2 for the details)

$$y_{k+1} = \begin{cases} y_k - h\ \mathrm{sgn}(y_k) & \text{if} \quad |y_k| > h \\ 0 \quad \text{if} \quad |y_k| \leq h \end{cases}$$

$$u_k = \begin{cases} -\mathrm{sgn}(y_k) & \text{if} \quad |y_k| > h \\ -\frac{y_k}{h} \quad \text{if} \quad |y_k| \leq h. \end{cases}$$

Obviously, if $|x_k| \neq 0$, then

$$|x_{k+1}| \neq 0 \quad \text{and} \quad |x_{k+1}| = \gamma(x_k)|x_k|$$

with

$$\gamma(x_k) \stackrel{\Delta}{=} \left(\sqrt{\frac{h^2}{|x_k|} + 1} - \sqrt{\frac{h^2}{|x_k|}} \right)^2 \in (0,1), \quad k = 1, 2, \ldots .$$

In other words, the implicit discretization of the first equation is just asymptotically stable, but the implicit discretization of the second equation remains finite-time stable, see Theorem 1. We infer that the implicit discretization of the considered equivalent systems does not yield equivalent discrete-time models. Therefore, a reasonable way to discretize consistently the first (continuous) system is to use its equivalence with the second (discontinuous) one. Indeed, using solutions to the discretized second system we can recover the finite-time convergent solutions to the first dynamics by means of posterior transformation of coordinates $x = y^2\mathrm{sgn}(y)$. The proposed scheme is depicted in Figure 12, where $\Phi(\cdot)$ denotes a coordinate transformation to an equivalent system. It gives the following discrete-time model for the first system

$$\hat{x}_{k+1} = \begin{cases} (\sqrt{|\hat{x}_k|} - h)^2 \mathrm{sgn}(\hat{x}_k) & \text{if} \quad |\hat{x}_k| > h^2 \\ 0 \quad \text{if} \quad |\hat{x}_k| \leq h^2, \end{cases}$$

$$\hat{u}_k = \begin{cases} (h - 2\sqrt{|\hat{x}_k|})\ \mathrm{sgn}(\hat{x}_k) & \text{if} \quad |\hat{x}_k| > h^2 \\ -\frac{\hat{x}_k}{h} \quad \text{if} \quad |\hat{x}_k| \leq h^2, \end{cases}$$

with $\hat{x}_0 = x_0$. This system is expected to be finite-time stable. Indeed, if $|\hat{x}_0| > h^2$ then

$$|\hat{x}_{k+1}| = \hat{\gamma}(\hat{x}_k)|\hat{x}_k| \quad \text{with} \quad \hat{\gamma}(\hat{x}_k) \stackrel{\Delta}{=} \left(1 - \frac{h}{\sqrt{|\hat{x}_k|}}\right)^2 < \hat{\gamma}(\hat{x}_0) \in (0,1), \quad k = 1, 2, \ldots ,$$

and there exists $k_h \in \mathbb{N}$ such that $|\hat{x}_{k_h}| \leq h^2$, that is, $x_{k_h+1} = 0$. This example motivates us to conjecture that even continuous finite-time stable systems may have *a consistent discrete-time approximation* that preserves the finite-time stability property. A design of the corresponding discretization scheme is expected to be based on the transformation of the original system to an equivalent one, which admits a finite-time stable implicit discretization. Such an approach is useful for the discretization of the so-called quasi-continuous HOSM algorithms[12],[105-107] which, in some particular cases, may have a discontinuity only in one point of the state space.

[12]Quasi-continuous HOSM algorithms are continuous everywhere except at the HOSM set where the sliding variable and its derivatives vanish.[106] They are an extension of the so-called unit vector controllers.

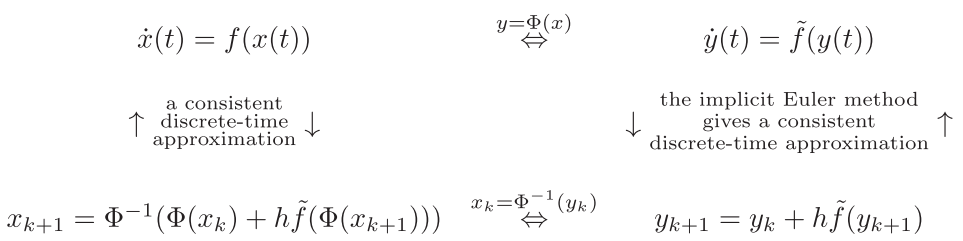

FIGURE 12 The proposed scheme of the consistent implicit discretization of $\dot{x}(t) = f(x(t))$

The key question is the existence of a coordinate transformation $\Phi(\cdot)$ (*see Figure* 12), *which allows the consistent discretization of the system in* $\mathbb{R}^n$. *In Reference* 34 *it has been shown that such a discretization exists for so-called* **d***-homogeneous differential equations and inclusions.*

5.2 | Homogeneity

5.2.1 | Linear dilations

In mathematical analysis, the symmetry of a function $f(\cdot)$ with respect to the *uniform dilation* of its argument $x \mapsto e^s x$, where $s \in \mathbb{R}$, is known as *homogeneity*. In the simplest case, it is defined as follows

$$f(e^s x) = e^{\nu s} f(x), \quad \text{for all } s \text{ and } x,$$

where $\nu \in \mathbb{R}$ is a constant parameter. In other words, homogeneity is a dilation symmetry. The latter is always needed for linearity that requires additionally the central symmetry $f(-x) = -f(x)$ and the additivity $f(x+y) = f(x) + f(y)$. Thus, all linear functions are homogeneous with respect to the uniform dilation. A *homogeneous mapping* is somewhere in-between essentially nonlinear and linear ones. In the 18th century the homogeneity with respect to the uniform dilation (the *standard homogeneity*) has been studied by Leonhard Euler. His notion of homogeneity is still well known in the context of the so-called homogeneous polynomials. Homogeneity of nonlinear systems is studied, for example, in References 95,108-112, see Reference 113 for a general presentation. Obviously, the sign function is standard homogeneous, indeed: $\operatorname{sgn}(e^s x) = e^{0s}\operatorname{sgn}(x) = \operatorname{sgn}(x)$ (at $x = 0$ this is understood as equality of sets). The standard homogeneity considered above has been introduced by means of the uniform dilation $x \mapsto e^s x$, $s \in \mathbb{R}$. It is clear that if we change the dilation rule to a nonuniform one, then another type of homogeneity can be defined. Below we deal with the so-called linear dilation,[114] which in $\mathbb{R}^n$ is given by the following definition.

Definition 5. A map $\mathbf{d} : \mathbb{R} \to \mathbb{R}^{n\times n}$ is called a linear **dilation** in $\mathbb{R}^n$ if it satisfies the three properties:

1. Group property: $\mathbf{d}(0) = I_n$ and $\mathbf{d}(t+s) = \mathbf{d}(t)\mathbf{d}(s) = \mathbf{d}(s)\mathbf{d}(t)$ for all $t, s \in \mathbb{R}$;
2. Continuity property: $\mathbf{d}(\cdot)$ is a continuous map, that is,

$$\forall t \in \mathbb{R}, \quad \forall \varepsilon > 0, \quad \exists \delta = \delta(t,\varepsilon) > 0 \quad : \quad |s-t| < \delta \quad \Rightarrow \quad \|\mathbf{d}(s) - \mathbf{d}(t)\| \le \varepsilon;$$

3. Limit property: $\lim_{s\to-\infty} \|\mathbf{d}(s)x\| = 0$ and $\lim_{s\to+\infty} \|\mathbf{d}(s)x\| = +\infty$ uniformly on the unit sphere $S \triangleq \{x \in \mathbb{R}^n \mid \|x\| = 1\}$.

The dilation $\mathbf{d}(\cdot)$ is a continuous group of invertible matrices $\mathbf{d}(s) \in \mathbb{R}^{n\times n}$, $\mathbf{d}(-s) = [\mathbf{d}(s)]^{-1}$. The dilation $\mathbf{d}(\cdot)$ can be utilized for the scaling of any vector x in $\mathbb{R}^n$ as $x \mapsto \mathbf{d}(s)x$. The most popular dilations in $\mathbb{R}^n$ are:

- *uniform-or standard-dilation* (L. Euler, 18th century) :

$$\mathbf{d}_1(s) = e^s I_n, \quad s \in \mathbb{R}, \tag{59}$$

- *weighted dilation*:[108]

$$\mathbf{d}_2(s) = \begin{pmatrix} e^{r_1 s} & 0 & \dots & 0 \\ 0 & e^{r_2 s} & \dots & 0 \\ \dots & \dots & \dots & \dots \\ 0 & 0 & \dots & e^{r_n s} \end{pmatrix}, \quad s \in \mathbb{R}, \quad r_i > 0, \quad i = 1, \dots, n. \tag{60}$$

The matrix $G_{\mathbf{d}} \in \mathbb{R}^{n\times n}$ defined as $G_{\mathbf{d}} = \lim_{s\to 0} \frac{\mathbf{d}(s)-I_n}{s}$, is known [115, chapter 1] as the generator of the group $\mathbf{d}(\cdot)$. It satisfies the property $\frac{d}{ds}\mathbf{d}(s) = G_{\mathbf{d}}\mathbf{d}(s)$, that is,

$$\mathbf{d}(s) = e^{G_{\mathbf{d}}s} = \sum_{i=0}^{+\infty} \frac{s^i G_{\mathbf{d}}^i}{i!}, \quad s \in \mathbb{R}. \tag{61}$$

The limit property implies that the generator $G_{\mathbf{d}}$ is an anti-Hurwitz matrix [13]. Obviously, the generator of the standard dilation is the identity matrix I_n, and the generator of the weighted dilation is a diagonal matrix with r_i on the main diagonal.

Definition 6. The dilation $\mathbf{d}(\cdot)$ is said to be *strictly monotone* if there exists $\beta > 0$ such that $\|\mathbf{d}(s)\| \le e^{\beta s}$ as $s \le 0$.

Strictly monotone dilations satisfy a coercivity condition [113, proposition 6.5]. The monotonicity of a dilation may depend on a norm $\|\cdot\|$ in $\mathbb{R}^n$. A dilation $\mathbf{d}$ in $\mathbb{R}^n$ is *strictly* monotone (see References 113,114 for more details) with respect to the weighted Euclidean norm $\|x\|_{\mathrm{P}} \stackrel{\Delta}{=} \sqrt{x^\top P x}$, provided that the matrix $P \in \mathbb{R}^{n\times n}$ satisfies the matrix inequalities

$$PG_{\mathbf{d}} + G_{\mathbf{d}}^\top P \succ 0, \quad P = P^\top \succ 0. \tag{62}$$

5.2.2 | Homogeneous functions and vector fields

Vector fields which are homogeneous with respect to dilation $\mathbf{d}(\cdot)$, have many properties useful for control design and state estimation of linear and nonlinear plants, as well as for analysis of convergence rates.[110,111,116] Most HOSM controllers are homogeneous[95,112] with respect to the weighted dilation (see above).

Definition 7. *A vector field $f : \mathbb{R}^n \to \mathbb{R}^n$ (resp. a function $h : \mathbb{R}^n \to \mathbb{R}$) is said to be $\mathbf{d}$-homogeneous if there exists $\nu \in \mathbb{R}$* such that

$$f(\mathbf{d}(s)x) = e^{\nu s}\mathbf{d}(s)f(x), \quad \forall x \in \mathbb{R}^n \setminus \{0\}, \quad \forall s \in \mathbb{R}. \tag{63}$$

$$(\text{resp. } h(\mathbf{d}(s)x) = e^{\nu s}h(x), \quad \forall x \in \mathbb{R}^n \setminus \{0\}, \quad \forall s \in \mathbb{R}.) \tag{64}$$

The number $\nu \in \mathbb{R}$ is called the homogeneity degree of the vector field $f(\cdot)$ (resp., of the functional $h(\cdot)$).

Example 3 (Homogeneity of the second-order sliding mode algorithms). Let $n = 2$ and

$$\mathbf{d}(s) = \begin{pmatrix} e^{2s} & 0 \\ 0 & e^{s} \end{pmatrix}, \quad s \in \mathbb{R}. \tag{65}$$

It is easy to check that the second-order sliding-mode control algorithms:[117]

- *twisting controller* : $u(x) \in -\alpha\mathrm{sgn}(x_1) - \beta\mathrm{sgn}(x_2), \alpha > 0, \beta > 0$,

[13] The matrix $G_{\mathbf{d}} \in \mathbb{R}^n$ is anti-Hurwitz if $-G_{\mathbf{d}}$ is Hurwitz.

- *nested controller* : $u(x) \in -\alpha \text{sgn}(x_1 + \beta x_2 |x_2|)$,
- *quasi-continuous controller*: $u(x) = -\alpha \frac{x_1 + \beta x_2 |x_2|}{|x_1| + \beta x_2^2}$,

are $\mathbf{d}$-homogeneous functions $\mathbb{R}^2 \to \mathbb{R}$, namely, $u(\mathbf{d}(s)x) = u(x)$, where $x = (x_1, x_2)^\top \in \mathbb{R}^2$.

For monotone dilations, the so-called *canonical homogeneous norm* $\|\cdot\|_{\mathbf{d}} : \mathbb{R}^n \to \mathbb{R}_+$ can be introduced as follows

$$\|x\|_{\mathbf{d}} = e^{s_x} \quad \text{where} \quad s_x \in \mathbb{R} \ \text{ is such that } \ \|\mathbf{d}(-s_x)x\| = 1. \tag{66}$$

Obviously, $\|\cdot\|_{\mathbf{d}}$ is a $\mathbf{d}$-homogeneous function, $\|\mathbf{d}(s)x\|_{\mathbf{d}} = e^s \|x\|_{\mathbf{d}}$. The homogeneous norm is not a norm in the usual sense, since, for example, the triangle inequality may not hold. However, it can be shown that it is a norm in a Euclidean space homeomorphic to $\mathbb{R}^n$. If $\mathbf{d}(\cdot)$ is the standard dilation (see (59)), then $\|u\|_{\mathbf{d}} = \|u\|$.

Proposition 4. [114] *If* $\mathbf{d}(\cdot)$ *is a strictly monotone dilation then :*

- *the canonical homogeneous norm* $\|\cdot\|_{\mathbf{d}}$ *is Lipschitz continuous on* $\mathbb{R}^n \setminus \{0\}$*;*
- *if a norm* $\|\cdot\|$ *is smooth outside the origin, then the homogeneous norm* $\|\cdot\|_{\mathbf{d}}$ *is also smooth outside the origin,* $\frac{d\|\mathbf{d}(-s)x\|}{ds} < 0$ *if* $s \in \mathbb{R}$, $x \in \mathbb{R}^n \setminus \{0\}$ *and*

$$\frac{\partial \|x\|_{\mathbf{d}}}{\partial x} = \left. \frac{\|x\|_{\mathbf{d}} \frac{\partial \|z\|}{\partial z}\Big|_{z=\mathbf{d}(-s)x}}{\frac{\partial \|z\|}{\partial z}\Big|_{z=\mathbf{d}(-s)x} G_{\mathbf{d}} \mathbf{d}(-s)x} \right|_{s=\ln \|x\|_{\mathbf{d}}}. \tag{67}$$

The canonical homogeneous norm is utilized in most of the constructions below.

5.2.3 | Homogeneous differential equations

The homogeneity can be inherited by other mathematical objects induced by homogeneous functions. For example, solutions to homogeneous differential equations are symmetric in a certain sense.[108,110,111,118] Namely, if $f : \mathbb{R}^n \to \mathbb{R}^n$ is $\mathbf{d}$-homogeneous of degree $\nu \in \mathbb{R}$, and if $\varphi_{x_0} : [0, T) \to \mathbb{R}^n$ is a solution to

$$\dot{x}(t) = f(x(t)), \tag{68}$$

with the initial condition $x(0) = x_0 \in \mathbb{R}^n$, then $\varphi_{\mathbf{d}(s)x_0} : [0, e^{-\nu s}T) \to \mathbb{R}^n$ defined as

$$\varphi_{\mathbf{d}(s)x_0}(t) = \mathbf{d}(s)\varphi_{x_0}(te^{\nu s}), \quad s \in \mathbb{R}$$

is a solution to (68) with the initial condition $x(0) = \mathbf{d}(s)x_0$. The latter property implies many corollaries. For instance, local asymptotic stability is equivalent to global asymptotic stability.

Theorem 6 [114] *Let the vector field* $f : \mathbb{R}^n \to \mathbb{R}^n$ *be* $\mathbf{d}$*-homogeneous of degree* $\nu \in \mathbb{R}$ *and continuous on* $\mathbb{R}^n \setminus \{0\}$*. The following five claims are equivalent one to each other:*

1) *The origin of the system (68) is asymptotically stable.*
2) *There exists a* $\mathbf{d}$*-homogeneous Lyapunov function* $V \in C(\mathbb{R}^n) \cap C^\infty(\mathbb{R}^n \setminus \{0\})$ *for the system (68).*
3) *The origin of the system*

$$\dot{y}(t) = \|y(t)\|_P^{1+\nu} \left(\frac{(I_n - G_{\mathbf{d}})y(t)y(t)^\top P}{y(t)^\top P G_{\mathbf{d}} y(t)} + I_n \right) f\left(\frac{y(t)}{\|y(t)\|_P} \right) \tag{69}$$

is asymptotically stable, where we recall that $\|y\|_P \stackrel{\Delta}{=} \sqrt{y^\top P y}$*, and the matrix* $P \in \mathbb{R}^{n \times n}$ *satisfies (62).*

4) *For any matrix $P \in \mathbb{R}^{n\times n}$ satisfying (62), there exists a* $\mathbf{d}$*-homogeneous vector field $\Psi : \mathbb{R}^n \to \mathbb{R}^n$ of degree zero such that $\Psi \in C(\mathbb{R}^n) \cap C^\infty(\mathbb{R}^n \setminus \{0\})$, $\Psi(\cdot)$ is a diffeomorphism on $\mathbb{R}^n \setminus \{0\}$, a homeomorphism on $\mathbb{R}^n$, $\Psi(0) = 0$ and*

$$\frac{\partial(\Psi^\top(x)P\,\Psi(x))}{\partial x} f(x) < 0 \quad \text{if} \quad \Psi^\top(x)P\Psi(x) = 1. \tag{70}$$

Moreover, $\|\Psi\|_{\mathbf{d}} \in C(\mathbb{R}^n) \cap C^\infty(\mathbb{R}^n \setminus \{0\})$ is a Lyapunov function for the system (68).

5) *For any matrix $P \in \mathbb{R}^{n\times n}$ satisfying (62), there exists a matrix-valued mapping $\Xi \in C^\infty(\mathbb{R}^n \setminus \{0\}, \mathbb{R}^{n\times n})$ such that*

$$\det(\Xi(y)) \neq 0, \quad \frac{\partial \Xi(y)}{\partial y_i} y = 0, \quad \Xi(e^s y) = \Xi(y)$$

$$\text{for } y = (y_1, \dots, y_n)^\top \in \mathbb{R}^n \setminus \{0\}, \quad s \in \mathbb{R}, \quad i = 1, \dots, n$$

and

$$y^\top \Xi^\top(y) P \Xi(y) \left(\frac{(I_n - G_{\mathbf{d}})yy^\top P}{y^\top P G_{\mathbf{d}} y} + I_n \right) f\left(\frac{y}{\|y\|_P} \right) < 0. \tag{71}$$

This theorem proves the following important facts:

- Any $\mathbf{d}$-homogeneous system (68) is homeomorphic on $\mathbb{R}^n$ and diffeomorphic on $\mathbb{R}^n \setminus \{0\}$ to the standard homogeneous one (69). The corresponding change of coordinates is given by

$$y = \Phi(x) \stackrel{\Delta}{=} \|x\|_{\mathbf{d}} \mathbf{d}(-\ln \|x\|_{\mathbf{d}})x, \tag{72}$$

while the inverse transformation is as follows:

$$x = \Phi^{-1}(y) \stackrel{\Delta}{=} \mathbf{d}(\ln \|y\|_P) \frac{y}{\|y\|_P}. \tag{73}$$

The transformation $\Phi(\cdot)$ is utilized below for a construction of the consistent discretization of the differential Equation (68) (see Figure 12). For the motivating example in Figure 12, one has $r = 2$, $\mathbf{d}(s) = e^{2s}$, $\nu = -1$, $|x|_{\mathbf{d}} = \sqrt{|x|}$, and $\mathbf{d}(-\ln \|x\|_{\mathbf{d}})x = \frac{x}{|x|} = \operatorname{sgn}(x)$, and $\mathbf{d}(\ln(|y|)) = y^2$ so that $x = |y|y = y^2\operatorname{sgn}(y)$.

- As a consequence of Theorem 6, item 4), we conclude that if the inequalities (62) and

$$x^\top P f(x) < 0 \quad \text{for all } x \in \mathbb{R}^n \text{ such that } \|x\|_P = 1 \tag{74}$$

hold, then the canonical homogeneous norm $\|\cdot\|_{\mathbf{d}}$ is a Lyapunov function for the system (68). Indeed, from the formula (67) and $\mathbf{d}$-homogeneity of $f(\cdot)$ we derive

$$\frac{\partial \|x\|_{\mathbf{d}}}{\partial x} f(x) < 0, \quad \forall x \in \mathbb{R}^n \setminus \{0\} \quad \Leftrightarrow \quad z^\top P f(z) < 0, \quad \|z\|_P = 1,$$

provided that $\|x\|_{\mathbf{d}}$ is induced by the norm $\|x\|_P$ with P satisfying (62).

- Any asymptotically stable generalized homogeneous system is homeomorphic on $\mathbb{R}^n$ and diffeomorphic on $\mathbb{R}^n \setminus \{0\}$ to a quadratically stable one. Indeed, let

$$\dot{\xi} = g(\xi) \tag{75}$$

be an asymptotically stable $\mathbf{d}$-homogeneous system. Then making the change of variables

$$x = \Psi(\xi),$$

$$\Psi(\xi) = \mathbf{d}\left(\ln \frac{V^{1/\mu}(\xi)}{\|\xi\|_{\mathbf{d}}}\right)\xi, \qquad \Psi^{-1}(x) = \mathbf{d}\left(-\ln \frac{V^{1/\mu}(x)}{\|x\|_{\mathbf{d}}}\right)x, \tag{76}$$

where $\mu > 0$ is the homogeneity degree of the $\mathbf{d}$-homogeneous Lyapunov function $V(\cdot)$, we derive

$$\dot{x}(t) = f(x(t)) \stackrel{\Delta}{=} \frac{\partial \Psi}{\partial \xi}(\xi(t))g(\xi(t))\Big|_{\xi(t)=\Psi^{-1}(x(t))}. \tag{77}$$

Since $\|x\|_{\mathbf{d}} = \|\Psi(\xi)\|_{\mathbf{d}} = V^{1/\mu}(\xi)$ then the canonical homogeneous norm $\|\cdot\|_{\mathbf{d}}$ induced by $\|x\|_P$ with P satisfying (62) is a Lyapunov function to the latter system and $x(t)^\top P\dot{x}(t) < 0$ if $x(t)^\top Px(t) = 1$. Finally, the change of variable $y = \Phi(x) = \|x\|_{\mathbf{d}}\mathbf{d}(-\ln\|x\|_{\mathbf{d}})x$ gives $\|x\|_{\mathbf{d}} = \|y\|_P$, so the transformed system

$$\dot{y}(t) = \tilde{f}(y(t)) \tag{78}$$

is quadratically stable with the Lyapunov function $V(\cdot)$ defined as $V(y) = \|y\|_P^2$, where

$$\tilde{f}(y) \stackrel{\Delta}{=} \|y\|_P^{1+\nu}\left(\frac{(I_n - G_{\mathbf{d}})yy^\top P}{y^\top PG_{\mathbf{d}}y} + I_n\right) f\left(\frac{y}{\|y\|_P}\right). \tag{79}$$

Notice that the latter theorem has been originally proven for vector fields continuous outside the origin (like, eg, quasi-continuous sliding mode algorithms). Recently,[119] this result has been extended to discontinuous differential equations and to differential inclusions.

5.3 | Consistent discretization of finite-time stable homogeneous systems

Let us consider the nonlinear system

$$\dot{x}(t) = f(x(t)), \quad t > 0, \quad x(0) = x_0, \tag{80}$$

where $x(t) \in \mathbb{R}^n$ is the system's state and the nonlinear function $f : \mathbb{R}^n \to \mathbb{R}^n$ is continuous on $\mathbb{R}^n \setminus \{0\}$, that is, the only possible discontinuity point of $f(\cdot)$ is the origin. Such a vector field is said to be quasi-continuous. The system (80) is assumed to be forward complete for solutions understood in the sense of Filippov:[120] an absolutely continuous function $\phi(\cdot, x_0) : [0, +\infty) \to \mathbb{R}^n$ is a solution to (80) if $\phi(0, x_0) = x_0$ and for almost all $t > 0$ it satisfies the differential inclusion

$$\dot{x}(t) \in F(x(t)) = \bigcap_{\varepsilon>0}\bigcap_{\mu(N)=0} \overline{\text{co}} f(x(t) + \varepsilon\mathbb{B}_n \setminus \{N\}), \tag{81}$$

where co denotes the convex hull, $\overline{\text{co}}$ is its closure, and $\mu(N) = 0$ means that the Lebesgue measure of the set $N \subset \mathbb{R}^n$ is zero. Thus, in our case, $F(x) = \{f(x)\}$ is a singleton for $x \in \mathbb{R}^n \setminus \{0\}$, but $F(0) = \cap_{\varepsilon>0}\overline{\text{co}} f(\varepsilon\mathbb{B}_n \setminus \{0\})$ is a set if $f(\cdot)$ is discontinuous at 0. Recall[95,121,122] that the origin of the system (80) is said to be globally uniformly *finite-time stable*, if it is Lyapunov stable and there exists a locally bounded function $T : \mathbb{R}^n \to [0, +\infty)$ such that any solution $\phi(\cdot, x_0)$ to (80) satisfies $\phi(t, x_0) = 0$ for $t \geq T(x_0)$.

Remark 10. Notice that the vector fields $f(\cdot)$ for the twisting and the supertwisting algorithms studied in Section 4 have discontinuities outside the origin, thus they cannot be studied by results presented in this section. However, the material presented in Reference 34 can be extended the more general case of discontinuous ODEs embedded into Filippov's framework, see Reference 123.

The consistency of the discretization scheme for the finite-time stable system (80) is understood in the sense of the following definition.

Definition 8 [34] A (possibly) set-valued mapping $Q : \mathbb{R}_+ \times \mathbb{R}^n \times \mathbb{R}^n \rightrightarrows \mathbb{R}^n$ is said to be a consistent discrete-time approximation of the globally uniformly finite-time stable system (80) if

1. Existence property: for any $\tilde{x} \in \mathbb{R}^n$ and any $h > 0$, there exists $\tilde{x}_h \in \mathbb{R}^n$ such that:

$$0 \in Q(h, \tilde{x}, \tilde{x}_h), \tag{82}$$

and $\tilde{x}_h = 0$ is the unique solution to the GE: $0 \in Q(h, 0, \tilde{x}_h)$.
2. Finite-time convergence property: for any $h > 0$ each sequence

$$\{x_k\}_{k=0}^{+\infty} \tag{83}$$

generated by the GE

$$0 \in Q(h, x_k, x_{k+1}), \quad k = 0, 1, 2, \ldots . \tag{84}$$

converges to zero in a finite number of steps, that is, for any $x_0 \in \mathbb{R}^n \setminus \{0\}$ there exists $k^* > 0$ such that

$$x_k = 0 \quad \text{for} \quad k \geq k^*.$$

3. Approximation property: for any $\varepsilon > 0$ and any $R > \varepsilon$, there exists $\omega \in \mathcal{K}$ such that any sequence (83) generated by (84) satisfies

$$\|\phi(h, x_k) - x_{k+1}\| \leq h\ \omega(h), \tag{85}$$

provided that $\|x_{k+1}\|, \|x_k\| \in [\varepsilon, R]$, where $\phi(\cdot, x_k)$ is a solution to (80) with the initial condition $x(0) = x_k$.

Notice that the last property in this definition requires the existence of the conventional estimate (85) for the discretization error on any compact set from $\mathbb{R}^n \setminus \{0\}$ (since $\varepsilon > 0$ and $R > \varepsilon$ can be selected arbitrary small and arbitrary large, respectively). The origin is excluded because of a possible singularity of the vector field $f(\cdot)$ at zero (it can be discontinuous at the origin). The inequality (85) describes local (one-step) approximation error. An approximation error on the time interval $[0, T(x_0)]$ is $O(\omega(h))$ provided that $h = \frac{T(x_0)}{N}$ with $N \in \mathbb{N}$. This error tends to zero as $h \to 0$, that is, as $N \to +\infty$.

In Sections 2 to 5, the implicit discretization is essentially based on maximal monotone operators. Such maximal monotonicity of the set-valued operator in a GE like (82) guarantees existence and uniqueness of its solution. Homogeneity is an another sort of monotonicity. Below we show that it always guarantees an existence of solutions to GE, but the uniqueness of solutions is not proven in the general case.

The next theorem formalizes the scheme in Figure 12.

Theorem 7 [34] *Let a vector field $f : \mathbb{R}^n \to \mathbb{R}^n$ be uniformly continuous on the unit sphere $S = \{x \in \mathbb{R}^n \mid \|x\| = 1\}$ and $\mathbf{d}$-homogeneous of degree -1. Let*

$$\tilde{f}(y) \triangleq \left(\frac{(I - G_{\mathbf{d}})yy^\top P}{y^\top G_{\mathbf{d}} P y} + I_n \right) f\left(\frac{y}{\|y\|_P} \right), \quad y \in \mathbb{R}^n \setminus \{0\}, \tag{86}$$

where $G_{\mathbf{d}}$ is the generator of the dilation $\mathbf{d}(\cdot)$ and $P \in \mathbb{R}^{n \times n}$ satisfies (62). If the condition (71) holds with $\Xi = I_n$, then the map $Q : \mathbb{R}_+ \times \mathbb{R}^n \times \mathbb{R}^n \rightrightarrows \mathbb{R}^n$ defined as

$$\begin{aligned} Q(h, x_k, x_{k+1}) &= \tilde{Q}(h, \Phi(x_k), \Phi(x_{k+1})), \\ \Phi(x) &= \|x\|_{\mathbf{d}}\ \mathbf{d}(-\ln \|x\|_{\mathbf{d}})x \end{aligned} \tag{87}$$

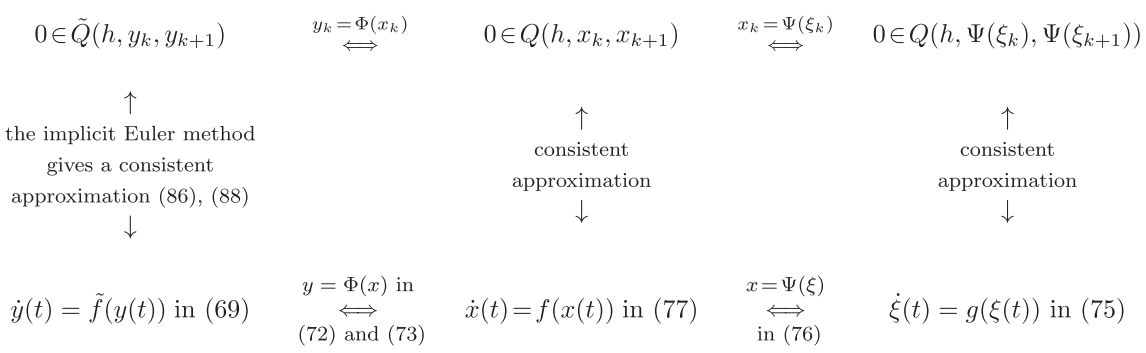

FIGURE 13 Recapitulation of various state space changes

where $h>0$ and

$$\begin{aligned}\tilde{Q}(h,y_k,y_{k+1})&=y_{k+1}-y_k-h\tilde{F}(y_{k+1}),\\ \tilde{F}(y)&=\bigcap_{\varepsilon>0}\overline{\text{co}}\tilde{f}(y+\varepsilon\mathbb{B}_n\setminus\{0\}),\end{aligned}\tag{88}$$

is a consistent discrete-time approximation of the finite-time stable system (80).

Notice that the change of the dilation $\mathbf{d}_\alpha(s)\overset{\Delta}{=}\mathbf{d}(\alpha s),\alpha>0$, implies the change of the homogeneity degree $\nu_\alpha\overset{\Delta}{=}\alpha\nu$ of the vector field $f(\cdot)$. If the homogeneous is finite-time stable then $\nu<0$ and selecting $\alpha=1/|\nu|$, we derive $\nu_\alpha=-1$. Therefore, the assumption that the homogeneity degree of $f(\cdot)$ equals to -1, is not restrictive at all. The latter theorem is also based on the assumption that the system $\dot{y}(t)=\tilde{f}(y(t))$ admits a quadratic Lyapunov function (see the condition (71) with Ξ =const). Notice that if the canonical homogeneous norm $\|\cdot\|_{\mathbf{d}}$ is a Lyapunov function of the system (80) then $\Xi=I_n$ and $y^\top P\tilde{f}(y)=y^\top Pf(y)<0$. However, since any stable homogeneous system is equivalent to a quadratically stable one (see the remarks after Theorem 6), then we conclude the following:

Any **d***-homogeneous finite-time stable system as* (80) *with a possible discontinuity at the origin satisfies all conditions of Theorem* 7 *possibly after the change of coordinate $x\mapsto\Psi(x)$ and the change of the dilation group $\mathbf{d}_\alpha(s)=\mathbf{d}(\alpha s),\alpha>0$.*

5.4 | Recapitulation

The foregoing developments which form the basis for the design of consistent numerical schemes, are summarized in Figure 13. The transformation $\Psi(\cdot)$ brings the original system to a system, which has a Lyapunov function in the form of the canonical homogeneous norm induced by $\|\cdot\|_P$. This transformation is not required if the original system has a strictly positively invariant ellipsoidal set $\{x|x^\top Px\le 1\}$ with a shape matrix P satisfying (62). In the latter case the inequality (70) holds for $\Psi(x)=x$. All examples considered in this section do not require the transformation coordinate $\Psi(\cdot)$.

Example 4 (Homogeneous system, $n=3$). Let us consider the chain of integrators $\dot{x}_1(t)=x_2(t),\dot{x}_2(t)=x_3(t),\dot{x}_3(t)=u(t)$. It is known [111, proposition 8.1] that the continuous, non-Lipschitz controller

$$u(x)=-k_1\text{sgn}(x_1)|x_1|^{\frac{\alpha}{3-2\alpha}}-k_2\text{sgn}(x_2)|x_2|^{\frac{\alpha}{1-\alpha}}-k_2\text{sgn}(x_3)|x_3|^{\alpha}\tag{89}$$

renders the origin globally finite-time stable provided that the matrix $\begin{pmatrix}0&1&0\\0&0&1\\-k_1&-k_2&-k_3\end{pmatrix}$ is Hurwitz and $\alpha\in(0,1)$ is sufficiently close to 1. One can check that the closed-loop system is **d**-homogeneous with degree $\nu=-1$, and the weighted dilation $\mathbf{d}(s)=\begin{pmatrix}e^{\frac{3-2\alpha}{1-\alpha}s}&0&0\\0&e^{\frac{2-\alpha}{1-\alpha}s}&0\\0&0&e^{\frac{1}{1-\alpha}s}\end{pmatrix}$. Let us discretize the system with an implicit method as follows:

$$\begin{pmatrix} x_{1,k+1} = x_{1,k} + hx_{2,k+1} \\ x_{2,k+1} = x_{2,k} + hx_{3,k+1} \\ x_{3,k+1} = x_{3,k} + hu_k \\ u_k = -\mathrm{sgn}(x_{1,k+1})|x_{1,k+1}|^{\frac{1}{2}} - \frac{3}{2}\mathrm{sgn}(x_{2,k+1})|x_{2,k+1}|^{\frac{3}{5}} - \frac{3}{2}\mathrm{sgn}(x_{3,k+1})|x_{3,k+1}|^{\frac{3}{4}} \end{pmatrix}. \tag{90}$$

Few manipulations yield $x_{1,k+1} = x_{1,k} + hx_{2,k} + h^2x_{3,k} + h^3u_k$, that is:

$$\begin{aligned} x_{1,k+1} = \; & x_{1,k} + hx_{2,k} + h^2x_{3,k} - \underbrace{h^3\mathrm{sgn}(x_{1,k+1})|x_{1,k+1}|^{\frac{1}{2}}}_{\triangleq f_1(x_{1,k+1})} - \underbrace{\frac{3}{2}h^{\frac{12}{5}}\mathrm{sgn}(x_{1,k+1} - x_{1,k})|x_{1,k+1} - x_{1,k}|^{\frac{3}{5}}}_{\triangleq f_2(x_{1,k+1})} \\ & \underbrace{-\frac{3}{2}h^{\frac{9}{4}}\mathrm{sgn}(x_{1,k+1} - x_{1,k} - hx_{2,k})|x_{1,k+1} - x_{1,k} - hx_{2,k}|^{\frac{3}{4}}}_{\triangleq f_3(x_{1,k+1})}. \end{aligned} \tag{91}$$

The function $x_{1,k+1} \mapsto f_1(x_{1,k+1}) + f_2(x_{1,k+1}) + f_3(x_{1,k+1})$ defines a strictly monotone (increasing) function of $x_{1,k+1}$, hence one infers that the nonlinear equation (91) possesses a unique solution for any $x_{1,k} + hx_{2,k} + h^2x_{3,k}$ (we do not discuss here the numerical algorithm needed to solve on-line this nonlinear non-Lipschitz equation). Moreover, the sliding surface $\Sigma_d = \{(x_{1,k}, x_{2,k}, x_{3,k}) \mid x_{1,k} = 0, x_{2,k} = 0, x_{3,k} = 0\}$ is invariant, as it follows from the dynamics

$$x_{1,k+1} = -\left(h^3|x_{1,k+1}|^{\frac{1}{2}} + \frac{3}{2}h^{\frac{12}{5}}|x_{1,k+1}|^{\frac{3}{5}} + \frac{3}{2}h^{\frac{9}{4}}|x_{1,k+1}|^{\frac{3}{4}}\right)\mathrm{sgn}(x_{1,k+1})$$

obtained from (91), setting $x_{1,k} = 0, x_{2,k} = 0, x_{3,k} = 0$: the only solution to this equation is $x_{1,k+1} = 0$, and invariance follows from $x_{2,k+1} = \frac{x_{1,k+1} - x_{1,k}}{h} = 0$, $x_{3,k+1} = \frac{x_{2,k+1} - x_{2,k}}{h} = 0$. This is the first property of the consistency in [34, definition 2.1]. The scalar example treated in [34, section 1.1] shows that it is hopeless to guarantee finite-time convergence of the scheme in (91). Let us now proceed with the derivation of a consistent method. Let $P = P^\top \in \mathbb{R}^{3\times 3}$ be selected such that

$$P\begin{pmatrix} 0 & 1 & 0 \\ 0 & 0 & 1 \\ -k_1 & -k_2 & -k_3 \end{pmatrix} + \begin{pmatrix} 0 & 1 & 0 \\ 0 & 0 & 1 \\ -k_1 & -k_2 & -k_3 \end{pmatrix}^\top P \prec 0, \quad PG_{\mathbf{d}} + G_{\mathbf{d}}P \succ 0, \quad P \succ 0,$$

where $G_{\mathbf{d}} = \begin{pmatrix} \frac{3-2\alpha}{1-\alpha} & 0 & 0 \\ 0 & \frac{2-\alpha}{1-\alpha} & 0 \\ 0 & 0 & \frac{1}{1-\alpha} \end{pmatrix}$ is the generator of the dilation. Such selection is always possible provided that $\alpha \in (0, 1)$ is sufficiently close to 1. This immediately implies that the canonical homogeneous norm $\|\cdot\|_{\mathbf{d}}$ is a Lyapunov function of the considered system. It can be checked that all conditions of Theorem 7 are fulfilled for

$$f(x) = \begin{pmatrix} x_2 \\ x_3 \\ u(x) \end{pmatrix}.$$

From Theorem 6 and the degree $\nu = -1$, we conclude that the equivalent system has the form

$$\dot{y}(t) = \tilde{f}(y) = \frac{y^T P f(\frac{y}{\|y\|_P})}{y^T P G_{\mathbf{d}} y}(I_3 - G_{\mathbf{d}})y + f\left(\frac{y}{\|y\|_P}\right),$$

and it is asymptotically stable, where $P = P^T \succ 0$ and $y = \Phi(x) = \|x\|_{\mathbf{d}}\mathbf{d}(-\ln\|x\|_{\mathbf{d}})x$. We therefore obtain that a consistent discrete-time mode of the considered system is given by (87),(88) with

$$\tilde{F}(y) = \begin{cases} \tilde{f}(y) & \text{if} \quad y \neq 0 \\ \overline{\text{co}}\tilde{f}(\mathbb{B}_3^P) & \text{if} \quad y = 0, \end{cases}$$

where $\mathbb{B}_3^P$ is the unit ball in the metric defined by P.

Remark 11. Some comments arise about the Lyapunov function. Under homogeneity and asymptotic stability, [111, theorem 6.2] states the existence of a homogeneous Lyapunov function, and [34, theorem 3.8 (1)] states the existence of a homogeneous and infinitely differentiable Lyapunov function. In Reference 124 Lyapunov functions of arbitrarily large degree of differentiability are derived for similar controllers as (89). Their use to derive consistent numerical schemes is not trivial, however, as they may be lacking the central symmetry property.

5.5 | Maximal monotonicity and homogeneity

As alluded to above, first-order SMCs rely essentially on maximal monotonicity of the set-valued operators, which greatly facilitates the design of efficient GE solvers, while HOSMCs in this section rely on homogeneity. It is of interest to study the relationship between both properties. Since $\tilde{F}(x) = \{\tilde{f}(x)\}$ for $x \neq 0$ we conclude that $-\tilde{F}(\cdot)$ in (88) may be a maximal monotone operator only if $-\tilde{f}(\cdot)$ is a monotone operator on $\mathbb{R}^n \setminus \{0\}$. A necessary and sufficient condition of maximal monotonicity of the vector field $-\tilde{f}(\cdot)$ is given below.

Lemma 1. *Let $\tilde{f}(\cdot)$ satisfy all conditions of Theorem 7. Then the mapping $-\tilde{f}(\cdot)$ is a maximal monotone operator on $\mathbb{R}^n \setminus \{0\}$ if and only if*

$$\tilde{f}^\top(y_1)Py_1 \leq \tilde{f}^\top(y_2)Py_1 \quad \text{for all } \; y_1, y_2 \in S \stackrel{\Delta}{=} \{y \in \mathbb{R}^n \mid y^\top Py = 1\}. \tag{92}$$

Proof. Sufficiency $\Leftarrow=$: By definition, $-\tilde{f}(\cdot)$ is monotone on $\mathbb{R}^n \setminus \{0\}$ if

$$(-\tilde{f}(x_1) + \tilde{f}(x_2))^\top P(x_1 - x_2) \geq 0, \quad \text{for all } x_1, x_2 \in \mathbb{R}^n \setminus \{0\},$$

with the inner product $\langle x,y\rangle = x^T Py$. Since $\tilde{f}(x) = \tilde{f}(x/\|x\|_P)$ for all $x \neq 0$, then dividing both sides of the latter inequality by $\|x_1\|_P$ we conclude that the monotonicity condition is equivalent to

$$m(\alpha, y_1, y_2) \stackrel{\Delta}{=} (-\tilde{f}(y_1) + \tilde{f}(\alpha y_2))^\top P(y_1 - \alpha y_2) \geq 0 \quad \text{for all } y_1, y_2 \in S \text{ and for all } \alpha > 0.$$

We have $m(\alpha, y_1, y_2) = -\tilde{f}^\top(y_1)Py_1 - \alpha\tilde{f}^\top(y_2)Py_2 + \tilde{f}^\top(y_2)Py_1 + \alpha\tilde{f}^\top(y_1)Py_2$, and

$$\frac{\partial m}{\partial \alpha} = -\tilde{f}^\top(y_2)Py_2 + f^\top(y_1)Py_2 \geq C \stackrel{\Delta}{=} \inf_{y_1, y_2 \in S}(-\tilde{f}^\top(y_2)Py_2 + f^\top(y_1)Py_2 \geq 0.$$

On the other hand, we have

$$m(\alpha) \to m_0(y_1, y_2) \stackrel{\Delta}{=} -\tilde{f}^\top(y_1)Py_1 + \tilde{f}^\top(y_2)Py_1 \quad \text{as} \quad \alpha \to 0.$$

Thus, using (92) it follows that $\inf_{y_1, y_2 \in S} m_0(y_1, y_2) = C \geq 0$, and $m(\alpha, y_1, y_2) \geq 0$ for all $y_1, y_2 \in S$ and all $\alpha > 0$, that is, $-\tilde{f}(\cdot)$ is monotone on $\mathbb{R}^n \setminus \{0\}$.

Necessity $\Rightarrow$: If $-\tilde{f}(\cdot)$ is monotone then letting $\alpha \to 0$ yields (92). The proof is complete. ∎

The condition of maximal monotonicity given in Lemma 1 *is a very rare property. It holds, for example, if* $\tilde{f}(y) = -\frac{y}{\|y\|}$. *By contrast to the case of monotone operators, computational schemes for solving of GE with homogeneous operators are not developed yet in the general case. However, in some particular cases, solutions can be found by means of proper computational algorithms.*

5.6 | On step-varying discretization of homogeneous systems

A rather simple scheme for numerical simulation of nonlinear homogeneous systems has been proposed in Reference 125. Key idea consist in a scaling of a discretization step dependently of the homogeneous norm of the state and the homogeneity degree of the system. The Euler explicit scheme in this case becomes

$$x_{i+1} = x_i + \frac{h}{p^{\nu}(x_i)} f(x_i), \quad x_i, x_{i+1} \in \mathbb{R}^n, \tag{93}$$

where ν is homogeneity degree of the vector field $f(\cdot)$ and $p : \mathbb{R}^n \to \mathbb{R}$ is a homogeneous norm in $\mathbb{R}^n$, that is, $p(\cdot)$ is positive definite and $p(\mathbf{d}(s)x) = e^s p(x)$, for all $x \in \mathbb{R}^n$, for all $s \in \mathbb{R}$. Obviously that the term $\frac{h}{p^{\nu}(x)}$ defines a discretization step of the explicit Euler method. For the weighted dilation

$$\mathbf{d}(s) = \mathrm{diag}\{e^{r_1 s}, e^{r_2 s}, \ldots, e^{r_n s}\}, \quad r_i > 0, \quad s \in \mathbb{R},$$

the authors of Reference 125 suggest the following selection of the homogeneous norm

$$p(z) = \|z\|_r \stackrel{\Delta}{=} \left(\sum_{i=1}^{n} |z_i|^{\frac{\rho}{r_i}} \right)^{\frac{1}{\rho}}, \quad \rho > 0, \quad z = (z_1, \ldots z_n)^{\top} \in \mathbb{R}^n,$$

and show that for a sufficiently small $h > 0$ the discrete-time system (93) is globally uniformly asymptotically stable, provided that the original system (80) is asymptotically stable as well. Recall that the classical explicit Euler discretization (with a constant step) is never globally asymptotically stable for homogeneous systems with positive degrees[17] and never locally asymptotically stable for homogeneous systems with negative degrees.[18] The suggested state-dependent discretization scheme solves this problem.

For $\nu < 0$ the asymptotically stable homogeneous system (80) is finite-time stable. In this case the discretization step $\frac{h}{\|x\|_r^{\nu}} \to 0$ as $\|x\| \to 0$. This does not allow the system (93) to converge to zero in a finite-time number of steps and, formally, it is not consistent in the sense of the above definition. However, the sum of the discretization steps always remains bounded

$$\tilde{T}(x_0) = \sum_{i=0}^{\infty} \frac{h}{\|x_i\|_r} < +\infty,$$

where the number can be treated as estimation of the settling time of the original continuous-time system. A trajectory of the finite-time stable continuous-time system (80) on a time interval $[0, T(x_0)]$, where T is the settling-time function, is approximated by a trajectory of the discrete-time system (93) for $i \to +\infty$ and $\tilde{T}(x_0) \to T(x_0)$ as $h \to 0$. In Reference 125 it shown that the implicit scheme

$$x_{i+1} = x_i + \frac{h}{p^{\nu}(x_{i+1})} f(x_{i+11}), \quad x_1, x_{i+1} \in \mathbb{R}^n,$$

has the same properties.

5.7 | Example 1: Discretization of the quasi-continuous second-order SMC

Let us now proceed in the following sections, with examples of homogeneous controllers.

5.7.1 | Quasi-continuous SMC

Let us consider the system

$$\dot{x}(t) = f(x(t)) = \begin{pmatrix} 0 & 1 \\ 0 & 0 \end{pmatrix} x(t) + \begin{pmatrix} 0 \\ 1 \end{pmatrix} u(x(t)), \quad x = (x_1, x_2)^\top \in \mathbb{R}^2,$$

where $u(\cdot)$ is given by $u(x) = -\alpha \frac{x_1 + \beta x_2 |x_2|}{|x_1| + \beta x_2^2}$, and $\alpha, \beta > 0$ are constant parameters to be defined. Such a controller is a so-called quasi-continuous control,[106] because it has discontinuities only at $x_1 = x_2 = 0$, where those variables define the sliding variable x_1 and its derivative x_2. The closed-loop system can be embedded into Filippov's framework (81). The vector field $f(\cdot)$ has a unique discontinuity at zero, and $F(0) = (0, [-\alpha, \alpha])^\top$. One can check that the vector field $f(\cdot)$ is $\mathbf{d}$-homogeneous of degree -1 with respect to the dilation $\mathbf{d}(\cdot)$ given by (65), that is,

$$f(e^{sG_\mathbf{d}} x) = e^{-s} e^{sG_\mathbf{d}} f(x), \quad \text{for all } x \in \mathbb{R}^2 \setminus \{0\}, \quad \text{for all } s \in \mathbb{R}, \quad G_\mathbf{d} = \begin{pmatrix} 2 & 0 \\ 0 & 1 \end{pmatrix}.$$

To fulfill the requirements of Theorem 7, the parameters $\alpha > 0$ and $\beta > 0$ should be selected such that the canonical homogeneous norm $\|\cdot\|_\mathbf{d}$ is a Lyapunov function of the system. To this purpose we use the inequality (74) and (62). For example, the matrix

$$P = \begin{pmatrix} 1 + \varepsilon & 1 \\ 1 & 1 \end{pmatrix} \text{ with } \varepsilon > 1/8,$$

satisfies the inequality (62). Due to the symmetry property $f(-x) = -f(x)$, we may consider only the case $x_1 \geq 0$. Hence, taking into account

$$x^\top P x = 1 \quad \Leftrightarrow \quad (1 + \varepsilon) x_1^2 + 2 x_1 x_2 + x_2^2 = 1 \quad \Leftrightarrow \quad x_2 = -x_1 \pm \sqrt{1 - \varepsilon x_1^2},$$

we derive that the inequality (74) becomes

$$\begin{pmatrix} x_1 \\ x_2 \end{pmatrix}^T \begin{pmatrix} 1 + \varepsilon & 1 \\ 1 & 1 \end{pmatrix} \begin{pmatrix} x_2 \\ -\alpha \frac{x_1 + \beta |x_2| x_2}{|x_1| + \beta x_2^2} \end{pmatrix} < 0, \quad x_2 = -x_1 \pm \sqrt{1 - \varepsilon x_1^2}, \quad 0 \leq x_1 \leq \frac{1}{\sqrt{\varepsilon}},$$

or, equivalently,

$$\tilde{q}(x_1) < 0, \quad \text{for all } x_1 \in \left[0, \frac{1}{\sqrt{\varepsilon}}\right],$$

where

$$\tilde{q}(x_1) \stackrel{\Delta}{=} \max_{x_2 \in \{-x_1 + \sqrt{1 - \varepsilon x_1^2}, -x_1 - \sqrt{1 - \varepsilon x_1^2}\}} \begin{pmatrix} x_1 \\ x_2 \end{pmatrix}^T \begin{pmatrix} 1 + \varepsilon & 1 \\ 1 & 1 \end{pmatrix} \begin{pmatrix} x_2 \\ -\alpha \frac{x_1 + \beta |x_2| x_2}{|x_1| + \beta x_2^2} \end{pmatrix}.$$

Given $\alpha > 0, \beta > 0$ and $\varepsilon > 0$, the latter inequality can be easily checked (eg, numerically). For $\alpha = 1.5$, $\beta = 1$ and $\varepsilon = 1$, the plot for $\tilde{q}(\cdot)$ is depicted in Figure 14. Therefore, the canonical homogeneous norm $\|\cdot\|_\mathbf{d}$ induced by the norm $\|x\| = \sqrt{(1 + \varepsilon) x_1^2 + 2 x_1 x_2 + x_2^2}$ (see the formula (66), with s_x solving $(1 + \epsilon) e^{-4 s_x} x_1^2 + 2 e^{-3 s_x} x_1 x_2 + e^{-2 s_x} x_2^2 = 1$ using Ferrari's formula) is a Lyapunov function for the considered system, with $\alpha = 1.5$ and $\beta = 1$.

5.7.2 | Consistent discretization

According to the discretization scheme presented above (see Figure 12), a computational scheme first needs to be developed for the transformed system (88). Let us denote $y = q\tilde{z}$, where $q = \|y\|_P$ and $\tilde{z} = (\tilde{z}_1, \tilde{z}_2)^\top \in S \stackrel{\Delta}{=} \{z \in \mathbb{R}^2 \mid \|z\|_P = 1\}$.

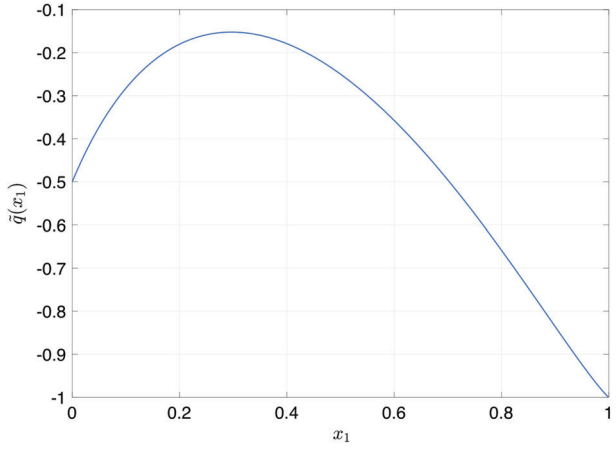

FIGURE 14 The function $\tilde{q}(\cdot)$ for $\alpha = 1.5, \beta = 1, \varepsilon = 1$ [Colour figure can be viewed at wileyonlinelibrary.com]

In this case, using (86) it follows that

$$\tilde{f}(y) = \left(\frac{(I - G_{\mathbf{d}})\tilde{z}\tilde{z}^\top P}{\tilde{z}^\top P G_{\mathbf{d}} \tilde{z}} + I_2 \right) f(\tilde{z}) = \begin{pmatrix} -\tilde{z}_1 \frac{\tilde{z}^\top P f(\tilde{z})}{\tilde{z}^\top P G_{\mathbf{d}} \tilde{z}} + \tilde{z}_2 \\ -\alpha \frac{\tilde{z}_1 + \beta |\tilde{z}_2| \tilde{z}_2}{|\tilde{z}_1| + \beta \tilde{z}_2^2} \end{pmatrix} = \tilde{f}(\tilde{z}).$$

Let $q_k = \|y_k\|_P$ and $z_k = \frac{y_k}{q_k}$. Hence, for $-\frac{y_k}{h} \in \tilde{F}(0) = \overline{\text{co}} \cup_{\tilde{z} \in S} \tilde{f}(\tilde{z})$, the GE($y_{k+1}$): $0 \in \tilde{Q}(h, y_k, y_{k+1})$ (see (88) and Definition 8) gives $q_{k+1} = 0$ and $y_{k+1} = 0$. But if $-\frac{y_k}{h} \notin \tilde{F}(0)$, then the GE($y_{k+1}$) becomes

$$\begin{aligned} & q_{k+1} z_{k+1} - y_k = h \tilde{f}(z_k), \\ & q_{k+1} > 0, \quad z_{k+1}^\top P z_{k+1} = 1. \end{aligned}$$

Simple computations show that

$$q_{k+1} = z_{k+1}^\top P y_k + h z_{k+1} P f(z_{k+1})$$

and

$$e_2^\top \tilde{f}(z_{k+1}) = e_2^\top f(z_{k+1}),$$

where $e_2 = (0,1)^\top \in \mathbb{R}^2$. Therefore, we derive the system of two equations

$$(h z_{k+1}^\top P f(z_{k+1}) + z_{k+1}^\top P y_k) e_2^\top z_{k+1} - e_2^\top y_k - h e_2^\top f(z_{k+1}) = 0, \quad z_{k+1}^\top P z_{k+1} = 1,$$

with respect to two variables $(a,b)^T \stackrel{\Delta}{=} z_{k+1} \in \mathbb{R}^2$. Notice that multiplying the first equation by $|a| + \beta b^2$ yields a polynomial-like equation:

$$m(a,b) \stackrel{\Delta}{=} (|a| + \beta b^2)\{(a \quad b) P y_k + h(2a + b) b\} b - (|a| + \beta b^2) e_2^\top y_k + \alpha h (a + \beta b |b|)(1 - (a+b)b) = 0.$$

Since

$$z_{k+1}^\top P z_{k+1} = 1 \quad \Leftrightarrow \quad b = -a \pm \sqrt{1 - \varepsilon a^2}, \quad -\frac{1}{\sqrt{\varepsilon}} \le a \le \frac{1}{\sqrt{\varepsilon}},$$

solving the GE(y_{k+1}) implies to find a real root of one of the two scalar equations:

$$\begin{aligned} & (a) \ \tilde{m}_1(a, -a + \sqrt{1 - \varepsilon^2 a}) = 0, \quad -\frac{1}{\sqrt{\varepsilon}} \le a \le \frac{1}{\sqrt{\varepsilon}} \\ & (b) \ \tilde{m}_2(a, -a - \sqrt{1 - \varepsilon^2 a}) = 0, \quad -\frac{1}{\sqrt{\varepsilon}} \le a \le \frac{1}{\sqrt{\varepsilon}}. \end{aligned} \tag{94}$$

Theorem 7 implies that such a root (at least of one of these two equations) always exists.

Algorithm 5 (consistent scheme for the quasi-continuous SMC in Example 1):

- **data**: y_k, $h>0$, ϵ, P, $G_{\mathbf{d}}$, α, β, $\Phi^{-1}(y)=\begin{pmatrix}\|y\|_P\, y_1\\ y_2\end{pmatrix}$.
- Calculate $\tilde{F}(0)$:
  - **if** $-\frac{y_k}{h}\in\tilde{F}(0)$ **then** $y_{k+1}=0$.
  - **else if** $-\frac{y_k}{h}\notin\tilde{F}(0)$ **then**
    - **if** the polynomial equation (94) (a) has a solution $a\in\mathbb{R}$, **then** $z_{1,k+1}=a$ and $z_{2,k+1}=-a+\sqrt{1-\epsilon^2 a}$,
    - **else if** the polynomial equation (94) (b) has a solution $a\in\mathbb{R}$, **then** $z_{1,k+1}=a$ and $z_{2,k+1}=-a-\sqrt{1-\epsilon^2 a}$,
  - **then** $q_{k+1}=z_{k+1}^{\top}Py_k+hz_{k+1}Pf(z_{k+1})$ and $y_{k+1}=q_{k+1}z_{k+1}$.
- **then** $x_{k+1}=\Phi^{-1}(y_{k+1})=\begin{pmatrix}q_{k+1}y_{1,k+1}\\ y_{2,k+1}\end{pmatrix}$.
- **terminate**

In practice, a Newton method can be used to compute the real root. The example in Section 5.8 presents an HOSM control system which admits an explicit solution to the GE(y_{k+1}) when $n=2$.

5.8 | Example 2: Discretization of an HOSM algorithm

5.8.1 | An homogeneous HOSM algorithm

Let us consider the homogeneous control system[105,114]

$$\dot{x}=f(x)\overset{\Delta}{=}Ax+B(u+\gamma(t,x)),\quad A=\begin{pmatrix}0&1&0&\dots&0\\0&0&1&\dots&0\\\vdots&\vdots&\vdots&\vdots&\vdots\\0&0&0&\dots&1\\0&0&0&\dots&0\end{pmatrix},\quad B=\begin{pmatrix}0\\\vdots\\0\\1\end{pmatrix},\tag{95}$$

where $x=(x_1,x_2,\dots,x_n)^{\top}$, $\gamma:\mathbb{R}\times\mathbb{R}^n\to\mathbb{R}$, describes a bounded matched disturbance and the HOSM algorithm[105] is given using the quasi-continuous controller[14]:

$$u=u(x)\overset{\Delta}{=}\sum_{j=1}^{n}\frac{k_jx_j}{\|x\|_{\mathbf{d}}^{n+1-j}},\tag{96}$$
$$K=\begin{pmatrix}k_1&k_2&\dots&k_n\end{pmatrix}\in\mathbb{R}^n,$$

and $\|\cdot\|_{\mathbf{d}}:\mathbb{R}^n\to\mathbb{R}_+$ is the canonical $\mathbf{d}$-homogeneous norm for the dilation $\mathbf{d}(s)=e^{sG_{\mathbf{d}}}$, $s\in\mathbb{R}$ with

$$G_{\mathbf{d}}=\begin{pmatrix}n&0&\dots&0\\0&n-1&\dots&0\\\vdots&\vdots&\vdots&\vdots\\0&0&\dots&1\end{pmatrix}.$$

[14]See the end of Section 5.1 for the definition.

One has $u(\mathbf{d}(s)x) = u(x)$ and the right-hand side $f(\cdot)$ of the closed-loop system (95) (96) is homogeneous of degree -1:

$$f(\mathbf{d}(s)x) = A\mathbf{d}(s)x + Bu(\mathbf{d}(s)x) = e^{-s}\mathbf{d}(s)(Ax + Bu(x)) = e^{-s}\mathbf{d}(s)f(x), \quad x \in \mathbb{R}^n \setminus \{0\}.$$

Let the gain vector K and a matrix $P = P^\top > 0$ be selected as follows:

$$(A + BK + \alpha G_{\mathbf{d}})^\top P + P(A + BK + \alpha G_{\mathbf{d}}) = 0, \quad PG_{\mathbf{d}} + G_{\mathbf{d}}^\top P > 0, \quad \alpha > 0. \tag{97}$$

Such a selection is always possible.[126] Moreover, if

$$|\gamma(t,x)| < \alpha \frac{\lambda_{\min}(P^{1/2}G_{\mathbf{d}}P^{-1/2} + P^{-1/2}G_{\mathbf{d}}^\top P^{1/2})}{2\sqrt{B^\top PB}}, \quad \forall (t,x) \in \mathbb{R} \times \mathbb{R}^n,$$

then the origin of the closed-loop system (95) and (96) is globally uniformly finite-time stable (see Reference 126 for more details). Notice also that

$$u^\top(x)u(x) \le \lambda_{\max}(P^{-1/2}K^\top KP^{-1/2}), \quad \forall x \in \mathbb{R}^n \setminus \{0\},$$

that is, the control input is globally bounded.

5.8.2 | Consistent discretization

The equivalent homogeneous system with $y = \Phi(x) \overset{\Delta}{=} \|x\|_{\mathbf{d}}\mathbf{d}(-\ln\|x\|_{\mathbf{d}})x$ has the form

$$\dot{y} = \|y\|_P^{1+\nu}\left(\frac{(I_n - G_{\mathbf{d}})yy^\top P}{y^\top PG_{\mathbf{d}}y} + I_n\right) f\left(\frac{y}{\|y\|_P}\right),$$

where $f\left(\frac{y}{\|y\|_P}\right) = \frac{1}{\|y\|_P}\begin{pmatrix} y_2 \\ \vdots \\ y_{n-1} \\ \sum_{j=1}^n k_j y_j \end{pmatrix} = (A + BK)\frac{y}{\|y\|_P}$, and recall that $\|y\|_P = \sqrt{y^\top Py}$ with P satisfying (62). In this case, we derive

$$\begin{aligned}\tilde{f}(y) &\overset{\Delta}{=} \left(\frac{(I_n - G_{\mathbf{d}})yy^\top P}{y^\top PG_{\mathbf{d}}y} + I_n\right)(A + BK)\frac{y}{\|y\|_P} = \frac{1}{\|y\|_P}\frac{(I_n - G_{\mathbf{d}})yy^\top P(A + BK)y}{y^\top PG_{\mathbf{d}}y} + (A + BK)\frac{y}{\|y\|_P} \\ &= \frac{1}{\|y\|_P}\frac{(I_n - G_{\mathbf{d}})y(-y^\top PG_{\mathbf{d}}y)}{y^\top PG_{\mathbf{d}}y} + (A + BK)\frac{y}{\|y\|_P} = (A + BK + G_{\mathbf{d}} - I_n)\frac{y}{\|y\|_P}.\end{aligned}$$

According to Theorem 7, the consistent implicit discretization scheme has the form (88) with $\tilde{F}(y) = (\tilde{A} - I_n)\tilde{N}(y)$ or, equivalently,

$$y_i \in y_{i+1} + h(I_n - \tilde{A})\tilde{N}(y_{i+1}), \quad h > 0, \quad i = 0, 1, 2, \ldots \tag{98}$$

where $\tilde{A} = A + BK + G_{\mathbf{d}}$ is such that $\tilde{A}^\top P + P\tilde{A} = 0$ (see (97)) and

$$\tilde{N}(y) = \begin{cases} \left\{\frac{y}{\|y\|_P}\right\} & \text{if} \quad y \neq 0 \\ \mathbb{B}_n^P & \text{if} \quad y = 0, \end{cases}$$

where $\mathbb{B}_n^P$ is the unit ball in $\mathbb{R}^n$ with the norm $\|\cdot\|_P$. Notice that the condition (97) implies that $I_n - \tilde{A}$ is invertible. Let us denote $q_{i+1} = \|y_{i+1}\|_P$ and $z_{i+1} = \frac{y_{i+1}}{\|y_{i+1}\|_P}$. Then the inclusion (98) has the following solution

- if $y_i^\top (I_n - \tilde{A})^{-\top} P (I_n - \tilde{A})^{-1} y_i \le h^2$ then

$$q_{i+1} = 0 \quad \text{and} \quad z_{i+1} = h^{-1}(I_n - \tilde{A})^{-1} y_i. \tag{99}$$

- Otherwise, q_{i+1} and z_{i+1} are derived as the solution to

$$((q_{i+1} + h) I_n - h\tilde{A}) z_{i+1} = y_i, \quad z_{i+1}^\top P z_{i+1} = 1, \tag{100}$$

where $y_i = \|x_i\|_{\mathbf{d}} \mathbf{d}(-\ln \|x_i\|_{\mathbf{d}}) x_i$. A solution to (100) always exists due to Theorem 7. It can be found in two steps. First, a positive real root of the polynomial (with respect to q_{i+1}) equation

$$y_i^\top ((q_{i+1} + h) I_n - h\tilde{A})^{-\top} P ((q_{i+1} + h) I_n - h\tilde{A})^{-1} y_i = 1,$$

must be solved. The vector z_{i+1} is given by

$$z_{i+1} = ((q_{i+1} + h) I_n - h\tilde{A})^{-1} y_i.$$

For $n = 2$ the system (100) implies a quartic equation with respect to q_{i+1}:

$$y_i^\top \begin{pmatrix} q_{i+1} - k_2 h & h \\ k_1 h & q_{i+1} - h \end{pmatrix}^\top P \begin{pmatrix} q_{i+1} - k_2 h & h \\ k_1 h & q_{i+1} - h \end{pmatrix}^1 y_i = (q_{i+1} - h)^2 (q_{i+1} - k_2 h)^2,$$

so it can be solved *explicitly* using Ferrari formulas. In other cases some proper computational procedure can be utilized. Second, to transform the vector $x \in \mathbb{R}^2$ to $y = \|x\|_{\mathbf{d}} \mathbf{d}(-\ln \|x\|_{\mathbf{d}}) x$, the canonical homogeneous norm $\|\cdot\|_{\mathbf{d}}$ must be also computed. From its definition (see the formula (66)) we conclude that $\|x\|_{\mathbf{d}}$ also satisfies a polynomial equation (with respect to $\|x\|_{\mathbf{d}}$):

$$x^\top \begin{pmatrix} \|x\|_{\mathbf{d}}^{-n} & 0 & \dots & 0 \\ 0 & \|x\|_{\mathbf{d}}^{-(n-1)} & \dots & 0 \\ \dots & \dots & \dots & \dots \\ 0 & 0 & \dots & \|x\|_{\mathbf{d}}^{-1} \end{pmatrix} P \begin{pmatrix} \|x\|_{\mathbf{d}}^{-n} & 0 & \dots & 0 \\ 0 & \|x\|_{\mathbf{d}}^{-(n-1)} & \dots & 0 \\ \dots & \dots & \dots & \dots \\ 0 & 0 & \dots & \|x\|_{\mathbf{d}}^{-1} \end{pmatrix} x = 1.$$

Again for $n = 2$ we derive that the canonical homogeneous norm is a unique positive solution to the quartic equation

$$\|x\|_{\mathbf{d}}^4 = a\|x\|_{\mathbf{d}}^2 + 2b\|x\|_{\mathbf{d}} + c,$$

$$a = x^\top \begin{pmatrix} 0 & 0 \\ 0 & 1 \end{pmatrix} P \begin{pmatrix} 0 & 0 \\ 0 & 1 \end{pmatrix} x, \quad b = x^\top \begin{pmatrix} 0 & 0 \\ 0 & 1 \end{pmatrix} P \begin{pmatrix} 1 & 0 \\ 0 & 0 \end{pmatrix} x, \quad c = x^\top \begin{pmatrix} 1 & 0 \\ 0 & 0 \end{pmatrix} P \begin{pmatrix} 1 & 0 \\ 0 & 0 \end{pmatrix} x,$$

which again can be found using Ferrari's formulas. Therefore, for any $x_i \in \mathbb{R}^2$, the values (q_{i+1}, z_{i+1}), as well as x_{i+1}, can be easily computed.

5.8.3 | On the digital implementation of the implicit HOSM controller

Similarly to the methodology developed in Sections 2 to 4, let us suggest to use the obtained discretization scheme for digital (sampled-time) implementation of finite-time controllers. Taking into account $x = \mathbf{d}(\ln(\|y\|_P)) \frac{y}{\|y\|_P}$ and $u_\nu(\mathbf{d}(s)x) = u_\nu(x)$ for $\nu = -1$, we derive that the implicit discretization of the control law (96) can be defined as follows

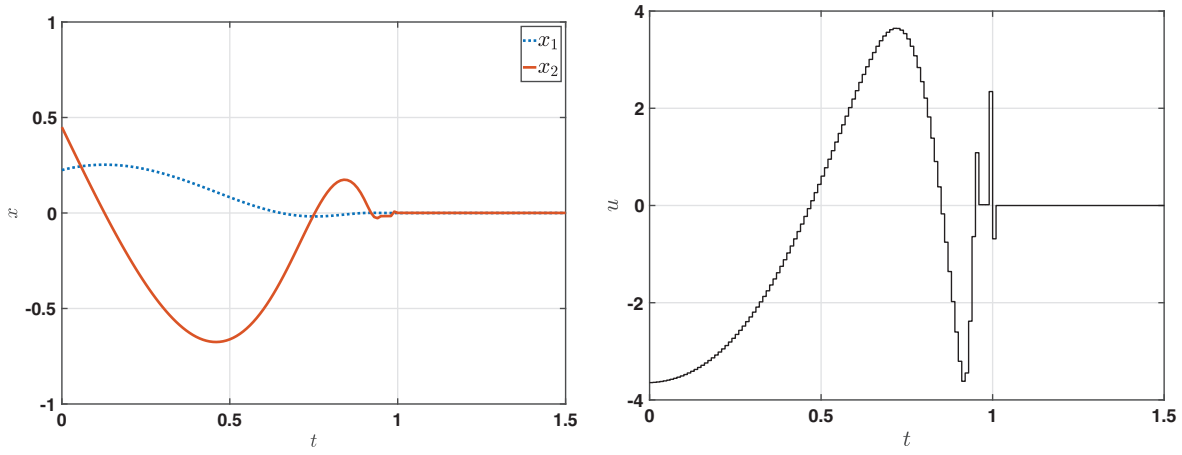

FIGURE 15 Evolution of the system (102) with the implicitly discretized control $u_i = Kz_{i+1}$, $h = 0.01$s [Colour figure can be viewed at wileyonlinelibrary.com]

$$u_v(x_{i+1}) = u_v\left(\frac{y_{i+1}}{\|y_{i+1}\|_P}\right) = u_v(z_{i+1}) = Kz_{i+1},$$

where z_{i+1} is given by (99) or (100) (dependently of y_i). According to the conventional implicit discretization technique (see Sections 2-4) this value is suggested to be selected for the time interval $[t_i, t_{i+1})$ during digital implementation of the control law (96) in the system (95), that is,

$$u(t) = u_i \stackrel{\Delta}{=} Kz_{i+1}, \quad t \in [ih, (i+1)h). \tag{101}$$

Notice that the controller (101) does not guarantee finite-time convergence of the system states to zero, since the *exact* solution to the system (95) in this case is given by

$$x(t) = e^{At}x_i + \int_0^t e^{A(t-s)}B(u_i + \gamma(s, x(s)))\, ds, \quad t \in [ih, (i+1)h), \quad x_i \stackrel{\Delta}{=} x(ih). \tag{102}$$

The following control parameters are used for the simulations

$$P = \begin{pmatrix} 9.1050 & 1.7829 \\ 1.7829 & 0.8914 \end{pmatrix}, \quad K = \begin{pmatrix} -10.2139 & -3.0000 \end{pmatrix}.$$

In the disturbance-free case $\gamma(t, x) \equiv 0$, the implicit sampled control (101) completely rejects the numerical chattering (see Figure 15), which always exists for the explicit implementation of the control law (96) (see Figure 16). Moreover, the numerical experiments show that the consistently discretized implicit HOSM control remains efficient for rejection of slowly varying perturbations $\gamma = 0.4\cos(2t)$ (see Figure 17). Noisy measurements imply an expectable degradation of chattering reduction (Figure 18).

However, the chattering magnitude of the implicitly discretized controller in the noisy and perturbed case, is still much smaller than the chattering magnitude of the explicitly discretized controller in the disturbance-free case.

The noisy measurement was modeled as $\tilde{x}_i = x_i + \eta_i$ and utilized for the computation of the control value u_i, where η_i is a uniformly distributed random noise with a certain magnitude. Notice that, the implicit control remains more precise than the explicit one even in the case of the higher noise magnitude (see Figure 19). Obviously, this conclusion needs to be confirmed theoretically, and numerically on other types of plants and controllers.

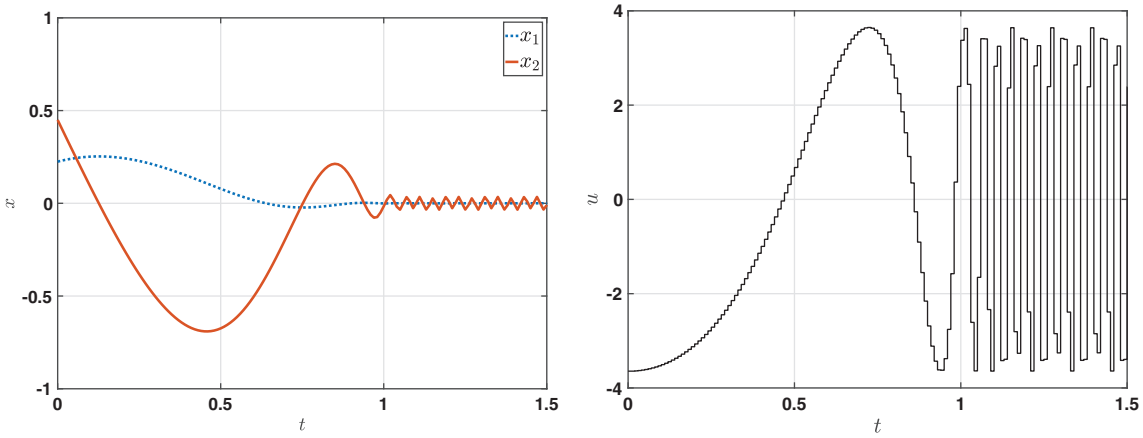

FIGURE 16 Evolution of the system (102) with the explicitly discretized control $u_i = u(x_i)$, $h = 0.01$s [Colour figure can be viewed at wileyonlinelibrary.com]

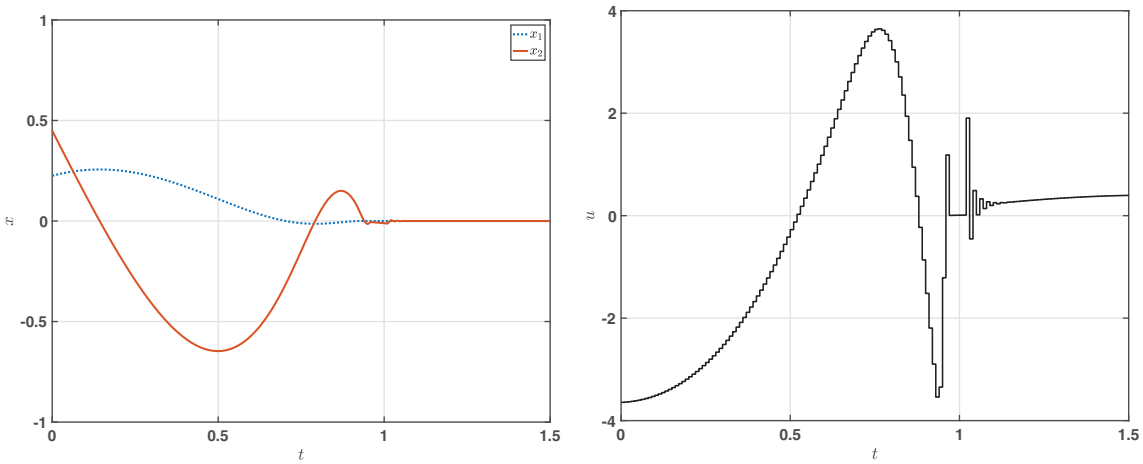

FIGURE 17 Evolution of the system (102) with the implicitly discretized control $u_i = Kz_{i+1}$, $h = 0.01$ in the perturbed case $\gamma = 0.4\cos(2t)$ [Colour figure can be viewed at wileyonlinelibrary.com]

6 | OPEN PROBLEMS AND CONCLUSIONS

This article is dedicated to present the implicit discrete-time implementation of various kinds of SMC and homogeneous systems. It is shown in each case how the implicit method can be implemented in practice, solving at each time step (usually simple) GEs, that take the form of low-dimension complementarity problems (in a sense this is similar to model-predictive control which requires to solve an optimization problem at each step). This article reviews the main results published to date (linear systems, nonlinear systems, with exogenous disturbances or parameter uncertainties, first-order, second-order SMC, homogeneous systems) and presents five algorithms for the implementation of the implicit discretization. Open problems are numerous:

- HOSM homogeneous differentiators: it is known that the explicit Euler method provides accuracy deterioration (or even instability issues[54]), and has to be enhanced to increase the precision.[52,127] Could the implicit method bring a solution to this discretization issue ? Do such discretized differentiators bring significant advantage with respect to "dirty" differentiators like linear filters, when used in a closed-loop system (see also Section 3.4.4 for related material)? In particular linear differentiator may decrease the accuracy.[21] Preliminary results in this direction are in Reference 40 where a twisting SMC is combined with a supertwisting observer, and[44] where two supertwisting algorithms are used for control and observation. First-order sliding-mode differentiators are proposed and analyzed in References 56,128,

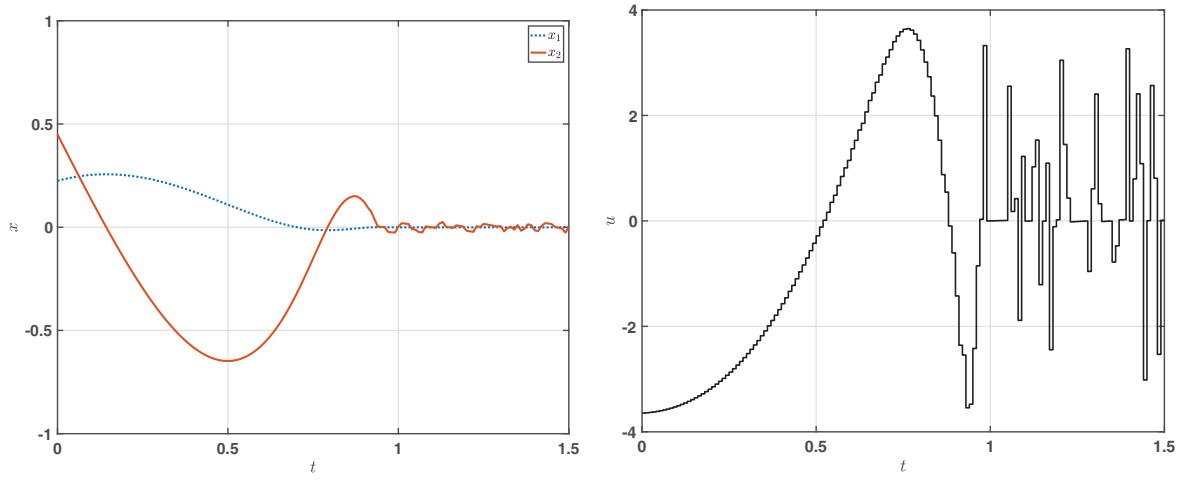

FIGURE 18 Evolution of the system (102) with the implicitly discretized control $u_i = Kz_{i+1}$, $h = 0.01$s in the perturbed case $\gamma = 0.4\cos(2t)$ with a uniformly distributed measurement noise with magnitude 10^{-3} [Colour figure can be viewed at wileyonlinelibrary.com]

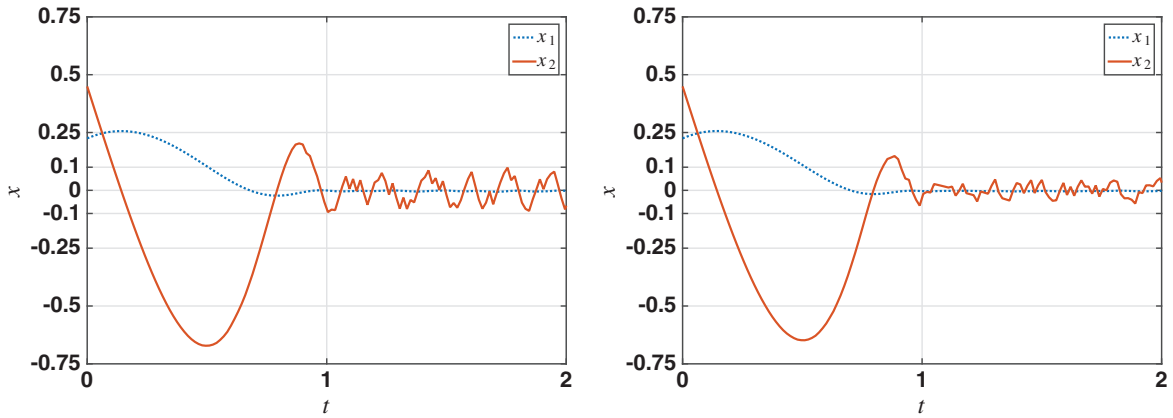

FIGURE 19 Comparison of the precision of the explicitly (left) and the implicitly (right) discretized control for the system (102) with $h = 0.01$s, $\gamma = 0.4\cos(2t)$ and the uniformly distributed measurement noise with magnitude $5{\cdot}10^{-3}$ [Colour figure can be viewed at wileyonlinelibrary.com]

with an implicit Euler discretization. Let us mention also the preliminary results in Reference 129, who generalize the results in Reference 36 to homogeneous differentiators. The extension of Algorithm 4 (which can be easily adapted to the supertwisting differentiator case) toward the supertwisting method proposed in Reference 130, could be of interest as well. Comparisons with the differentiators analyzed in Reference 74,75 seem to be unavoidable as well. The big challenge is the analysis of implicitly discretized differentiators in closed-loop systems. The case of closed-loop systems incorporating supertwisting state observers,[101] may also be worth investigating.

- Higher order sliding-mode controllers, other than twisting and supertwisting.
- Infinite dimensional homogeneous systems[113] (would maximal monotone operators as used for the first time in sliding-mode control in References 31-33,78, be useful in this context?).
- Improve the robustness with respect to noise on the sliding variable (despite of the fact that modern SMC possess good robustness properties in that respect, even enhanced by the use of proper differentiators).
- Backstepping control with nested controllers for uncertain triangular systems of dimension $n \geq 3$ (Section 3.4).
- Develop the use of maximal monotone operators as done in References 31-33,78 in a larger context.
- Nonconstant sampling period h (see Reference 125 for preliminary results).

- More experimental validations, comparisons between first-order and HOSMC (with correct discrete-time implementation), see [21, figure 22] for preliminary results, where it is shown that the twisting and a first-order SMC provide similar closed-loop performance.
- In case the "generalized equation" block is solved with an iterative algorithm (successive approximations method, or LCP solver), what is the influence of the solver precision on the closed-loop performance ?
- Implementation of SMC plus observers to decrease chattering: is it more efficient than implicit SMC without observer? In that same vein consider supertwisting observers combined with supertwisting or twisting controller,[93,131] and extend the results of Section 4.2.
- Develop user-friendly toolboxes to solve the "Generalized equation" block for different classes of systems, both for control and differentiation.
- Analyse the robustness and performances taking into account the quantization on the sliding variable.[132]
- When the SMC guarantees stability in the presence of parametric uncertainties, does its implicit discrete-time implementation behave better that an adaptive or an H_∞ controller? See Reference 33 for a preliminary analysis.
- Design a generic optimization procedure to compute the "extra" parameters usually needed to construct the sliding variable: elements of the output matrix C (with $\sigma = Cx$), time constants of the linear filters ("dirty" differentiators with transfer function $\frac{\tau s}{\tau+s}$) used to get higher degree derivatives of the measured output y. See [21, section 5] and [98, section 4.1.3] for an example of such a procedure.
- Design SMC for flexible mechanical systems: chattering is known to be particularly dangerous since it excites high-frequency oscillatory modes. The suppression of chattering through the implicit implementation, could represent a significant progress for the robust control of flexible systems.
- Compare the semi-implicit discretization methods proposed in References 52,53 with the above implicit ones, both for control and for differentiation algorithms. Compare also with the algorithm proposed in Reference 72. More generally, semi-implicit methods (keeping the implicit discretization of the set-valued part of the controllers) may constitute an acceptable compromise in some applications, with reduced computations and reduced chattering. This is an open problem.
- Continue the analysis of twisting and supertwisting algorithms in more general contexts with perturbation. Analyse also the discrete-time multivariable supertwisting scheme,[133] which uses the so-called unit vector controller, that is, maximal monotone [32, example 17].

ORCID

Bernard Brogliato https://orcid.org/0000-0002-6193-9404
Andrey Polyakov https://orcid.org/0000-0002-5894-1917

REFERENCES

1. Acary V, Brogliato B. *Numerical Methods for Nonsmooth Dynamical Systems. Lecture Notes in Applied and Computational Mechanics*. Vol 35. New York, NY: Springer-Verlag; 2008.
2. Brogliato B, Tanwani A. Dynamical systems coupled with monotone set-valued operators: formalisms, applications, well-posedness, and stability. *SIAM Rev*. 2020;62(1):3-129.
3. Jean M, Moreau JJ. Dynamics in the presence of unilateral contacts and dry friction: a numerical approach. In: Del Piero G, Maceri F, eds. *Unilateral Problems in Structural Analysis. International Centre for Mechanical Sciences (Courses and Lectures)*. Vol 304. Wien, Austria: Springer Verlag; 1987:151-196. https://hal.archives-ouvertes.fr/hal-01864213/document.
4. Moreau JJ. Unilateral contact and dry friction in finite freedom dynamics. In: Moreau JJ, Panagiotopoulos PD, eds. *Nonsmooth Mechanics and Applications. International Centre for Mechanical Sciences (Courses and Lectures)*. Vol 302. Vienna, Austria: Springer Verlag; 1988:1-82.
5. Baji B, Cabot A. An inertial proximal algorithm with dry friction: finite convergence results. *Set Valued Anal*. 2006;14(1):1-23.
6. Peypouquet J, Sorin S. Evolution equations for maximal monotone operators: asymptotic analysis n continuous and discrete time. *J Convex Anal*. 2010;17(3-4):1113-1163.
7. Moreau JJ. Propriétés des applications "prox". *C R Acad Sci*. 1963;256:1069-1071.
8. Bastien J, Schatzman M. Numerical precision for differential inclusions with uniqueness. *ESAIM: M2AN Math Modell Numer Anal*. 2002;36(3):427-460.
9. Bastien J, Schatzman M, Lamarque CH. Study of an elastoplastic model with an infinite number of internal degrees of freedom. *Europ J Mech A/Solids*. 2002;21:199-222.
10. Lippold G. Error estimates for the implicit Euler approximation of an evolution inequality. *Nonlinear Anal*. 1990;15:1077-1089.

11. Galias Z, Yu X. Complex discretization behaviours of a simple sliding-mode control system. *IEEE Trans Circ Syst–II Exp Briefs*. 2006;53(8):652-656.
12. Galias Z, Yu X. Euler's discretization of single input sliding-mode control systems. *IEEE Trans Autom Control*. 2007;52(9):1726-1730.
13. Galias Z, Yu X. Analysis of zero-order holder discretization of two-dimensional sliding-mode control systems. *IEEE Trans Circ Syst–II Expr Briefs*. 2008;55(12):1269-1273.
14. Yan Y, Galias Z, Yu X, Sun C. Euler's discretization effect on a twisting algorithm based sliding mode control. *Automatica*. 2016;68:203-208.
15. Wang B, Brogliato B, Acary V, Boubakir A, Plestan F. Experimental comparisons between implicit and explicit implementations of discrete-time sliding mode controllers: toward input and output chattering suppression. *IEEE Trans Control Syst Technol*. 2015;23(5):2071-2075.
16. Huber O, Brogliato B, Acary V, Boubakir A, Plestan F, Wang B. Experimental results on implicit and explicit time-discretization of equivalent-control-based sliding-mode control. In: Fridman L, Barbot JP, Plestan F, eds. *Recent Trends in Sliding-Mode Control*. Control, Robotics and Sensors. Vol 102. London: IET Institution of Engineering and Technology; Londan: 2016;207-236.
17. Levant A. On fixed and finite time stability in sliding mode control. Paper presented at: Proceedings of the 52nd IEEE Conference on Decision and Control; 2013:4260-4265; Firenze, Italy.
18. Efimov D, Polyakov A, Levant A, Perruquetti W. Realization and discretization of asymptotically stable homogeneous systems. *IEEE Trans Autom Control*. 2017;62(11):5962-5969.
19. Du H, Zhai J, Chen MZQ, Zhu W. Robustness analysis of a continuous higher order finite-time control system under sampled-data control. *IEEE Trans Autom Control*. 2019;64(6):2488-2494.
20. Huber O, Acary V, Brogliato B. Lyapunov stability and performance analysis of the implicit discrete sliding mode control. *IEEE Trans Autom Control*. 2016;61(10):3016-3030.
21. Huber O, Acary V, Brogliato B, Plestan F. Implicit discrete-time twisting controller without numerical chattering: analysis and experimental results. *Control Eng Pract*. 2016;46(1):129-141.
22. Güler O. On the convergence of the proximal point algorithm for convex minimization. *SIAM J Control Optim*. 1991;29(2):403-419.
23. Leenaerts DMW. On linear dynamic complementary systems. *IEEE Trans Circ Syst I Fund Theory Appl*. 1999;46(8):1022-1026.
24. Camlibel MK. *Complementarity Methods in the Analysis of Piecewise Linear Dynamical Systems* (PhD thesis). Katholieke Universiteit Brabant (Tilburg University), Tilburg, NL; May 2001.
25. Acary V, Brogliato B. Implicit Euler numerical scheme and chattering-free implementation of sliding mode systems. *Syst Control Lett*. 2010;59:284-293.
26. Acary V, Brogliato B, Orlov Y. Chattering-free digital sliding-mode control with state observer and disturbance rejection. *IEEE Trans Autom Control*. 2012;57(5):1087-1101.
27. Acary V, Brogliato B, Orlov Y. Comments on "Chattering-free digital sliding-mode control with state observer and disturbance rejection". *IEEE Trans Automat Control*. 2016;61(11):3707.
28. Adly S, Brogliato B, Le BK. Implicit Euler time-discretization of a class of Lagrangian systems with set-valued robust controller. *J Convex Anal*. 2016;23(1):23-52.
29. Brogliato B, Polyakov A. Globally stable implicit Euler time-discretization of a nonlinear single-input sliding-mode control system. Paper presented at: Proceedings of the IEEE 54th International Conference on Decision and Control; December 2015:5426-5431; Osaka, Japan.
30. O. Huber, V. Acary, and B. Brogliato. Enhanced matching perturbation attenuation with discrete-time implementations of sliding-mode controllers. Paper presented at: Proceedings of the European Control Conference; 2014:2606-2611; Strasbourg, France.
31. Miranda-Villatoro F, Brogliato B, Castanos F. Multivalued robust tracking control of Lagrange systems: continuous and discrete-time algorithms. *IEEE Trans Autom Control*. 2017;62(9):4436-4450.
32. Miranda-Villatoro F, Brogliato B, Castanos F. Set-valued sliding-mode control of uncertain linear systems: continuous and discrete-time analysis. *SIAM J Control Optim*. 2018;56(3):1756-1793.
33. Miranda-Villatoro F, Castanos F, Brogliato B. Continuous and discrete-time stability of a robust set-valued nested controller. *Automatica*. 2019;107:406-417.
34. Polyakov A, Efimov D, Brogliato B. Consistent discretization of finite-time and fixed-time stable systems. *SIAM J Control Optim*. 2019;57(1):78-103.
35. Huber O, Acary V, Brogliato B. Lyapunov stability analysis of the implicit discrete-time twisting control algorithm. *IEEE Trans Autom Control*. 2020;65(6):2619-2626.
36. Brogliato B, Polyakov A, Efimov D. The implicit discretization of the super-twisting sliding-mode control algorithm. *IEEE Trans Automat Control*. 2020.
37. Aung MTS, Shi Z, Kikuuwe R. A new parabolic sliding mode filter augmented by a linear low-pass filter and its application to position control. *ASME J Dyn Syst Measur Control*. 2018;140:041005.
38. Kikuuwe R, Fujimoto H, Yasukouchi S, Yamamoto M. Proxy-based sliding mode control: a safer extension of PID position control. *IEEE Trans Robot*. 2010;26(4):670-683.
39. Baiomy N, Kikuuwe R. Parameter selection procedure for an amplitude- and rate-saturated controller. *Int J Control Automat Syst*. 2019;17(4):926-935.
40. Luo D, Xiong X, Jin S, Chen W. Implicit Euler implementation of twisting controller and super-twisting observer without numerical chattering: precise quasi-static MEMS mirrors control. Paper presented at: Proceedings of the MATEC Web of Conferences, volume 256. ICMME; 2019:03004.

41. Jin S, Kikuuwe R, Yamamoto M. Improving velocity feedback for position control by using a discrete-time sliding mode filtering with adaptive windowing. *Adv Robot*. 2014;14:943-953.
42. Kikuuwe R, Takesue N, Sano A, Mochiyama H, Fujimoto H. Admittance and impedance representations of friction based on implicit Euler integration. *IEEE Trans Robot*. 2006;22(6):1176-1188.
43. Jin S, Kikuuwe R, Yamamoto M. Parameter selection guidelines for a parabolic sliding mode filter based on frequency and time domain characteristics. *J Control Sci Eng*. 2012;2012:923679.
44. Xiong X, Kikuuwe R, Yamamoto M. Backward-Euler discretization of second-order sliding mode control and super-twisting observer for accurate position control. Paper presented at: Proceedings of the ASME Dynamic Systems and Control Conference DSCC2013, V003T44A002; 2013:DSCC2013-3872; Palo Alto.
45. Xiong X, Kikuuwe R, Yamamoto M. A differential algebraic method to approximate nonsmooth mechanical systems by ordinary differential equations. *J Appl Math*. 2013;2013:320276.
46. Kikuuwe R. A sliding-mode-like position controller for admittance control with bounded actuator force. *IEEE/ASME Trans Mechatron*. 2014;19(5):1489-1500.
47. Kikuuwe R, Kanaoka K, Kumon T, Yamamoto M. Phase-lead stabilization of force-projecting master-slave systems with a new sliding mode filter. *IEEE Trans Control Syst Technol*. 2015;23(6):2182-2194.
48. Baiomy N, Kikuuwe R. An amplitude-and rate-saturated controller for linear plants. *Asian J Control*. 2019;21(6):1-15.
49. Kikuuwe R. Some stability proofs on proxy-based sliding mode control. *IMA J Math Control Inf*. 2018;35:1319-1341.
50. Xiong X, Chen W, Jin S, Kamal S. Discrete-time implementation of continuous terminal algorithm with implicit-Euler method. *IEEE Access*. 2019;7:175940-175946.
51. Xiong X, Kikuuwe R, Kamal S, Jin S. Implicit-Euler implementation of super-twisting observer and twisting controller for second-order systems. *IEEE Trans Circ Syst II Expr Briefs*. 2020.
52. Koch S, Reichhartinger M, Horn M. Discrete-time equivalents of the super twisting algorithm. *Automatica*. 2019;107:190-199.
53. S. Koch, M. Reichhartinger, and M. Horn. On the discretization of the super-twisting algorithm. Paper presented at: Proceedings of the IEEE 58th Conference on Decision and Control; 2019:5989-5994; Nice, France.
54. Wetzlinger M, Reichhartinger M, Horn M, Fridman L, Moreno JA. Semi-implicit discretization of the uniform robust exact differentiator. Paper presented at: Proceedings IEEE 58th Conference on Decision and Control; 2019:5995-6000, Nice, France.
55. Drakunov SG, Utkin VI. On discrete-time sliding modes. Paper presented at: Proceedings of the Nonlinear Control Design Conference; 1989:273-278; Capri, Italy, IFAC
56. Jin S, Kikuuwe R, Yamamato M. Real-time quadratic sliding mode filter for removing noise. *Adv Robot*. 2012;26(8-9):877-896.
57. Hiriart-Urruty JB, Lemaréchal C. *Fundamentals of Convex Analysis*. Grundlehren Text Editions. Berlin, Heidelberg/Germany: Springer-Verlag; 2001.
58. Robinson SM. Generalized equations. In: Bachem A, Groetschel M, Korte B, eds. *Mathematical Programing: The State of the Art, Bonn 1982*. New York, NY: Springer Verlag; 1983:346-367.
59. Facchinei F, Pang JS. *Finite-Dimensional Variational Inequalities and Complementarity Problems. Operations Research*. Vol I. New York, NY: Springer-Verlag; 2003.
60. Addi K, Brogliato B, Goeleven D. A qualitative mathematical analysis of a class of linear variational inequalities via semi-complementarity problems. *Appl Electron Math Progr Ser A*. 2011;126(1):31-67.
61. Nguyen T, Ewards C, Azimi V, Su WC. Improving control effort in output feedback sliding mode control of sampled-data systems. *IET Control Theory Appl*. 2019;13(13):2128-2137.
62. Utkin VI. Sliding-mode control in discrete-time and difference systems. In: Zinober ASI, ed. *Variable Structure and Lyapunov Control. Lecture Notes in Control and Information Sciences*. Vol 193. Berlin, Heidelberg/Germany: Springer Verlag; 1994:87-107.
63. Dontchev A, Lempio F. Difference methods for differential inclusions: a survey. *SIAM Rev*. 1992;34(2):263-294.
64. Yu X, Chen G. Discretization behaviors of equivalent control based sliding-mode control systems. *IEEE Trans Autom Control*. 2003;48(9):1641-1646.
65. Yu X, Wang B, Galias Z, Chen G. Discretisation effect on equivalent control-based multi-input sliding-mode control systems. *IEEE Trans Autom Control*. 2008;53(6):1563-1569.
66. Wang B, Yu X, Chen G. ZOH discretisation effect on single-input sliding mode control systems with matched uncertainties. *Automatica*. 2009;45(1):118-125.
67. Young KD, Utkin VI, Ozguner U. A control engineer's guide to sliding mode control. *IEEE Trans Control Syst Technol*. 1999;7(3):328-342.
68. Alexander JC, Seidman T. Sliding modes in intersecting switching surfaces: blending. *Houst J Math*. 1998;24:545-569.
69. Barbot JP, Monaco S, Normand-Cyrot D, Pantalos N. Discretization schemes for nonlinear singularly perturbed systems. Paper presented at: Proceedings of the IEEE International Conference on Decision and Control; December 1991:443-448; Brighton, UK.
70. Barbot JP, Djemai M, Monaco S, Normand-Cyrot D. Analysis and control of nonlinear singularly perturbed systems under sampling. In: Leondes CT, ed. *Digital Control Systems Implementations and Computational Techniques. Control and Dynamic Systems. Advances in Theory and Applications*. Vol 79. San Diego, New York, Boston, London, Sydney, Tokyo, Toronto: Academic Press; 1996:203-246.
71. Wu C, van der Schaft AJ, Chen J. Robust trajectory tracking for incrementally passive nonlinear systems. *Automatica*. 2019;107(9):595-599.
72. Su WC, Drakunov SV, Ozguner U. Robust trajectory tracking for incrementally passive nonlinear systems. *IEEE Trans Automat Control*. 2000;45(3):482-485.
73. Levant A. Robust exact differentiation via sliding mode technique. *Automatica*. 1998;34(3):379-384.

74. Mboup M, Join C, Fliess M. Numerical differentiation with annihilators in noisy environment. *Numer Alg*. 2009;50(4):439-467.
75. Mboup M, Riachy S. Frequency-domain analysis and tunig of the algebraic differentiators. *Int J Control*. 2018;91(9):2073-2081.
76. Brogliato B, Lozano R, Maschke B, Egeland O. *Dissipative Systems Analysis and Control. Theory and Applications*. Communications and Control Engineering. 3rd ed. Springer Nature Switzerland AG; 2020.
77. Utkin VI. *Sliding Modes in Control Optimization*. Communications and Control Engineering. Berlin, Heidelberg/Germany: Springer Verlag; 1992.
78. Miranda-Villatoro F, Castanos F. Robust output regulation of strongly passive linear systems with multivalued maximally monotone controls. *IEEE Trans Autom Control*. 2017;62(1):238-249.
79. Adly S, Brogliato B, Le BK. Well-posedness, robustness and stability analysis of a set-valued controller for Lagrangian systems. *SIAM J Control Optim*. 2013;51(2):1592-1614.
80. Miranda-Villatoro F, Brogliato B, Castanos F. Errata to "Multivalued robust tracking control of Lagrange systems: continuous and discrete-time algorithms". *IEEE Trans Automat Control*. 2018;63(8):2750.
81. Kolmogorov AN, Fomin SV. *Elements of the Theory of Functions and Functional Analysis*. Vol 1. New York, NY: Graylock Press; 1957.
82. Utkin VI, Drakunov SV, Izosimov DE, Lukyanov AG, Utkin VA. A hierarchical principle of the control system decomposition based on motion separation. Paper presented at: Proceedings 9th IFAC Triennal World Congress; July 1984:1553-1558; Budapest, Hungary.
83. Drakunov SV, Izosimov DB, Luk'yanov AG, Utkin VA, Utkin VI. The block control principle I. *Autom Remote Control*. 1990;51:601-608.
84. Drakunov SV, Izosimov DB, Luk'yanov AG, Utkin VA, Utkin VI. The block control principle II. *Autom Remote Control*. 1990;51:737-746.
85. Utkin VI, Chen DS, Chang HC. Block control principle for mechanical systems. *ASME J Dyn Syst Measur Control*. 2000;122:1-10.
86. Jin S, Lv Z, Xiong X, Yu J. A chattering-free sliding mode filter enhanced by first order derivative feedforward. *IEEE Access*. 2020;8:41175-41185.
87. Lv Z, Jin S, Xiong X, Yu J. A new quick-response sliding mode tracking differentiator with its chattering-free discrete-time implementation. *IEEE Access*. 2019;7:130236-130245.
88. Kikuuwe R, Fujimoto H. Proxy-based sliding mode control for accurate and safe position control. Paper presented at: Proceedings of IEEE International Conference on Robotics and Automation; 2006:25-30; Orlando, Florida.
89. Prieto PJ, Rubio E, Hernandez L, Urquijo O. Proxy-based sliding mode control on platform of 3 degree of freedom (3-DOF). *Adv Robot*. 2013;27(10):773-784.
90. Huo W, Arnez-Paniagua V, Ding G, Amirat Y, Mohammed S. Adaptive proxy-based controller of an active ankle foot orthosis to assist lower limb movements of paretic patients. *Robotica*. 2019;37:2147-2164.
91. Gu GY, Zhu LM, Su CY, Ding H, Fatikow S. Proxy-based sliding-mode tracking control of piezoelectric-actuated nanopositioning stages. *IEEE/ASME Trans Mechatron*. 2015;20(4):1956-1965.
92. Shtessel YB, Moreno JA, Fridman LM. Twisting sliding mode control with adaptation: Lyapunov design, methodology and application. *Automatica*. 2017;75:229-235.
93. Chalanga A, Kamal S, Fridman LM, Bandyopadhyay B, Moreno JA. Implementation of super-twisting control: super-twisting and higher order sliding-mode observer-based approaches. *IEEE Trans Ind Electron*. 2016;63(6):3677-3685.
94. Levant A. Sliding order and sliding accuracy in sliding mode control. *Int J Control*. 1993;58(6):1247-1263.
95. Orlov Y. Finite time stability and robust control synthesis of uncertain switched systems. *SIAM J Control Optim*. 2005;43(4):1253-1271.
96. Koch S, Reichhartinger M, Horn M, Fridman LM. Discrete implementation of sliding mode controllers satisfying accuracy level specifications. Paper presented at: Proceedings of the 14th International Workshop on Variable Structure Systems (VSS); 2016:154-159; Nanjing, China.
97. Cao M, Ferris MC. A pivotal method for affine variational inequalities. *Math Oper Res*. 1996;21:44-64.
98. Huber O. *Analyse et implémentation du contrôle par modes glissants en temps discret* (PhD thesis). Université Grenoble-Alpes, Grenoble, France, May 2015. https://hal.inria.fr/tel-01194430.
99. Torres-Gonzales V, Sanchez T, Fridman LM, Moreno JA. Design of continuous twisting algorithm. *Automatica*. 2017;80:119-126.
100. Yan Y, Yu X, Sun C. Discretization behaviors of a super-twisting algoriothm based sliding mode control system. Paper presented at: Proceedings of the International Workshop on Recent Advances in Sliding Modes (RASM); 2015; Istanbul, Turkey.
101. Zhang K, Hatano T, Tien Nguyen T, et al. A super-twisting observer for atomic-force reconstruction in a probe microscope. *Control Eng Pract*. 2020;94:104191.
102. Moreno JA, Osorio M. Strict Lyapunov functions for the super-twisting algorithm. *IEEE Trans Automat Control*. 2012;57(4):1035-1040.
103. Polyakov A, Poznyak A. Reaching time estimation for "super-twisting" second order sliding mode controller via Lyapunov function designing. *IEEE Trans Autom Control*. 2009;54(8):1951-1955.
104. Seeber R, Horn M. Stability proof for a well-established super-twisting parameter setting. *Automatica*. 2017;84:241-243.
105. Polyakov A, Efimov D, Perruquetti W. Finite-time and fixed-time stabilization: implicit Lyapunov function approach. *Automatica*. 2015;51(1):332-340.
106. Levant A. Quasi-continuous high-order sliding-mode controllers. *IEEE Trans Autom Control*. 2005;50(11):1812-1816.
107. Dvir Y, Efimov D, Levant A, Polyakov A, Perruquetti W. Acceleration of finite-time-stable homogeneous systems. *Int J Robust Nonlinear Control*. 2018;28(5):1757-1777.
108. Zubov VI. On systems of ordinary differential equations with generalized homogenous right-hand sides. *Izvestia vuzov. Mathematica (in Russian)*. 1958;1:80-88.
109. Hermes H. Nilpotent approximations of control systems and distributions. *SIAM J Control Optim*. 1986;24(4):731-473.

110. Rosier L. Homogenous Lyapunov function for homogenous coninuous vector field. *Syst Control Lett*. 1992;19:467-473.
111. Bhat SP, Bernstein DS. Geometric homogeneity with applications to finite-time stability. *Math Control Signals Syst*. 2005;17:101-127.
112. Levant A. Homogeneity approach to high-order sliding mode design. *Automatica*. 2005;41:823-830.
113. Polyakov A. Generalized homogeneity in systems and control. *Communications and Control Engineering*. Switzerland: Springer Nature Switzerland; 2020.
114. Polyakov A. Sliding mode control design using canonical homogeneous norm. *Int J Robust Nonlinear Control*. 2018;29(3):682-701.
115. Pazy A. *Semigroups of Linear Operators and Applications to Partial Differential Equations*. New York, NY: Springer; 1983.
116. Perruquetti W, Floquet T, Moulay E. Finite-time observers: application to secure communication. *IEEE Trans Autom Control*. 2008;53(1):356-360.
117. Levant A. Construction principles of 2-sliding mode design. *Automatica*. 2007;43(4):576-586.
118. Kawski M. Geometric homogeneity and stabilization. In: Krener A, Mayne D, eds. *Proceedings of the IFAC Nonlinear Control Symposium*. Lake Tahoe, CA; 1995:164-169.
119. Zimenko K, Polyakov A, Efimov D. On dynamical feedback control design for generalized homogeneous differential inclusions. Paper presented at: Proceedings IEEE Conference on Decision and Control; December 2018:4785-4790; Miami Beach, FL.
120. Filippov AF. *Differential equations with discontinuous right-hand sides*. Dordrecht: Kluwer; 1988.
121. Roxin E. On finite stability in control systems. *Rendiconti del Circolo Matematico di Palermo*. 1966;15(3):273-283.
122. Polyakov A, Fridman L. Stability notions and Lyapunov functions for sliding mode control systems. *J Frankl Inst*. 2014;351(4):1831-1865.
123. Polyakov A, Brogliato B. On consistent discretization of finite-time stable homogeneous differential inclusions; March 2020. https://hal.inria.fr/hal-02514847/document.
124. Sanchez T, Moreno JA. Design of Lyapunov functions for a class of homogeneous systems: Generalized forms approach. *Int J Robust Nonlinear Control*. 2019;29(3):661-681.
125. Efimov D, Polyakov A, Aleksandrov A. Discretization of homogeneous systems using Euler method with a state-dependent step. *Automatica*. 2019;108546.
126. Polyakov A, Efimov D, Perruquetti W. Robust stabilization of MIMO systems in finite/fixed time. *Int J Robust Nonlinear Control*. 2016;26(1):69-90.
127. Livne M, Levant A. Proper discretization of homogeneous differentiators. *Automatica*. 2014;50:2007-2014.
128. Kikuuwe R, Pasaribu R, Byun G. A first-order differentiator with frst-order sliding mode filtering. Paper presented at: Proceedings 11th IFAC Symposium on Nonlinear Control Systems (NOLCOS2019); September 2019:1383-1388; Vienna, Austria.
129. Carjaval-Rubio JE, Loukianov AG, Sanchez-Torres JD, Defoort M. On the discretization of a class of homogeneous differentiators. Paper presented at: Proceedings of the 16th International Conference on Electrical Engineering, Computing Science and Automatic Control (CCE); 2019; Mexico City, Mexico.
130. Cruz-Zavala E, Moreno J, Fridman LM. Uniform robust exact differentiator. *IEEE Trans Autom Control*. 2011;56(11):2727-2733.
131. Moreno JA. A Lyapunov approach to output feedback control using second-order sliding modes. *IMA J Math Control Inf*. 2012;29(3):291-308.
132. Yan Y, Yu S, Yu X. Quantized super-twisting algorithm based sliding mode control. *Automatica*. 2019;105:43-48.
133. Nagesh I, Edwards C. A multivariable super-twisting sliding mode approach. *Automatica*. 2014;50:984-988.
134. Cottle RW, Pang JS, Stone RE. *The Linear Complementarity Problem*. Computer Science and Scientific Computing: Academic Press; 1992.

How to cite this article: Brogliato B, Polyakov A. Digital implementation of sliding-mode control via the implicit method: A tutorial. *Int J Robust Nonlinear Control*. 2021;31:3528–3586. https://doi.org/10.1002/rnc.5121

APPENDIX A. COMPLEMENTARITY PROBLEM FOR (22)

The hypercube $[-g,g]^p = \{z \in \mathbb{R}^p \mid Hz + \overline{g} \geq 0\}$, with $H = \begin{pmatrix} I_p \\ -I_p \end{pmatrix}$ and $\overline{g} = (g, g, \dots, g)^\top \in \mathbb{R}^{2p}$. Then since $[-g,g]^p$ is convex polyhedral, one has $\mathcal{N}_{[-g,g]^p}(u_k^s) = \{w \in \mathbb{R}^p \mid w = -H^\top \overline{\Gamma}_k,\ 0 \leq \overline{\Gamma}_k \perp Hu_k^s + \overline{g} \geq 0\}$. Therefore, we obtain the equivalent formulation of (22):

$$\begin{cases} CB^* u_k^s + \sigma_k = H^\top \overline{\Gamma}_k \\ 0 \leq \overline{\Gamma}_k \perp Hu_k^s + \overline{g} \geq 0, \end{cases} \tag{A1}$$

which is a Mixed LCP.[1] Using the fact that $CB^* \succ 0$, we obtain the LCP:

$$\begin{aligned} &0 \le \bar{\Gamma}_k \perp H(CB^*)^{-1}H^\top \bar{\Gamma}_k + \bar{g} - H(CB^*)^{-1}\sigma_k \ge 0 \\ &u_k^s = (CB^*)^{-1}H^\top\bar{\Gamma}_k - (CB^*)^{-1}\sigma_k \end{aligned} \tag{A2}$$

which reduces to (17) when $p=1$, $g=1$, $C=B=1$, $B^*=h$ (it suffices to change $\overline{\Gamma}_k$ to $\frac{\overline{\Gamma}_k}{h}$ in (A1) to take into account the fact that (17) stems from (12) while (A2) stems from (22)).

APPENDIX B. LMIS FOR X AND K

The stabilizability of (A,B) implies that for some $a>0$ such that $0<2ha<1$, there exists an $n\times n$ matrix $X=X^\top \succ 0$ satisfying the matrix inequality:

$$B_\perp^\top(AX + XA^\top + 2aX)B_\perp + hB_\perp^\top(XA^\top B_\perp(B_\perp^\top XB_\perp)^{-1}B_\perp^\top AX)B_\perp \prec 0. \tag{B1}$$

The matrix X should also satisfy $X - I_n \succ 0$. Finally the next LMI should hold:

$$\begin{pmatrix} R_{11} & R_{12} \\ R_{12}^\top & R_{22} \end{pmatrix} \succ 0, \tag{B2}$$

where,

$$\begin{aligned} R_{11} &\stackrel{\Delta}{=} \begin{pmatrix} B_\perp^\top(aX - I_n)B_\perp & -\frac{1}{2}B_\perp^\top AB & -hB_\perp^\top XA^\top B_\perp \\ -\frac{1}{2}B^\top A^\top B_\perp & K & -hB^\top A^\top B_\perp \\ -hB_\perp^\top AXB_\perp & -hB_\perp^\top AB & 2hB_\perp^\top XB_\perp \end{pmatrix} \\ R_{12} &\stackrel{\Delta}{=} \begin{pmatrix} -hB_\perp^\top XA^\top B_\perp & 0 & B_\perp^\top X & 0 \\ 0 & -hB^\top A^\top B_\perp & 0 & B^\top \\ 0 & 0 & 0 & 0 \end{pmatrix} \\ R_{22} &\stackrel{\Delta}{=} \begin{pmatrix} 2hB_\perp^\top XB_\perp & 0 & 0 & 0 \\ 0 & hB_\perp^\top XB_\perp & 0 & 0 \\ 0 & 0 & \frac{2}{1+2h}\Lambda & 0 \\ 0 & 0 & 0 & \frac{2}{1+2h}\Lambda \end{pmatrix}. \end{aligned}$$

APPENDIX C. ON THE GE (41)

Let us choose $\Phi(\sigma) = \alpha\ \|\sigma\|_1, \alpha > 0$. From (40), we obtain $\hat{\mathcal{A}}_k\tilde{\sigma}_{k+1} - \hat{M}_k\sigma_k \in -hg\alpha\ \partial\|\tilde{\sigma}_{k+1}\|_1$. Let us now see how we could use (1) and (2) to get an explicit expression for $\tilde{\sigma}_{k+1}$, by inverting this inclusion. Using that the conjugate function of $f(\sigma) = \|\sigma\|_1$ is $f^\star(y) = \psi_{[-1,1]}(y_1) + \ \dots\ + \psi_{[-1,1]}(y_p)$, with $\partial f^\star(y) = \mathcal{N}_{[-1,1]^p}(y)$, it follows that the above inclusion is equivalent to:

$$\begin{aligned} &\tilde{\sigma}_{k+1} \in \mathcal{N}_{[-1,1]^p}\left(\frac{\hat{\mathcal{A}}_k\tilde{\sigma}_{k+1} - \hat{M}_k\sigma_k}{-hg\alpha}\right) \\ &\Leftrightarrow\ \tilde{\sigma}_{k+1} \in -\mathcal{N}_{[-hg\alpha,hg\alpha]^p}(\hat{\mathcal{A}}_k\tilde{\sigma}_{k+1} - \hat{M}_k\sigma_k) \\ &\qquad\qquad\qquad\qquad\qquad\qquad\qquad\qquad \stackrel{\Delta}{=} z_{k+1} \\ &\Leftrightarrow\ \hat{\mathcal{A}}_k^{-1}z_{k+1} + \hat{\mathcal{A}}_k^{-1}\hat{M}_k\sigma_k \in -\mathcal{N}_{[-hg\alpha,hg\alpha]^n}(z_{k+1}) \\ &\Leftrightarrow\ z_{k+1} = \mathrm{proj}_{\hat{\mathcal{A}}_k^{-1}}[[-hg\alpha, hg\alpha]^n; -\hat{M}_k\sigma_k] \\ &\Leftrightarrow\ \hat{\mathcal{A}}_k\tilde{\sigma}_{k+1} + \hat{M}_k\sigma_k = \mathrm{proj}_{\hat{\mathcal{A}}_k^{-1}}[[-hg\alpha, hg\alpha]^n; -\hat{M}_k\sigma_k] \\ &\Leftrightarrow\ \tilde{\sigma}_{k+1} = -\hat{\mathcal{A}}_k^{-1}\hat{M}_k\sigma_k + \hat{\mathcal{A}}_k^{-1}\mathrm{proj}_{\hat{\mathcal{A}}_k^{-1}}[[-hg\alpha, hg\alpha]^n; -\hat{M}_k\sigma_k]. \end{aligned} \tag{C1}$$

The last equality is the generalization of (11) and (21) (23) to the more complex Lagrangian systems case. Algorithm 3 is in fact a way to compute the right-hand side of the last equality. Once $\tilde{\sigma}_{k+1}$ has been computed, then ζ_{k+1} is obtained from (41), and u_k^s is obtained from (38) as $-u_k^s = K_\sigma \tilde{\sigma}_{k+1} + g\,\zeta_{k+1}$. The inclusion into a normal cone in (C1), can be rewritten under a complementarity framework, doing as in Section A1. On has $\mathcal{N}_{[-hg\alpha,hg\alpha]^n}(z_{k+1}) = \{w \in \mathbb{R}^n \mid w = -H^\top \Gamma_k,\ 0 \le \Gamma_k \perp Hz_{k+1} + \overline{hg\alpha} \ge 0\}$, where the hypercube $[-hg\alpha, hg\alpha]^n = \{z \in \mathbb{R}^n \mid Hz + \overline{hg\alpha} \ge 0\}$ for suitable matrix H and vector $\overline{hg\alpha}$. Therefore, it follows that $\hat{\mathcal{A}}_k^{-1} z_{k+1} + \hat{\mathcal{A}}_k^{-1} \hat{M}_k \sigma_k = H^\top \Gamma_k$, $0 \le \Gamma_k \perp Hz_{k+1} + \overline{hg\alpha} \ge 0$. Thus, the LCP is:

$$
\begin{aligned}
&0 \le \Gamma_k \perp H\hat{\mathcal{A}}_k H^\top \Gamma_k + \overline{hg\alpha} - \hat{M}_k \sigma_k \ge 0\\
&\tilde{\sigma}_{k+1} = H^\top \Gamma_k\\
&\zeta_{k+1} = -\tfrac{1}{hg}\left(\hat{\mathcal{A}}_k H^\top \Gamma_k - \hat{M}_k \sigma_k\right)\\
&-u_k^s = K_\sigma \tilde{\sigma}_{k+1} + g\zeta_{k+1}.
\end{aligned}
\tag{C2}
$$

This corresponds to the "Generalized equation" feedback block in Figure 7.

APPENDIX D. ON THE GE (33)

Let us examine now (33) using a similar point of view. Choosing $\mathbf{M}(\cdot) = \alpha\, \|\sigma\|_1$, it can be rewritten equivalently as:

$$
(I_p + hK)\tilde{\sigma}_{k+1} - \sigma_k \in -gh\alpha\, \partial\|\tilde{\sigma}_{k+1}\|_1. \tag{D1}
$$

Notice that θ in (33) is like μ in (41): they are numerical parameters to be tuned properly for the iterative solver to be efficient. This is the reason why they no longer appear neither in (C1) nor in (D1). Doing as in (C1), yields the following:

$$
\begin{aligned}
(D1) \ &\Leftrightarrow\ \frac{1}{gh\alpha}((I_p + hK)\tilde{\sigma}_{k+1} + \sigma_k) \in \partial\|\tilde{\sigma}_{k+1}\|_1\\
&\Leftrightarrow\ \tilde{\sigma}_{k+1} \in \mathcal{N}_{[-1,1]^p}\left(-\frac{1}{gh\alpha}(I_p + hK)\tilde{\sigma}_{k+1} + \frac{1}{gh\alpha}\sigma_k\right)\\
&\Leftrightarrow\ \tilde{\sigma}_{k+1} \in -\mathcal{N}_{[-gh\alpha,gh\alpha]^p}((I_p + hK)\tilde{\sigma}_{k+1} - \sigma_k)\\
&\qquad\qquad\qquad\qquad \overset{\Delta}{=} z_{k+1}\\
&\Leftrightarrow\ (I_p + hK)^{-1} z_{k+1} + (I_p + hK)^{-1}\sigma_k \in -\mathcal{N}_{[-gh\alpha,gh\alpha]^p}(z_{k+1})\\
&\Leftrightarrow\ z_{k+1} = \mathrm{proj}_{(I_p+hK)^{-1}}[[-gh\alpha, gh\alpha]^p; -\sigma_k]\\
&\Leftrightarrow\ \tilde{\sigma}_{k+1} = (I_p + hK)^{-1}\sigma_k + (I_p + hK)^{-1}\mathrm{proj}_{(I_p+hK)^{-1}}[[-gh\alpha, gh\alpha]^p; -\sigma_k].
\end{aligned}
\tag{D2}
$$

The projection in the right-hand side of (D2) corresponds to solve the quadratic program:

$$
\begin{cases}
\min\ \ \frac{1}{2}(z + \sigma_k)^\top (I_p + hK)^{-1}(z + \sigma_k)\\
\text{subject to: } z \in [-gh\alpha, gh\alpha]^p\ \Leftrightarrow\ Hz + \overline{gh\alpha} \ge 0
\end{cases}
\tag{D3}
$$

where H and $\overline{gh\alpha} \in \mathbb{R}^p$ are constructed as in Section A1. Using the expression of the normal cone to a polyhedral convex set, one obtains similarly to (A1):

$$
\begin{cases}
(I_p + hK)^{-1} z_{k+1} + (I_p + hK)^{-1}\sigma_k = H^\top \Gamma_k\\
0 \le \Gamma_k \perp Hz_{k+1} + \overline{gh\alpha} \ge 0
\end{cases}
\tag{D4}
$$

This mixed LCP can be transformed readily into the LCP:

$$
\begin{aligned}
&0 \le \Gamma_k \perp H(I_p + hK)H^\top \Gamma_k + \overline{gh\alpha} - \sigma_k \ge 0\\
&\tilde{\sigma}_{k+1} = H^\top \Gamma_k\\
&u_k^s = \tfrac{1}{h}(\tilde{\sigma}_{k+1} - \sigma_k).
\end{aligned}
\tag{D5}
$$

We see once again in this article, that the "Generalized equation" block in Figure 5, can be solved a priori using different approaches. The LCPs in (A2), (C2), and (D5) have dimension p, the number of sliding surfaces. Consequently they are low-dimensional problems which can be solved online, with negligible computation time.

There exists a wealth of theoretical results on the existence and uniqueness of solutions to LCPs as (A2), (C2), and (D5), the main reference on the topic being.[134] In the above cases the LCP matrices should all be positive semidefinite (which, in general, does not guarantee the existence and uniqueness of solutions). However, in our case we know that solutions exist and are uniquely defined.